The Hyde-Macraes shear zone in Otago:

A result of continental extension or shortening?

A kinematic analysis of the Footwall Fault

A thesis submitted in partial fulfilment of the

requirements for the Degree

of Master of Science in Geology

in the University of Canterbury

by

Christoph Florian Butz

Department of Geological Sciences

University of Canterbury, Christchurch, New Zealand

September 2007

Abstract

Mineralised shear zones in Otago are often truncated by regional low-angle faults, which juxtapose schist of different metamorphic grade. The Footwall Fault and the Hyde-Macraes Shear Zone are one example for this kind of tectonic setting, and are the subject to this study. Although, the mechanisms for the development of the mineralised thrust-origin shear zones are well studied, the relationship to the truncating faults is still poorly understood. Currently, the truncating low-angle faults are assumed to be related to crustal extension, starting in the early Cretaceous after the schist passed the ductile-brittle transition.

This study presents new kinematic data for the Footwall Fault, suggesting development of normal sense movement under ductile conditions due to an abundant shear band cleavage in the footwall, which dynamically recrystallises quartz grains. However, brittle high-angle normal faults truncating these shear bands indicate either reactivation of normal sense movement after passing the ductile-brittle transition or continuous normal sense movement during the transition.

Furthermore, this study presents a model, which suggests a regional scale rolling hinge development, consisting of an array of individual low-angle normal faults along the boundary of the textural zone change from TZ IV to TZIII, and strike-parallel high-angle faults at the NE margin of the Otago schist.

Acknowledgements

This study has benefitted immensly from the contributions of many people:

First, I would like to thank my parents, Hildegard and Michael Butz, for funding my residence here in New Zealand, which made this study possible in the first place.

I am particularly grateful for the support and supervision of Uwe Ring who was a patient listener in the past year and had always an open door. I am especially appreciative to the Mason Trust who funded my field campaigns in Otago.

I would also like to express my thanks to Nick Mortimer for his great help and hospitality at many times during my studies.

To Rob Spiers, Kerry Swanson, John Southward and Vanessa Tappenden thank you for your assistance and help with equipment and laboratory work. Thanks to Oceana Gold Ltd. for generous access to their land.

I am also especially thankful to my office mates Anja Müller and Monica Gowan for all the nice chats and help.

Many thanks to Elke Hanenkamp and Florian Büch for reviewing my thesis and for being such good friends.

During my residence in New Zealand I have learned many great people (no particular order): Robert, Justin, Stefan, Craig, Antje, Lim & Jin, Joe, Daniel, David, Michelle, Jimmy, Heather thank you all very much for making this experience as great as it was.

Table of Contents

CHAPTER ONE

INTRODUCTION

1.1. General Introduction

Shear zones are a common geological feature in Otago and often the focus of scientific and economic attention. This attention is essentially caused by the occurrence of recoverable amounts of gold. However, the shear zones also provide insights into past tectonic processes and may contribute to a better understanding of the genesis of a large part of New Zealand's south island.

The exploration for gold contributed immensly to the present-day knowledge about Otago's shear zones, especially in terms of their location and areal extend. In contrast, the concern for the gold concentrated the efforts more or less completely on its extraction neglecting the importance of the geologic and tectonic context of the shear zones.

The most prominent of those shear zones in Otago is probably the Hyde-Macraes Shear Zone (HMSZ) in eastern Otago. This shear zone is the host of the currently biggest goldmine in New Zealand and probably the best studied one in Otago. Although many data about the HMSZ itself exist, tectonic relationship between the HMSZ and its footwall remains largely unknown. Drillhole investigations of the mining company and the occurrence of brittle normal faults together with the juxtaposition of schist with different metamorphic grade lead to the suggestion that there is a low angle normal fault truncating the footwall of the shear zone. This normal fault is called the Footwall Fault.

This study focuses on the regional setting of the HMSZ, especially its Footwall Fault, in order to provide data on the tectonic and kinematic evolution of the Footwall Fault and the relationship of the latter with structures in its foot- and hangingwall.

1.2. Regional Geology

1.2.1. South Island

Much of New Zealand formed in a mesozoic subduction complex at the southern margin of Gondwana. The subduction of the pacific plate underneath Gondwana resulted in the accretion of sediments during the "Rangitata I" orogeny which ended in the Cretaceous. The accreted sediments together with the fore-arc sediments now confine the Eastern Province of the South Island and consist essentially of graywackes (Korsch & Wellmann 1988). The different parts of the Eastern Province are classified from NE to SW in miscellaneous tectonostratigraphic terranes: Torlesse, Caples, Maitai, Murihiku and Brook Street (figure 1.1). From these terranes, only Torlesse and Caples belong to the actual accretionary prism. The other terranes, Maitai, Murihiku and Brook Street, belong to the fore-arc of the subduction complex. Subduction related arc magmatism is represented by the Median Batholith, the remnant of the magmatic arc which follows the Brook Street terrane to the west and south. The Median Batholith was active between the Carboniferous and the Early Cretaceous which indicates almost 250 Ma of subduction and convergence (Kimbrough et al. 1994). The Western Province contains much older rocks which are considered to be part of the old Gondwana continent. These rocks are essentially of Cambrian to Devonian age and are locally covered by sediments from the Permian to Triassic. During their development in the "Tuhua" orogeny (c. 380-365 Ma) they have been exposed to high pressure/high temperature (HP/HT) metamorphism (Korsch & Wellmann 1988).

The most conspicuous geological feature of the South Island is the Alpine fault which is traceable along the western margin of the Southern Alps over approximately 2/3 the length of the South Island. The Alpine Fault is part of an oblique collision zone that confines the boundary between the west moving Pacific and east moving Australian plate. The subduction direction changes across New Zealand. To the northeast of the North Island the Pacific plate is subducted under the Australian plate. The obliquity of the plate boundary increases southwards where the Alpine fault represents a zone dominated by dextral strike-slip and reverse faulting (Pettinga et al. 2001). South of Fjordland the Alpine Fault transfers the strike-slip off shore towards a diametrical subduction with the Australian plate moving beneath the Pacific plate.

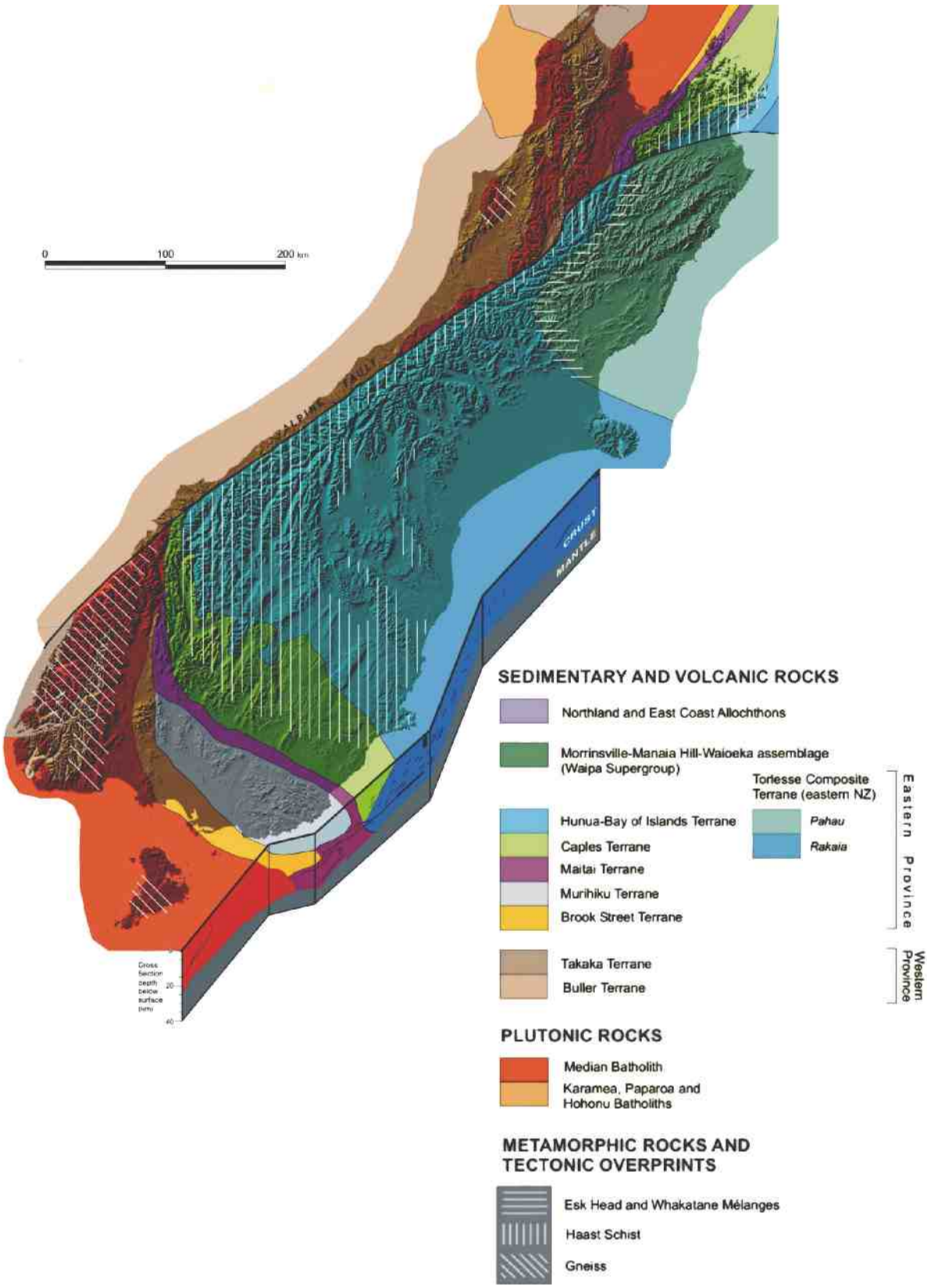

Figure 1.1: Tectonostratigraphic Terranes of the South Island (after Mortimer 2001)

1.2.2. Otago Schist

The Otago schist is a subdivision of the Haast schist which combines Otago-, Alpine- and Marlborough schist (figures 1.1/1.2a). It is located in the lower half of the South Island between the Livingstone and the Waitaki fault (figure 1.2b). To the north and west it passes into the Alpine schist. The areal extend of the schist has the shape of a two-sided arch and consists essentially of metamorphosed graywackes of different metamorphic grade. These metagraywackes belong to the Caples Terrane, Aspiring Lithologic Association (ALA, e.g. Craw & Norris 1991) and Rakaia (older Torlesse) Terrane and were deposited in the late Permian-Triassic. In the Jurassic to Cretaceous Rangitata I orogeny the Torlesse and Caples terranes were amalgamated. This introduced a regional metamorphism which formed the Otago Schist. Deeply buried parts reached the surface approximately 105 Ma ago during the initial rifting phase as indicated by the appearance of schist fragments in the Kyeburn formation, a sedimentary graben fill related to Albian rifting (Korsch 1988; Laird & Bradshaw 2004). However, the exhumation process is a subject of debate for about the past decade. Little et al. (1999) favor crustal thickening as a result of subduction related shortening and underplating until the Early-Cretaceous. They propose that this crustal thickening might have led to destabilistation of the wedge in the Mid-Cretacious causing syn-orogeny normal faulting in its rear (Little et al. 1999). Deckert et al. (2002) argued that strain data indicate extreme vertical contraction which would prevent overcritical tapering of the wedge, and thus rendering syn-orogeny normal faulting unlikely. Due to the first appearance of high grade schist fragments in the upper part of the Kyeburn Formation, Deckert et al. (2002) propose that deeper parts of the Otago schist could not be significantly exhumed and eroded before the development of the Kyeburn Formation. They therefore suggest that exhumation of the Otago schist is related to rifting throughout entire New Zealand in the Albian. This was accompanied by regional scale normal faulting creating a huge high angle fault system along the graben margin representing the younger equivalents of low angle structures in the inner part of the Otago schist (Deckert et al. 2002).

In stark contrast to these hypotheses, other authors (Forster & Lister 2003) relate the exhumation to crustal thinning caused by extensional tectonism in the Early-Cretaceous due to rollback of the pacific slab. This may have caused a switch from shortening to extension. This theory is based essentially on white mica Ar/Ar ages and the tectonic character of the Northburn shear zone in the Dunstan Range (Forster & Lister 2003).

Between 105 – 85 Ma significant erosion leveled wide areas of the South Island which resulted in an erosion surface which is often used as an indicator of the Late-Cretaceous paleosurface. Miocene to recent development of the Alpine Fault folded this surface and gave Otago the typical Basin and Range appearance (Jackson et al. 1996).

The metamorphic grade within the Otago schist belt increases from a prehnite-pumpellyite facies in the periphery to an upper greenschist facies in the center of the arch (Mortimer 2000). The greenschist facies rocks suggest peak pressures of about 8-10 kbar and temperatures of c. 350-400°C (Mortimer 2000). Common rocks in Otago are psammitic and pelitic grayschist, some greenschist, quarzite, very rare marble pods and ultramafic schist (Mortimer 2003). The monotonous Otago schist has been subdivided into various subdivisions called Textural Zones.

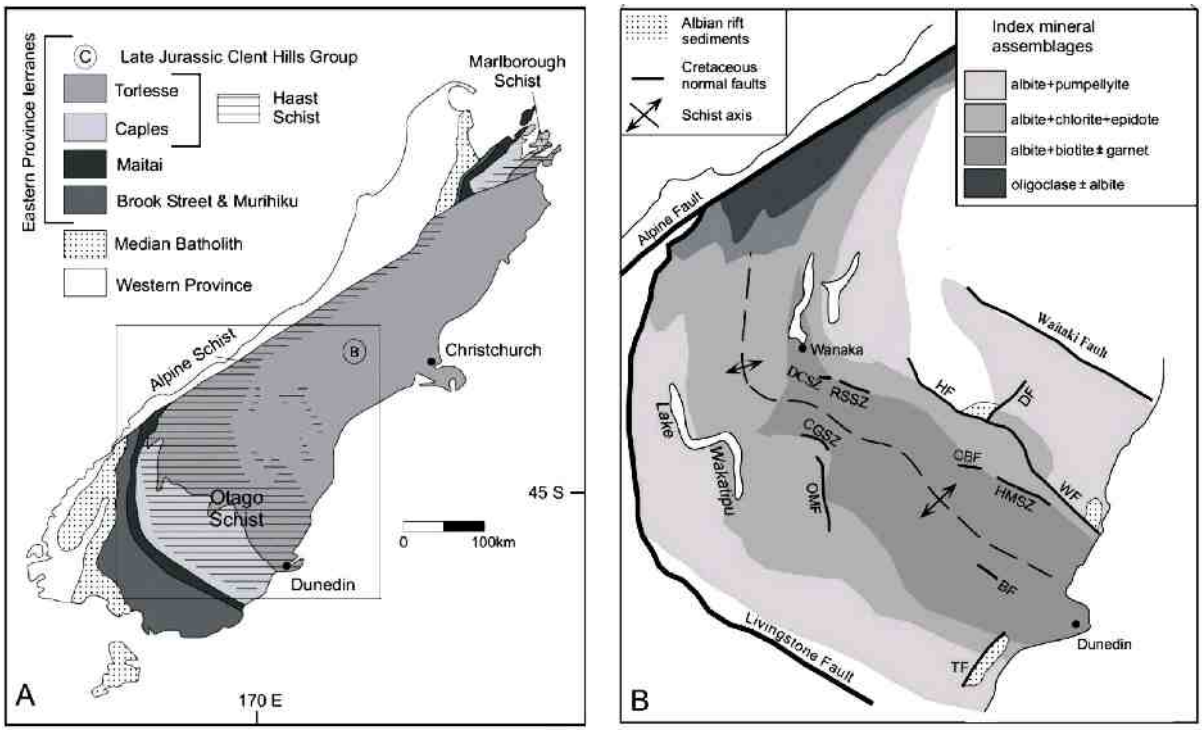

Figure 1.2: A) Simplified geologic Map of the South Island showing Eastern Province basement terranes, New Zealand (after Mortimer 2000). B) Distribution of metamorphic grade in the Otago schist. Also showing Cretaceous Faults and Albian rift sediments. HF, Hawkdun Fault; DF, Danseys Pass fault; WF, Waihemo Fault; HMSZ, Hyde-Macraes shear zone; BF, Barewood Fault system; TF, Titri Fault; OMF, Old Man Fault; CGSZ, Cromwell Gorge Shear Zone; RSSZ, Rise and Shine Shear Zone; DCSZ, Devils Creek Shear zone; CBF, Capburn Fault.

1.2.3. Textural Zones

The Textural Zonation system (TZ I – TZ IV) was originally introduced by Bishop (1972) and is based on a petrographic classification scheme established by Hutton & Turner (1936). Hutton & Turner established a system of four Chlorite Subzones which distinguished the schist by metamorphic quartz grain size relative to the parent rock and degree of textural reconstitution. When Bishop reviewed this system in 1972 he took into consideration that rocks of the first two subzones may not occur under greenschist conditions but may belong to a lower metamorphic facies (Turnbull et al. 2001). Furthermore, he recognized that mineralogical and textural criteria should be taken into account separately. On that basis Bishop (1972) modified the Hutton & Turner Chlorite scheme into four textural zones (TZ) with special regard to field application. The system distinguishes six types of schist considering different features like the protolith, grade of foliation, segregation and shape (including fissility) in hand specimen and at outcrop scale (table 1). Since then the Bishop system was modified several times by various authors (table 1). The last modification was made by Turnbull, Mortimer and Craw (2001) (table 2). They combined TZ IIIB and TZ IV to a new TZ IV and TZ IIIA became TZ III. TZ I, IIA and IIB were largely unchanged, although the criteria for their recognition have been modified (Turnbull et al. 2001). The new system is based on criteria such as metamorphic white mica grain size, also considering their length and habit, foliation features, quarz veins/segregation features, thin section textures, special features of the Otago schist and applicable rock names (table 2). In this thesis the scheme after Turnbull et al. (2001) is used to differentiate the schist unless stated otherwise.

Table 1: Summary of old schist definitions after Turnbull et al. 2001

Hutton & Turner (1936)	*Chl Subzone*	*HS foliation*	*HS segregation*	*TS grain size*	*TS textures*
	1	None	None	Average 0.3 mm, up to 1.5 mm (clastic)	Recrystallisation of clastic grains
	2	Distinct	None	Clastics reduced in size and number	Clastic structure partly obliterated
	3	Perfect	Distinct	0.1-0.15 mm xenoblastic	Some quartz feldspar augen
	4	Yes	Coarse (up to 10 mm)	0.2-0.4 mm (up to 1mm) xenoblastic	Grain size much coarser than in Chl 3
Bishop (1972)	*Textural Zone*	*HS foliation*	*HS segregation*	*HS Shape*	*Field outcrop and fabrics*
	I	None	None	Does not split in any preferred direction	Outcrops massive and blocky
	IIa	Slight	None	Tendency to split parallel to foliation	Platy outcrop; mica sheen and intersection lineations
	IIb	Penetrative	None	Parallel sided	Controlled by foliation; rootless folds in bedding
	IIIa	Strong	Incipient: 1-10 mm long	Foliation surfaces slightly rough	Steep dip gives lines of outcrop; lineations common
	IIIb	Strong	1-2 mm thick, >10 mm long	-	Mineral or lithologic lineations ubiquitious
	IV	Strong	> 2 mm thick	-	-
Norris & Bishop (1990)	*Textural Zone*	*TS detrital quartz*	*TS metamorphic quartz*	*TS metamorphic micas*	*TS Veins*
	I	Little deformation	-	Unoriented authigenic sericite	-
	II	Still well preserved, subgrains developed	Extensive strain shadow Overgrows, commonly amalgamated with detrital grains	Oriented: dark solution seams around detrital grains	Veins cut clasts and are rotated and boudined in matrix
	III	More subgrain development	Growth and homogenisation of adjacent strain shadow laminae	Mica fabric coarse and intergrown with quartz	Many segments of rotated veins lead to segregated schist

Note that in Bishops (1972) original definition, and in nearly all subsequent references, segregation thickness in TZ IIIB was given incorrectly as 0.1-0.2 mm. HS: hand specimen; TS: thin section.

Table 2: Modification of Textural Zones as presented in Turnbull et al. 2001.

Textural Zone	Metamorphic white mica thickness, length, habit	Hand specimen foliation features	Hand specimen quartz vein/segregation features	Thin section tectures	Special Otago schist features	Applicable rock names
I	<5 µm thick/<75 µm long. Naked eye and hand lens reveal only coarse detrital micas	None, or only a spaced fracture cleavage	Local veins	Detrital textures only; no preferred orientation of metamorphic white mica	-	Sandstone, mudstone, greywacke, argillite
IIA	<5 µm thick, <75 µm long. Pelites have a matt black colour and can be slaty. Naked eye and hand lens reveal only coarse detrital micas	Weak-mod, anastomosing, penetrative, stronger in fine-grained rocks. Bedding still dominates over cleavage. Hand samples break into wedge-shaped blocks	Local veins	Detrital quartz grains have undulose extinction. Weak preferred orientation of metamorphic micas	-	Foliated greywacke, semi-schist, slate
IIB	5-15 µm thick,<75µm long. Individual micas not visible through a hand lens. Pelites black but with distinct sheen, psammites grey	Strong, penetrative. Cleavage dominates over bedding which is transposed. Psammite-pelite contrasts still easily resolved through colour differences. Hand specimens break into parallel-sided slabs	Appearance of flattened detrital grains may be enhanced but there is no foliation parallel segregation. Veins locally common but these cut foliation at an angle	Detrital quartz grains still recognisable but mainly composed of subgrains. Strong preferred orientation of mica in anastomosing folia	F2 folds may develop and veins may be locally important. Pumpellyite-out isograd is within TZIIB	Psammitic or pelitic semi-schist, phyllite, slate
III	15-25 µm thick, 75-125 µm long (very fine sand size). Individual mica grains visible through hand lens, both pelites and psammites are silvery grey	Strong and penetrative but undulating on mm scale, less perfect than IIB. Where seen, psammitic-pelitic contacts are still sharp at mm scale.	Distributed foliation-parallel quartz lenses <1 mm thick, throughout rock. Different generations of mm-cm thick veins ubiquitious	Detrital quartz and mica unrecognisable; quartz and mica in rock are approximately equigranular and form sub-mm segregations	Maximum textural grade of volcaniclastic Caples psammites. F2 folds can start to dominate. Garnet-biotite isograd is within TZ III	Quartzofeldspathic schist, greyschist
IV	25-50µm thick, 125-500 µm long (fine-medium sand size). Individual mica grains clearly visible to naked eye	Strong and penetrative, undulating on mm-cm scale.Psammitic-pelitic contacts blurred at mm scale, but resolvable at cm scale.	Essential and widespread quartz veins/segregations >1 mm thick, mainly polydeformed quartz veins	Adjacent quartz and mica grains merge into segregations and folia of variable thickness and length	Main foliation is S2	Quartzofeldspathic schist, greyschist, gneiss

1.3. Low angle normal faults

In the last years the occurence of low angle normal faults (LANF) in Otago has been suggested in several places usually in connection with a semiductile shear zone. Although evidence through field data is quite rare and it is not fully understood when and how those faults formed. The scope of this chapter is to give an overview of low angle normal fault mechanics and characteristics as well as to present a few models which are capable of explaining their formation.

Low angle normal faults are a special type of fault (Axen 2004). They are characterised by a low dip angle of <30° and a large areal extend (10 km scale). LANFs first came into debate when they were discovered in the Basin and Range province in the United States in the late sixties to early seventies. The problem with this type of fault is that it can not be explained by standard fault mechanical theory. According to this theory, the friction on the fault surface in a brittle regime becomes too high if the angle of the dip is below 30°. This, and the fact that earthquakes are quite rare at low-angle normal faults, started a debate on how LANFs can develop in the first place (Axen 2004). Several models are capable of explaining the existence of low angle normal faults. All of them require large scale crustal extension.

(1) Block rotation.

In this model two crustal scale faults evolve parallel to each other in an extensional regime. The developing „block“ between those two faults rotates slowly into a horizontal position which changes the dip of the two faults to a lower angle (figure 1a).

(2) *A cordilleran style metamorphic core complex.*

This type of core complex may develop when a large scale moderately dipping fault with a listric shape is cutting through the brittle crust. On that fault, synthetic faults may develop en echelon in the hangingwall. Due to crustal thinning isostatic rebound lifts up the footwall changing the listric shape of the fault into a domal shape (figure 1b). Eventually, this process rotates the fault into a gentler angle and causes parts of the fault to dip into the opposite direction (figure 1b).

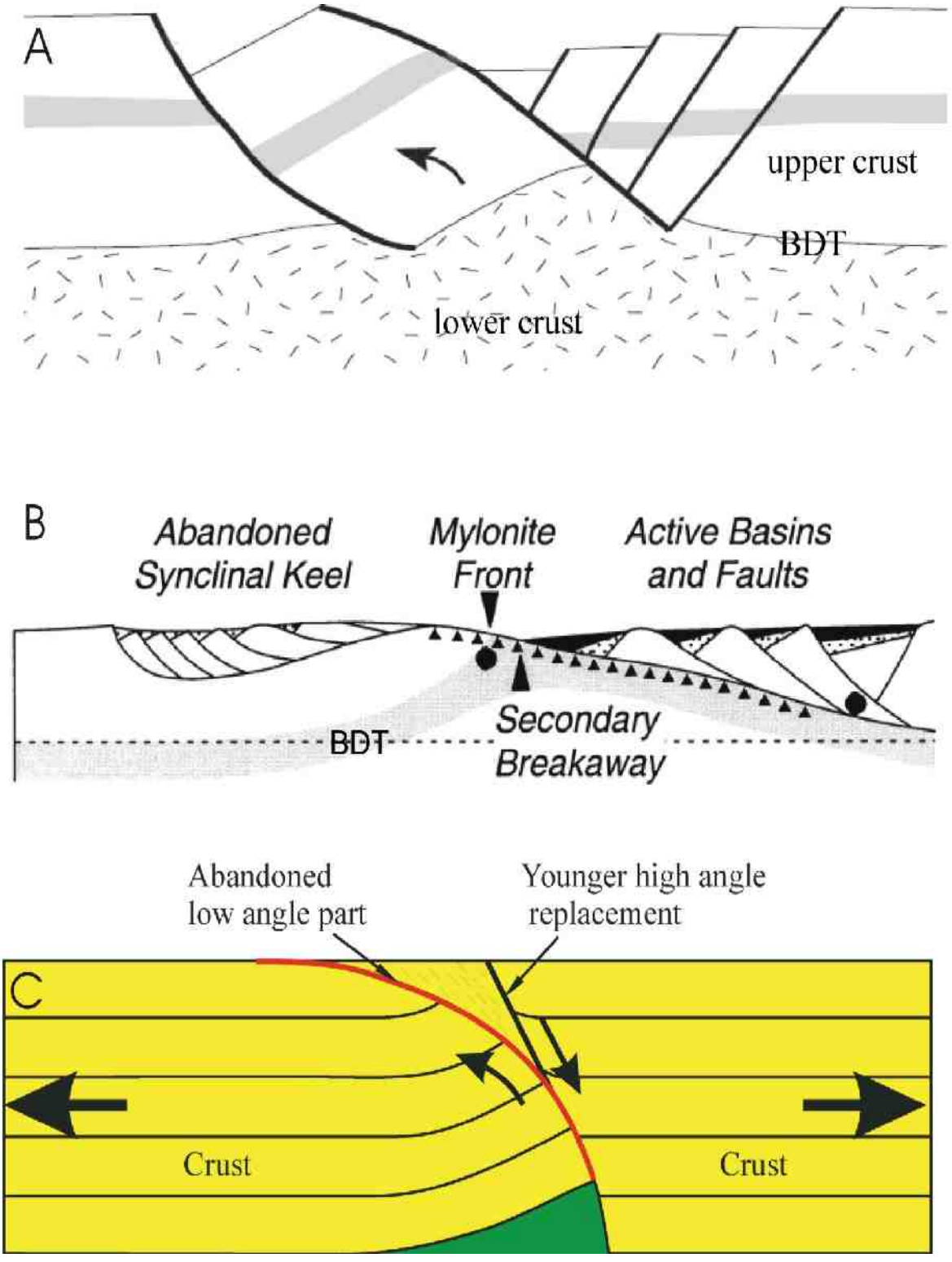

Figure 1.3: Models explaining the development of low angle faults. A) Block Rotation B) Metamorphic Core Complex (Axen 2004) C) Rolling Hinge. See text for explanation. BDT, brittle-ductile transition.

(3) *Rolling hinge*.

In the rolling hinge model, extension produces a large normal fault which cuts through the crust. This fault is a moderately to steeply dipping feature with a convex shape. Due to isostatic rebound the footwall rolls up on the fault surface. The rotation changes the dip angle of the fault to a lower angle the nearer it comes to the surface. Eventually, the shallower part will be abandoned if the angle becomes too shallow and a steeper fault will develop in dip direction (figure 1c).

1.4. Identification of Crustal Extension in Orogens

Extensional structures in orogens have been reported all over the world (e.g. western USA, Himalayas, etc.). However, it is not trivial to tell whether those structures are related to true crustal extension or not. A structure that shows extensional character relative to a previous layering does not necessarily indicate extension relative to the crust (Wheeler & Butler 1994). To identify true crustal extension, some criteria like those described by Wheeler & Butler (1994) have to be taken into account.

(1) Structural criteria

This criterion requires that relative movement of hangingwall and footwall can be obtained from offset of marker horizons or other kinematic indicators. “If the shear zone was related to crustal extension then, as it is followed in a direction opposite to that of the hangingwall transport, it should ultimately intersect the Earth's surface as it was at the time of movement, even if the shear zone was later folded” (Wheeler & Butler 1994, page 1024). In contrast to refering to the layering this criterion is less ambiguous. Layering can only be used if it is known to be parallel to the paleosurface at the time of shear zone activity.

Deposition can cause problems for this criterion due to burial of the intersection where the fault cuts the paleosurface. Another problem arises from later structures which intersect the shear zone because they may move key parts and thus destroying the information. Therefore, the ability to trace the entire structure is very important to determine the structural regime in which it developed.

(2) Metamorphic criteria

"If the shear zone was related to crustal extension then the pressure recorded by rocks in the footwall should, during shear zone movement, decrease faster than that recorded in the hangingwall" (Wheeler & Butler 1994, page 1025). It is not enough to relate a normal sense metamorphic break (low pressure rocks above high pressure rocks) as an indicator for crustal extension, because in zones where high pressure rocks have been thrust over low pressure rocks a later normal fault would still have a reversed stacking order. Problems also arise, when the metamorphism in hangingwall and footwall occurred at different times or when the footwall is much older than the shear zone. The latter could mean it was exhumed prior to shear zone activity.

(3) Geochronological criteria

For specific isotopic systems the closure temperature can be used to record different ages in hangingwall and footwall (Wheeler & Butler 1994). "If the shear zone was related to crustal extension, and the isothermal surfaces paralleled the Earth's surface then, along part of its length, the shear zone would juxtapose rocks with old cooling ages in its hangingwall against rocks with young ages in its footwall" (Wheeler & Butler 1994, page 1026). This argument depends among other things on a rather stable temperature field, because heat transfer between hangingwall and footwall may cause a partial reset of the isotopic system.

1.5. Shear Zones in Otago

1.5.1. Hyde-Macreas Shear Zone

The Hyde-Macraes shear zone is located in eastern Otago near the village of Macraes Flat (figure 1.2). The shear zone is gold-bearing and mining has begun already in the 19th century from 1862 until 1950. During this time miners produced c. 15,000 Oz gold and over 1,000 tons scheelite (Teagle et al. 1990). Primary target of the historic miners were metre-scale gold-bearing quarz veins which they locally exploited similiar to other gold deposits in Otago (Petrie & Craw 2005). After commencing the production at Round Hill in 1984 the mining is driven nowadays at a very large scale. Not only quarz veins are exploited but gold is also extracted from hydrothermally altered schists within the shear zone (Petrie & Craw 2005). With an estimated resource of over 100 tons and a current production rate of c. 5.7 t of gold per year the Macraes mining project is the largest in New Zealand (Mitchell 2005). Mining at other deposits in the Otago region is only marginal and is mainly confined to historic workings.

The Hyde-Macraes shear zone is a generally NW striking, NE dipping feature with a dip angle of less than 20° and is parallel to subparallel to the (hangingwall) foliation. Structurally the HMSZ is complex and originated as a thrust duplex system that passed the ductile-brittle transition (Teagle et al. 1990). This period of crustal shortening was followed by a period of extension (e.g. Teagle et al. 1990; Craw 2002). The mineralised thrust-type shear zone is restricted to Textural Zone III rock and has usually a well defined roof fault called the hangingwall shear and floor fault called footwall shear (Mitchell 2005). The schist in between is called intrashear schist. The thickness of the intrashear schist varies from 2 - 125 m (Teagle et al. 1990) and is traceable for ~30 km (Petrie & Craw 2005).

Intrashear schist of the HMSZ has undergone hydrothermal alteration and mineralisation through mixing with water rich fluids during the latter stages of lower greenschist facies metamorphism when the schist passed through the brittle - ductile transition. This happened at about 300° and at c.10km depth (De Ronde 2000). Because of that alteration, the intrashear schist is generally darker than the surrounding schist due to addition of hydrothermal graphite that accompanied gold and sulfide mineralisation (Petrie & Craw 2005). Other alterations include the substitution of titanite by rutile or epidote that was replaced by siderite, calcite and kaolinite as well as the recrystallisation of muscovite and chlorite.

The lower shear is trunchated by a regional scale normal fault that is responsible for the juxtaposition of TZ III schist above TZ IV schist (e.g.: Craw 2002; Mitchell 2005).

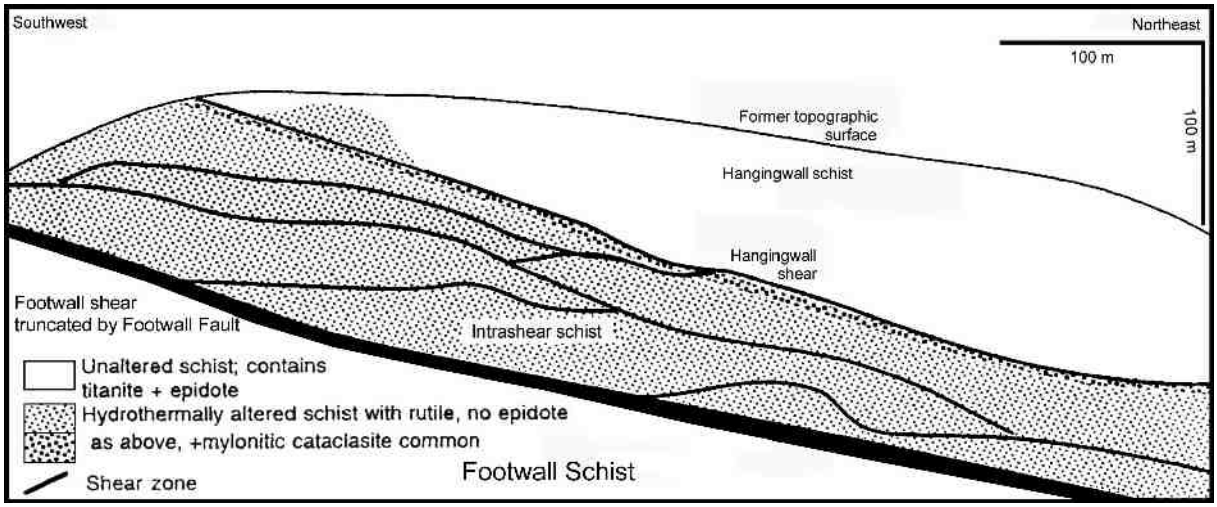

Figure 1.4: Cross section through the HMSZ illustrating terminology. (modified after Angus 1993 and Craw et al. 1999)

1.5.2. Rise and Shine Shear Zone

The Rise and Shine shear zone (RSSZ) is a low angle feature that crops out to the NW along strike of the HMSZ (Figure 1.2). Like the Hyde-Macraes shear zone the RSSZ startet as a shortening structure in a ductile environment (Cox et al. 2006). The shear zone is also gold-bearing but historic workings only produced a total of 393 oz (MacKenzie 2005). Nevertheless, this resulted in extensive exploration in the Dunstan Range over the past 20 years but has failed to determine recoverable amounts so far (Cox et al. 2006).

The shear zone is situatated in TZ IV rock and has a thickness of up to 50 m (MacKenzie 2005). Drillhole intersections and regional outcrops indicate a dip angle between 20° and 50° to the NE (MacKenzie 2005). The feature dips parallel to subparallel to the regional (host schist) foliation (Cox et al. 2006). The hangingwall shear is well defined and truncated by the Thompsons gorge fault (TGF), a normal fault that juxtaposes TZ III schist above TZ IV schist (MacKenzie 2005; Cox et al. 2006). The offset of this fault is supposed to be on a scale of several kilometres (Deckert et al. 2002; MacKenzie 2005; Cox et al. 2006). Because both the HMSZ and the RSSZ show the same kind of late brittle-ductile to brittle normal reactivation, it gave rise to the suggestion that normal faulting may be related (e.g. Deckert et al. 2002). The thrust features, on the other hand, show some differences: (1) The shear zones are situated in different structural settings (MacKenzie 2005; Cox et al. 2006). The RSSZ is hosted by TZ IV schist whereas the HMSZ is hosted by TZ III schist (MacKenzie 2005; Cox et al. 2006). (2) There are geochemical differences, i.e. the RSSZ is enriched in AS, U, Th and rare earth elements, whereas the HMSZ is enriched only in As and Cr (MacKenzie 2005; Cox et al. 2006).

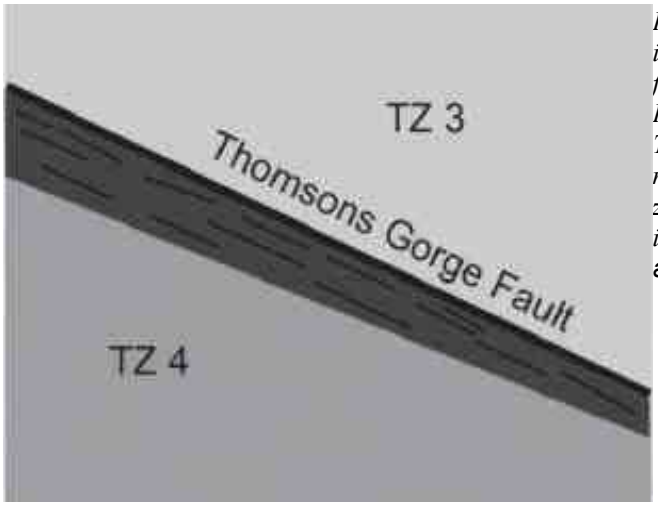

Figure 1.5: Scheme of the RSSZ, illustrating the textural change from TZ IV in the footwall to TZ III in the Hangingwall of the Thomsons Gorge Fault. The mineralised Rise and Shine shear zone (dark grey area under TGF) is hosted by TZ IV schist (Cox et al. 2006.)

1.5.3. Other Shear Zones

Apart from the HMSZ and RSSZ there are several other important shear zones in the Otago schist: e.g. the Cromwell Gorge Shear Zone (CGSZ) and the Northburn Shear Zone (NBSZ) (Figure 1.2). The Cromwell Gorge Shear Zone is located southwest of the RSSZ and recognised as a southwest-dipping, approximately 400m wide system of normal faults. The most prominent fault of this system is the for c.15 km traceable lower CGSZ (Deckert et al. 2002). Deckert et al. (2002) determined a southwest oriented normal sense of shear and suggested an overall listric shape.

The Northburn shear zone (NBSZ) is a north-south directed ductile normal sense shear zone in the southwest of the Dunstan Range (Forster & Lister 2003). White mica Ar/Ar ages suggest that the shear zone began to operate at c.110 Ma (Forster & Lister 2003). The NBSZ cuts through the east-west trending ductile Devils Creek Shear zone (DCSZ) which is trunchated by low angle faults (Forster & Lister 2003).

1.5.4. Waihemo Fault

The HMSZ dips NE and is truncated 10 km further to the NE by the steeply NE-dipping Waihemo Fault. Adams & Graham (1997) placed the time of mineralisation in the HMSZ between 158 Ma – 132 Ma. This constrains the time for the normal reactivation of the HMSZ, which resulted in the Footwall Fault, to an age <130 Ma. Age determinations for the Waihemo Fault (figure 1.2), place the time of its development at ~112-113 Ma (A.Tulloch, pers. com. 2007). These determinations were made by Ar/Ar dating of biotites in tuff in the Kyeburn Formation and by dating of zircons within the shag ignimbrite. Both the Kyeburn Formation and the Shag ignimbrite are considered to coincide with the development of the Waihemo Fault. Considering these ages, the time of the normal activation of the Footwall Fault lies between 112 and 130 Ma.

1.6. Scope Of Study

1.6.1. Relevance Of Study

The debate on the Cretaceous period of extensional tectonism in the Otago schist has increased. In the last decade different opinions developed about how and when the Otago schist was exhumed. This increases the need for additional structural data reflecting the relationship between low angle semiductile shear zones and adjacent regional structures. Deckert et al. (2002) proposed a common history of normal faulting in the Rise and Shine shear zone and the Hyde-Macraes shear zone at the northern periphery of the albite-biotite-garnet zone of the Otago schist. Although, a direct relationship between the two shear zones can be ruled out the question remains whether or not the two low-angle normal faults (Thompsons Gorge Fault and Footwall Fault) may be part of a New Zealand wide phase of Albian rifting. However, this requires new data regarding the relationship of the HMSZ and its Footwall Fault.

Structural mapping of foliation and kinematic indicators along the Deepdell Creek valley including a detailed cross section through the hangingwall and the footwall schist should reveal new aspects concerning the development of the Footwall Fault and its relationship to the HMSZ. At that scale this was never done by previous workers because these studies usually concentrate on gold mineralisations within the shear zone and were done along-strike. So, this study should provide new information for the formation of the biggest shear zones in Otago and may give new hints about the overall development of the region.

1.6.2. Thesis Objectives And Methodology

The main objective of this thesis is to determine the relationship of the Footwall Fault and the adjacent Hyde-Macraes Shear Zone and to use this information to reveal the geological history of both structures.

This objective has been achieved by the following methods:

- Literature review of articles concerning fault mechanics, local structures and the regional context.

- Detailed mapping of structural and petrological features across-strike of the Hyde-Macraes shear zone in the Deepdell creek transect using GPS and 1:50,000 topographical maps.

- Illustration of deformation processes in the low-angle normal fault (Footwall Fault) and its relationship to associated high angle faults.

- Detailed thin section investigations of shear bands.

1.7. Thesis organisation

Chapter One introduces the reader to the subject and provides background information on low-angle fault mechanics and crustal extension. Important regional structural features are described and the regional geology is presented. The relevance and scope of study are discussed and the methodology is outlined.

Chapter Two introduces the study area, gives background information on characteristical structural features to be found in the field and presents the data collected by structural mapping. The data will then be discussed and a model for the region will be presented.

Chapter Three is on the analysis of collected hand specimens, focussing in particular on shear bands. Also petrological aspects of the schist types will be presented.

Chapter Four summarizes the main findings, discusses pros and cons and presents suggestions for further studies.

CHAPTER TWO

Structural Mapping

2.1. Introduction

Mapping is the most important requirement to obtain field data and has been thoroughly carried out for the area around the historic battery near Macraes Flat as well as for the Deepdell creek valley (figure 2.1). Objectives of the field campaigns were to map changes in the orientation of the foliation, to map structural features such as faults, folds and kinematic indicators related to the Footwall Fault and change of textural zones to determine the shear zone boundaries. Data was obtained by using a Clar compass which measures dip direction and dip angle of planes. This notation will be used throughout the thesis unless indicated otherwise. Whenever possible slickenlines (groove lineations on slickensides) and/or stretching lineations (as expressed by mineral elongation and stretched quartz aggregates) were measured on foliation planes. Particularly in the hangingwall, it was not always possible to measure lineations due to the very fine grain size of the TZ III schist. However, the TZ IV schist in the footwall has a larger grain size which made it easier to obtain lineation data.

Figure 2.1: Airphoto showing the study area near Macraes Flat centered on the Round Hill pit, Macraes mine. Source: Google Earth, 2006

2.2. Background to Characteristic Structural Features in the Study Area

2.2. Shear Bands

Shear bands are small zones of concentrated shear which transect a mica preferred orientation (cleavage) at a low angle (figure 2.2). Two kinds of shear bands can be distinguished: c-type shear bands (part of a so called C-S fabric) and c'-type shear bands (part of a so-called C-C' fabric). The abbreviations C and S stand for “cisaillement” which is French for shear and “schistosité”, the French word for foliation.

In a C-S fabric (figure 2.2a) the foliation (S-planes) is transected by planar shears (C-planes). C-type shear bands in a C-S structure are parallel to the shear zone boundaries and develop early during shear zone activity where both foliation and shear bands form during a single event of deformation. The growth of C-S fabrics may continue until the shear zone stops its activity. C-S fabrics are especially common in deformed granites with medium-grade ductile shear zones. C-type shear bands are useful kinematic indicators because the S-foliation always points up the direction of shear.

C'-type shear bands usually form at a low angle to the shear zone boundaries. This angle lies between 15 to 30°. They are generally anastomosing, short and wavy and cut through an older (mylonitic) foliation (C-plane) by deflecting that foliation exactly like foliation curvature in a large scale shear zone (figure 2.2b). This type of shear band is expected to develop at a late stage during shear zone activity when the preferred mica orientation already exists. C-C' fabrics are most common in micaceous mylonites. Although their relationship to the strain field is not fully understood they are very good shear sense indicators because they dip always in the direction of the imposed shear (figure 2.2b). As there is also a component of normal sense displacement of the C-planes along the C'-surfaces, the latter develop parallel to the maximum extension direction within a shear zone. Although c'-type shear bands develop late in a ductile shear zone, the environment in which they develop is still ductile and exceeds temperatures of 300°C where quartz can be recrystallised.

Within this thesis the terms “shear bands” and “shear band cleavage” will be used referring to the C'-type shear bands as only those were found during the field campaigns.

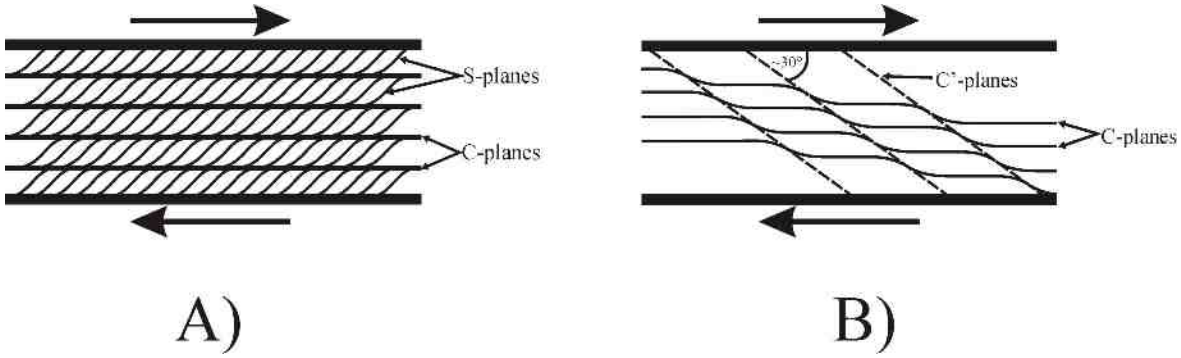

Figure 2.2: Schematic figure of C-S and C-C' structures. A) C-type shear bands (c-planes) cut through a foliation but are parallel to the shear zone boundaries (heavy black lines). B) C'-type shear bands (C'-planes) crosscutting the shear zone boundaries at a low angle. C-planes have been displaced in a normal sense.

2.2.1 Brittle Faults and brittle deformation

Brittle normal faults are one of the most common features in the study area, especially around the shear zone boundaries. Brittle faults in general reflect the latest component of movement in the Hyde-Macraes Shear Zone or rather the Footwall Fault. Due to their internal relationships (e.g. conjugation or Riedel arrangements), brittle faults may allow conclusions about the orientation of the strain regime in which they developed. Also, the frequency of their occurrence may give hints about the overall deformation pattern in a region.

Brittle deformation in a rock occurs as a response to a critical amount of stress applied to the rock body. If stress is applied to any kind of material, the material will first react in an elastic manner. This means that material, that has been strained in this way, will fully recover to its original shape when the stress is gone.

A critical amount of stress has been reached when the material has been stretched or shortened too far to recover completely, meaning, that the atomic bonds which form the material will break. This can happen in two ways: (1) The rock will deform in a ductile manner, which means, the material does not fully loose cohesion or (2) the rock deforms in a brittle manner and breaks.

A ductile behavior describes a state where strain is distributed throughout a material in a way that does not require the formation of mesoscopic discontinuities (the cohesion of the rock mass stays intact). The rock seems to flow like a viscous fluid.

Cataclastic flow is one example for a brittle deformation that has a ductile behavior. In a cataclastic flow, many fractures occur on a microscopic scale and individual grains are dislocated and rotated at these fractures by frictional sliding. Mesoscopically, this process makes the rock look like its flowing like a viscous fluid.

Brittle behavior means the loss of cohesion in a material, and can therefore only occur when the ability of the material to respond elastically and/or plasically to a certain amount of stress is exceeded. The ability of stress to induce brittle behavior strongly depends on pressure. However, high temperatures are not required. In fact, brittle behavior does generally not occur at high temperatures.

A brittle fault is a surface that offsets two blocks of rock using mainly brittle deformation mechanisms such as cataclastic flow or frictional sliding. To introduce brittle faulting, a differential stress has to be applied because slip only occurs parallel to a shear stress. That means, that the fault plane can not be perpendicular to one of the principal stress axes sigma 1 and 3 and sigma 1 must not equal sigma 3.

Brittle faulting can occur in two ways: (1) by shear fracturing of an intact rock body and (2) by activation of an existing zone of weakness such as a prexisting fault, or a change of competency in the material such as bedding. In contrast to an intact rock body, a zone of weakness in a rock may cause slip to happen earlier.

2.2.1.1 Methods to Determine Strain Axes

(A) Conjugated Faults

Strain directions can be calculated by means of stereographic projections if certain requirements are met. The conjugation of two brittle faults with the same shear sense in which one merges into the other is one example how to determine the strain axes. First, the two great circles of the fault planes are plot into an equal area, lower hemisphere stereo net (figure 2.3). The point of intersection of both great circles is a linear that equals the intersection direction. This direction is considered to be the axis of medium strain (S 2). Since the strain axes compose an orthogonal coordinate system, the strain axes for maximum shortening and maximum extension are found in a plane perpendicular to S 2. Each of the bisectors between the two linears, at which this perpendicular plane crosses the fault planes, represents one of the remaining strain axes.

Depending on whether the angle is acute or obtuse it is S 3 (axis of maximum shortening) or S 1 (axis of maximum lengthening), respectively. To be able to apply the technique it is crucial that the faults are indeed conjugated. This means that they must have formed during the same deformation event, must have the same sense of shear and the directions of transport must be approximately opposite. Furthermore, the angle between the faults should be high (~60°).

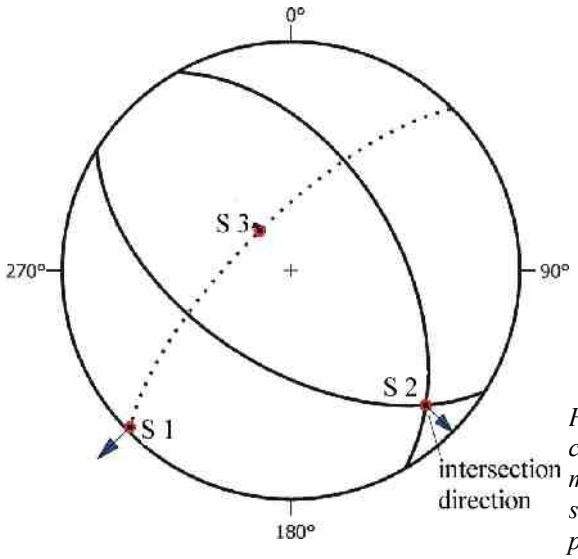

Figure 2.3: Determination of strain axes with conjugated faults. S 1 represents the direction of maximum extension, S 3 the direction of maximum shortening. Dashed great circle is the plane perpendicular to S 2.

(B) Riedel Arrangements

Another method to estimate strain axes is given by Riedel shear arrangements. Riedel shears are subsidiary shears which form at a certain angle to the main shear plane. In a Riedel arrangement, as it is defined by the Coulomb fracture criterion, two different subsidiary shears are distinguished: R-shears and R'-shears (figure 2.4). R-shears develop synthetically to the main shear direction at an angle of c.15°. R'-shears develop at an angle of c. 75° antithetically to the imposed shear having a movement opposite to the shear direction. The main shear is defined as a plane of pure shear stress which locates S 3, the axis of maximum shortening, per definition at an angle of 45° to the direction of shear. This means that S 3 is always oriented at an angle of c. 30° between R and R'. With an increase of deformation R-shears may be rotated to smaller angles which results in another subsidiary shear plane: the P-shears.
If either or more than one of these three shears can be identified in an outcrop it is possible to give an estimation of the direction of the strain axes. It is not possible to locate the exact positions of the strain axes by this approach because the process is usually much more complicated and would require more parameters to be calculated exactly. However, the more data about strain axes in a region is available, the better the mean axes will reflect the true strain field.

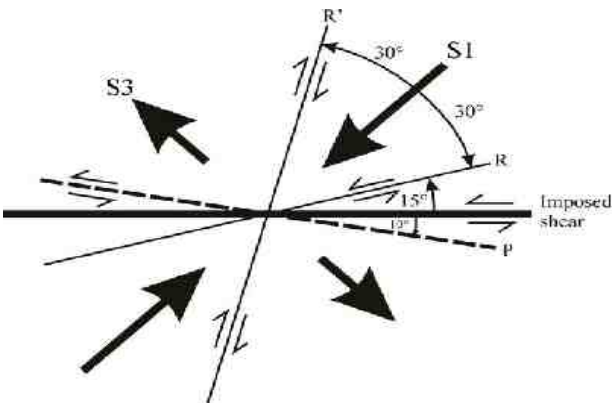

Figure 2.4: Illustration of the relationship of subsidiary fractures to the main shear as described by the Coulomb fracture criterion

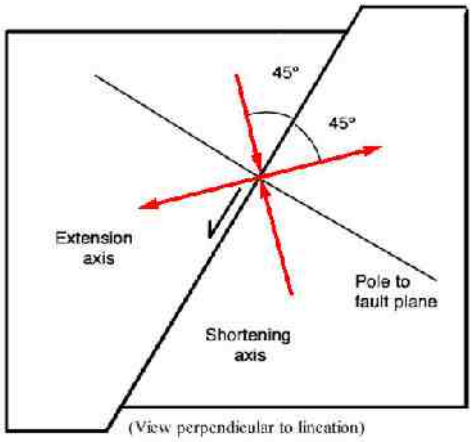

Figure 2.5: Bingham method to determine strain axes

C) Bingham Method

This is a very simple method using fault planes and lineations to determine the strain axes. This method assumes that the lineations give the direction of movement on the fault plane and that the axes for highest and lowest strain both occur at an angle of 45° to the slickenside parallel to the lineation. Per definition the intermediate strain axis S2 is perpendicular to the other axes.
By determination of the strain axes for several faults in the same area the mean strain axes can be calculated. In contrast to the conjugated fault method, this method has the advantage of using the direction of slip instead of an intersection direction to calculate the strain axes which produces better results. Furthermore, this method uses more than just two fault planes to estimate the strain pattern and calculates mean strain axes from all available axes, making the data more reliable.

All the methods discussed above give an estimation of the orientation of strain axes S 1, S 2 and S 3. It is often assumed that principal stress axes Sigma 1, Sigma 2 and Sigma 3 coincide with the strain axes.
Note that sigma 1 is the axis of maximum compressive stress and may coincide with strain axis S 3 which is the axis of maximum shortening. Likewise, Sigma 3 may coincide with S 1.
However, stress can not be measured directly in the field because stress is defined as force per unit area acting equally on a point from three perpendicular directions. This is valid if the point is in a state of equilibrium. If the three normal stresses increase or decrease at random, the stress in a point is not in equilibrium any more which results in shear stress that will eventually cause fracturing. This means that stress that causes faulting is a temporary condition that changes with time and usually changes when the fault becomes inactive. However, strain develops as a result of stress and leaves behind a pattern in the rock which can be measured. A deformation, however, consists of three distinct components: Strain, dislocation and rotation. Particularly, the rotational component reflects changes in the stress pattern. Therefore, it can only be assumed that the axes of stress and strain are oriented in the same way, if there is only small strain recorded in the rock and the deformation was non-rotational.

2.2.1.2 Foliation curvature as a kinematic indicator

On the basis of the behaviour of the foliation around a fault or shear zone, the sense of shear may be determined. When two blocks of schist move, the foliation is rotated passively reflecting the sense of movement. During normal movement the footwall can be viewed to be stable and the hangingwall slides down on a zone of weakness (fault). This movement displaces the foliation in a way that the footwall foliation adjacent to the zone of weakness is dragged down in the direction of movement. The hangingwall foliation shows the reverse pattern (figure 2.6a).

In a reverse or thrust sense of movement the foliation of the footwall will be dragged up, again pointing into the movement direction (figure 2.6b).

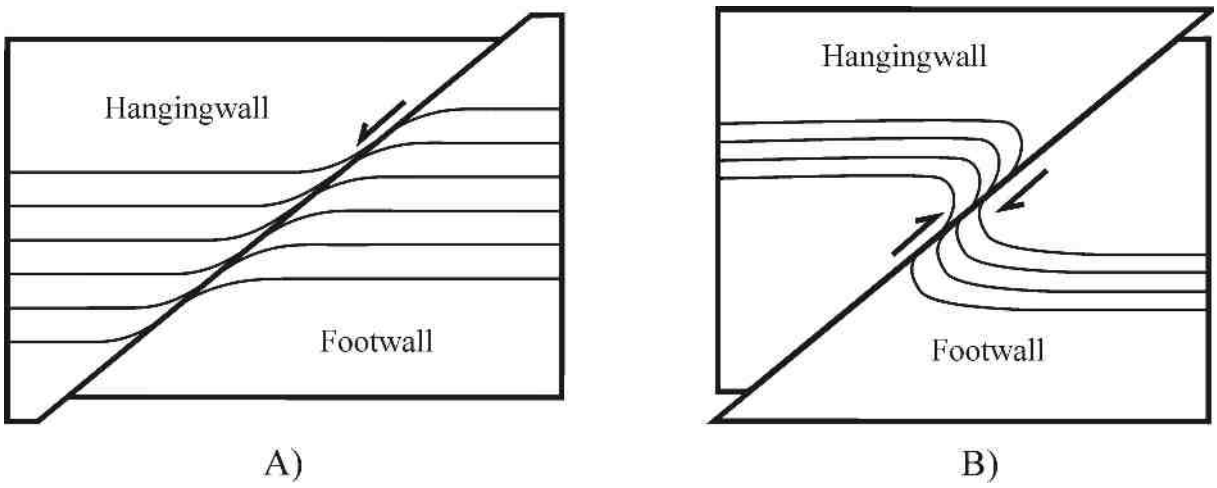

Figure 2.6: Deflection patterns for foliation in faults. A) normal sense B) Thrust/reverse sense

2.2.2 Kink Folds

Kink folds are commonly very small asymmetric folds which develop predominantly in finely laminated rocks. They are characterised by their straight limbs and sharp hinges (figure 2.7). Generally kink folds form due to displacement of individual foliation laminae. There are four different kinematic models describing kink fold formation. In the first model (figure 2.8a), the kink band develops around a line perpendicular to the lamination. Clockwise rotation from one end of this line and counterclockwise rotation from the other end forms the kink band boundaries. This changes the kink angle (κ) to a higher value the further the kink band grows. In the second model (figure 2.8b) this line is not perpendicular but oblique to the foliation and the kink band boundaries migrate into the undeformed material. In contrast to the first model, the kink angle stays constant.

The other two models (figure 2.8c/d) define the kink band boundaries as distinct shear zones on which the displacement occurs: (C) The kink band width stays constant during the process of kinking, however, the lamination within the band will first be decreased in length and increased in thickness and then decreased in thickness and increased in length. The kink angle also increases during this process. The last process (D) forms a kink fold by rigid rotation of the laminations. In this case the length of the lamination within the kink band boundaries stays constant. Thus, the width of the kink band increases and the volume increases which opens spaces between the individual laminae. When the angle yk reaches a certain degree the spaces will start to close. When yk=y the spaces are fully closed and the kinking process is finished and can not proceed any further.

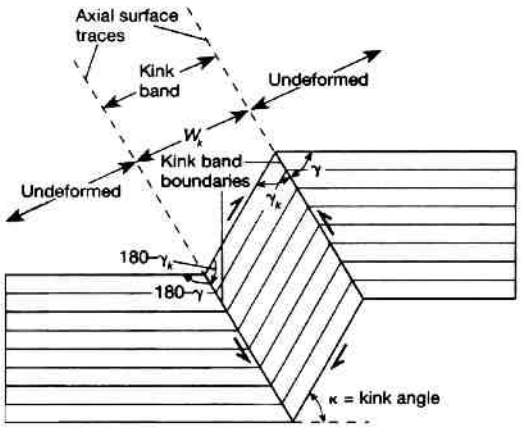

Figure 2.7: Scheme of a kink fold explaining basic terminology. Source: Twiss & Moores: Structural Geology

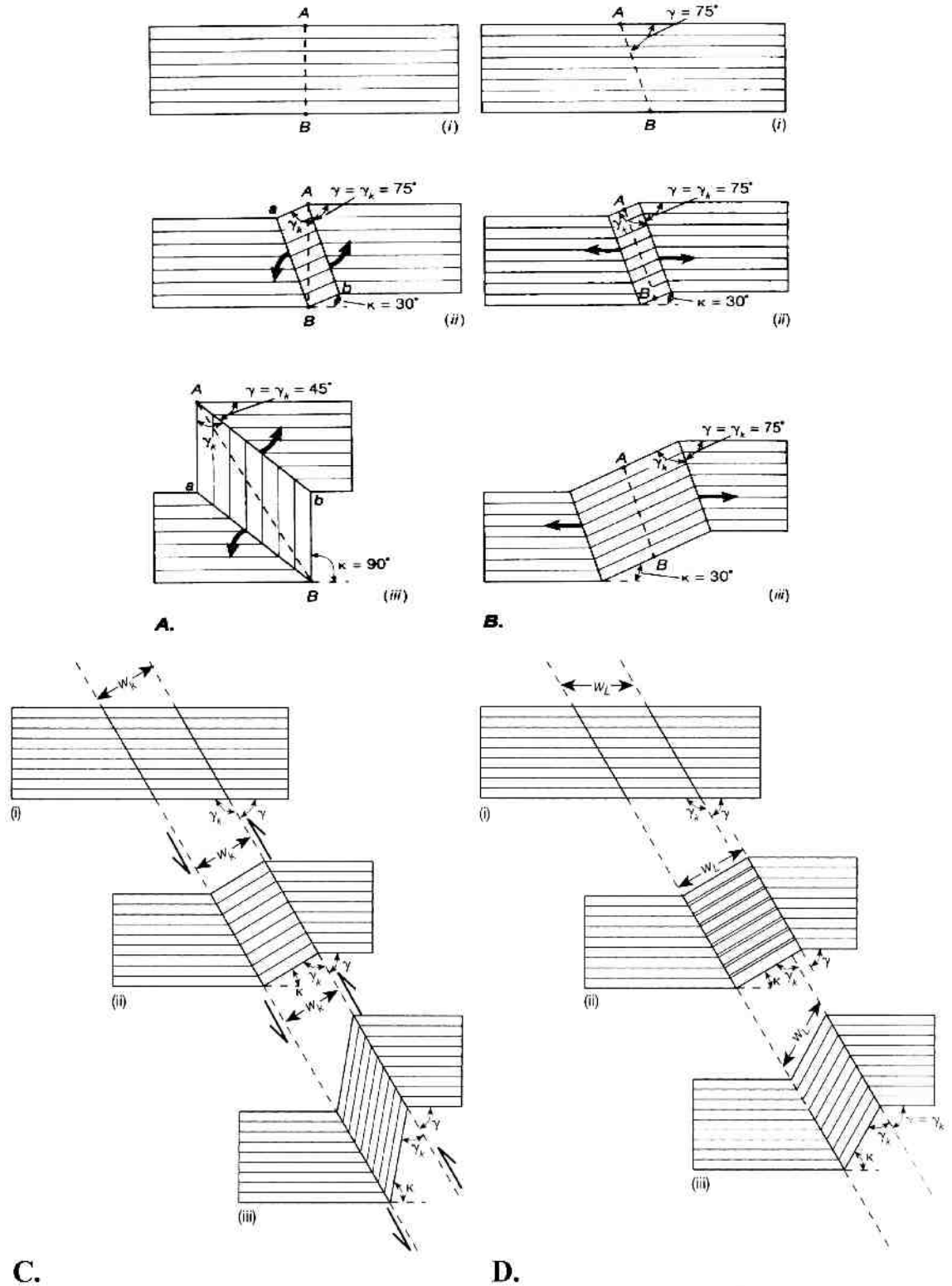

Figure 2.8: Scheme illustrating four different models of kink development: A/B development by migration of kink band boundaries into undeformed material; C/D, Kink band boundaries are distinct shear zones. A) Migration of kink band boundaries through rotation starting from a line perpendicular to the laminae. B) Migration by extension of the laminae considering a starting line oblique to the individual laminae C) Kink band width W_K stays constant during the process. D) The lamination length W_L between the kink band boundaries stays constant during kinking. Source: Twiss & Moores: Structural Geology

2.3. Data

In the following section the results of the structural mapping will be presented. Starting with the footwall of the Footwall Fault, there will be a short general introduction to the foliation pattern. After that the individual outcrops will be presented. Outcrops of the footwall have arabic numbers (1,2,3...), outcrops of of the hangingwall use letters (A,B,C....). Intrashear schist is identified by latin numbers (I,II). Figure 2.10 shows the locations of the outcrops in the field. A larger version of this map can be found in appendix A, map B.

2.3.1 Footwall of the Footwall Fault

2.3.1.1. Foliation pattern in footwall

Within the studied area the footwall of the Hyde-Macraes Shear zone consists of a psammitic TZ IV schist which becomes more and more pelitic closer to the Footwall Fault. The regional foliation changes its dip direction throughout the study area from NE to SW. In close proximity to the Footwall Fault, the foliation is almost horizontal and dips with c. 05° to the SW. In some locations near to the Footwall fault (e.g. at the Golden point road), the foliation dips gently to the NE. With increasing distance to the Footwall Fault the dip angle also increases (figure 2.9). Near the settlement Deepdell, the foliation on the NW side of the Deepdell creek commonly dips to the W and NW and on the southeastern margin the foliation dips to the SW.

Shear bands often form a second cleavage. This is the case, especially around the sample locations HM07/02, HM07/03 (appendix A, map C) and at the Golden point road. The shear bands generally dip to the NE.

The Footwall Fault is not exposed as identifiable structure, which made it impossible to determine its exact boundaries and the location of change in textural grade. However, thin section investigation indicates that the boundary lies somewhere between Outcrop 3, Outcrop 4 and Outcrop I.

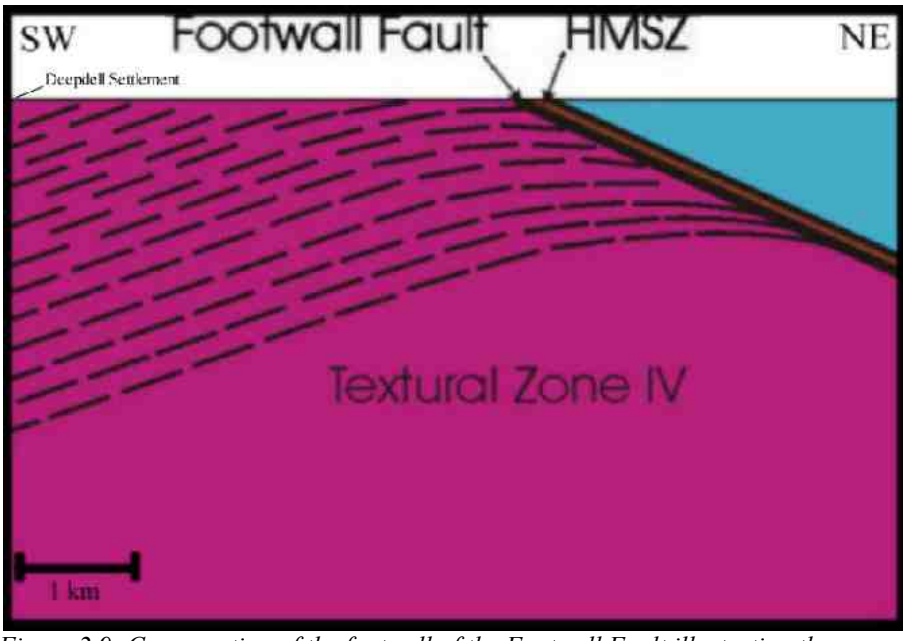

Figure 2.9: Cross section of the footwall of the Footwall Fault illustrating the foliation pattern in the footwall.

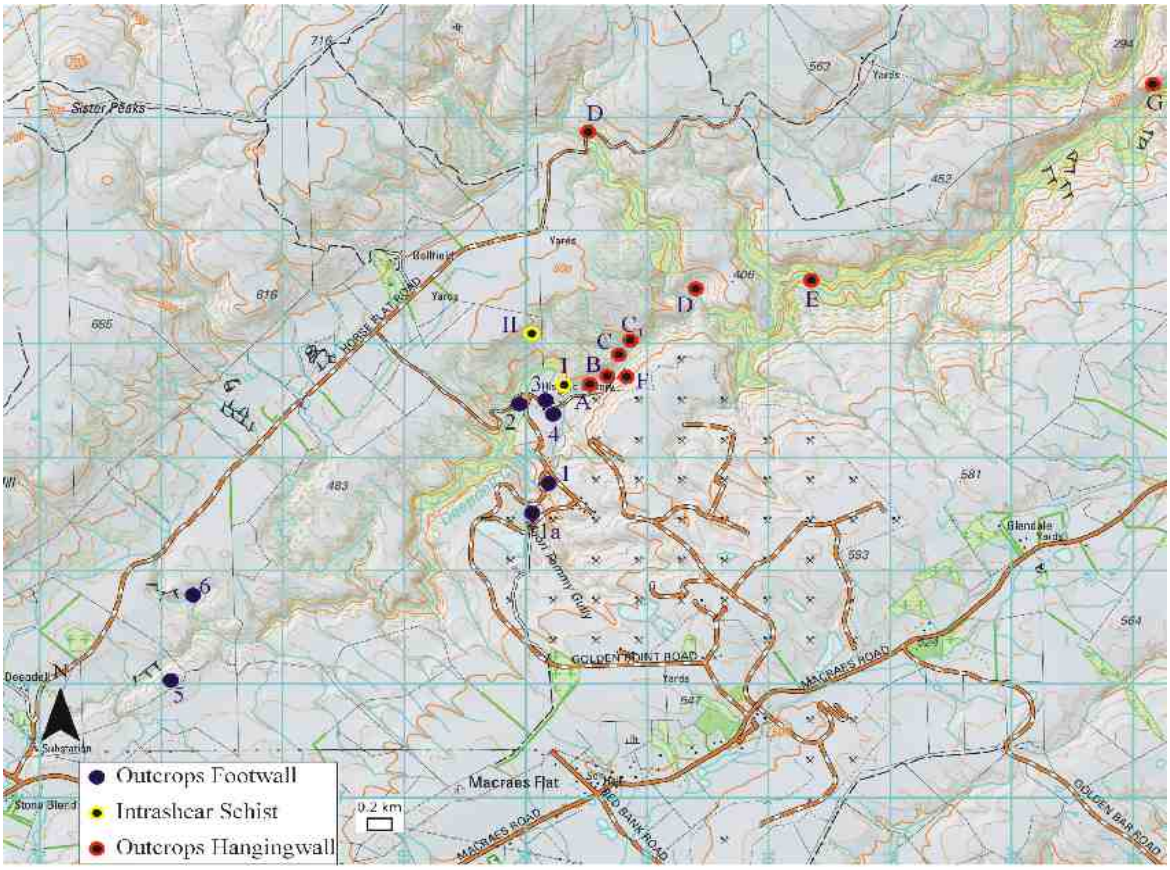

Figure 2.10: Map of the study area showing outcrop locations.

2.3.1.2. Outcrop Descriptions in Footwall

1) Golden Point Road

The most important outcrop is located at the Golden point road NW of the processing plant (figure 2.11). It is an approximately 200m long drive wall consisting of TZ IV schist. Structurally this outcrop lies directly below the Footwall Fault of the HMSZ. The drivewall is host to many structural features including late brittle faults and shear bands in particular. Investigation on these features showed that most of the brittle faults have a normal sense of shear. There are 20 major faults in this outcrop of which 19 have a normal sense and one a reverse sense of shear. Most of the normal faults dip approximately to the NE. Only a few of them have other dip directions (figure 2.12). The dips of those faults range from 37° - 75°. The reverse fault dips SW at c. 80°. The foliation in this drivewall is commonly almost horizontal and dips with c. 5° gently to the NE.

The most conspicuous feature is situated in the southern part of the drivewall. According to foliation curvature, it is a prominent high angle normal fault with an approximately 20 cm thick gouge zone (figure 2.13). It is accompanied by two parallel striking but shallower dipping normal faults in its footwall. Estimation of the strain field provides a NE-SW direction for the axis of maximum extension (S 1, figure 2.14).

Figure 2.11: Photography of the drive wall at the Golden Point Road. View is to the east. Also shows the Macraes mine processing plant and parts of the Round hill pit in the background.

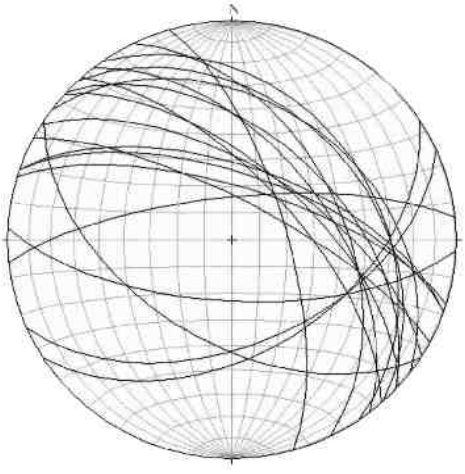

Figure 2.12: Great cirlces of late normal faults at the golden point road drivewall, equal area, lower hemisphere projection.

Figure 2.13: High angle normal fault in the southern part of the drivewall with two parallel dipping intermediate angle normal faults in its footwall. All three features have a similar strike and dip to the NE. Hammer for scale.

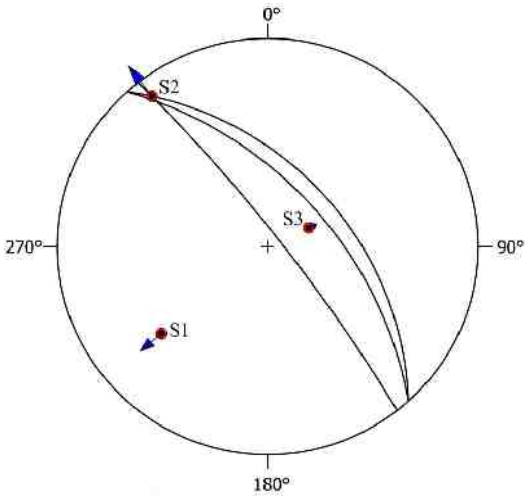

Figure 2.14: Great circles illustrating the orientation of the fault planes of a prominent brittle structure in the southern part of the drivewall. The plot is also showing principle strain axes S 1-3. Equal area, lower hemisphere projection.

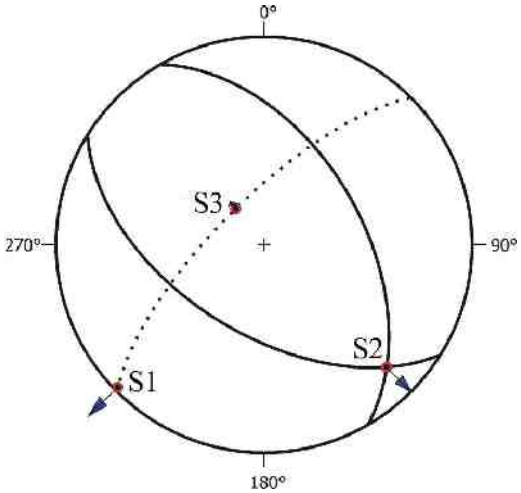

Figure 2.15: Great circles of two conjugated normal faults at the Golden point road drivewall. Determination of principle strain axes S 1-3 was done by the conjugated fault method.

Towards the northern end of the drive wall the gouge zones in the faults become thinner. After approximately 120m from the southern end there is very little gouge in the faults and the offset on the slickensides appears to be relatively small. At one fault the offset was measurable because this fault cuts through an older fault offsetting its fault plane. The offset is about 10cm. Due to the apparent conjugate nature of both faults it was possible to calculate strain axes (figure 2.15). According to the stereoplot the direction of maximum extension (S 1) trends NE – SW.

However, most attention was drawn to the occurrence of abundant shear bands in this outcrop (figure 2.16a). They form a second penetrative cleavage subparallel to the existing foliation and are commonly truncated by brittle normal faults. They also deform foliation-parallel quarz veins at some places (figure 2.16b). Although, they are relatively brittle features in this outcrop, subsequent thin section examination showed that in some of these shear bands quarz is recrystallised (Chapter 3, e.g. thin section HM06/13). Like the brittle normal faults, the shear bands dip to the NE and so do their slickenlines (figure 2.16c). Accordingly, the strain axes (as calculated using the Bingham method) indicate a direction of maximum extension trending NE-SW.

Adjacent to this drivewall c.100m to the south on the Goldenpoint road (figure 2.10, location 1a), there is another drivewall that consists more or less completely of polished surfaces (figure 2.17). A closer look at these surfaces identified them as slickensides of mainly N to NE dipping normal faults (figure 2.18). The relative offset on these surfaces has been determined by slickenfibres (figure 2.19a/b). Slickenfibres develop on slickensides during slow aseismic movement and fill gaps that open between the two blocks. Slickenfibres grow at a small angle from the shear boundary inwards in the direction of movement of the opposite block. This means that an arrow along the slickenfibre lineation starting at the point of their attachment to the shear boundary points into the movement direction of the opposite block. Thus, they are usefull kinematic indicators.

The slickensides also contain two different generations of slickenlines. The first one dips to the NE like the normal faults, the second generation of slickenlines dip gently to the west and represent possibly a stage of later reactivation (figure 2.20). Note that during reactivation also a second slickenfibre generation has developed.

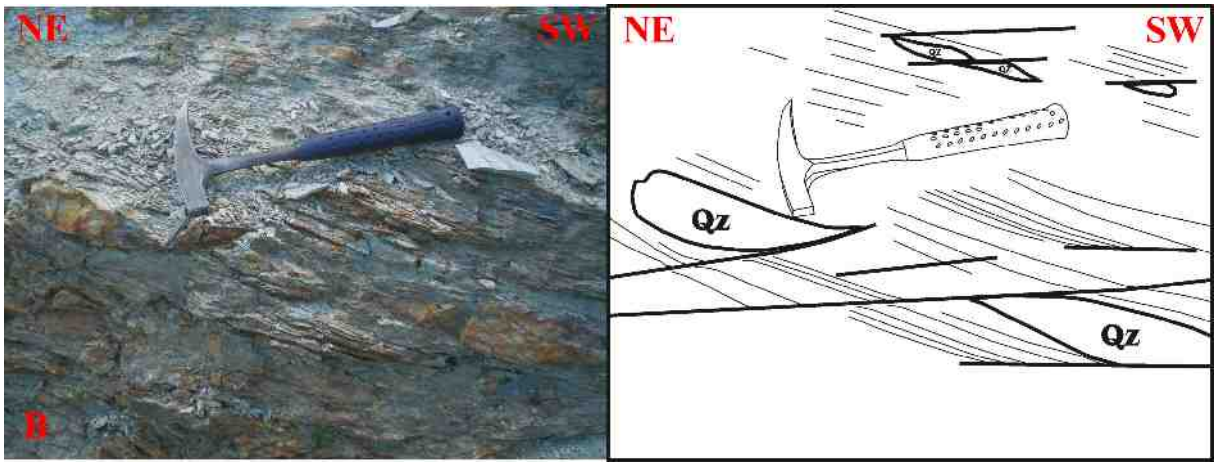

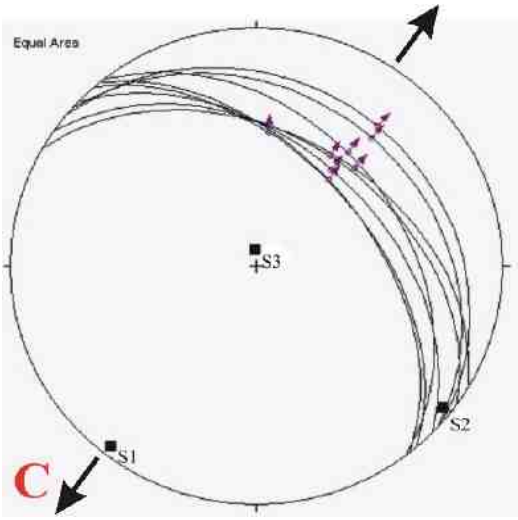

Figure 2.16:

A) Ductile shear bands in drive wall forming second penetrative cleavage.

B) Brittle-ductile shear bands deforming quartz veins. Shear bands are represented by heavy black lines in the drawing to the right.

C) Great circles representing shear band planes. The arrows mark the lineation trend with the sense of hangingwall displacement indicated by arrow head. Strain axes are represented by heavy black squares. Equal area projection, lower hemisphere.

Figure 2.17: Polished slickenside of a high angle normal fault.

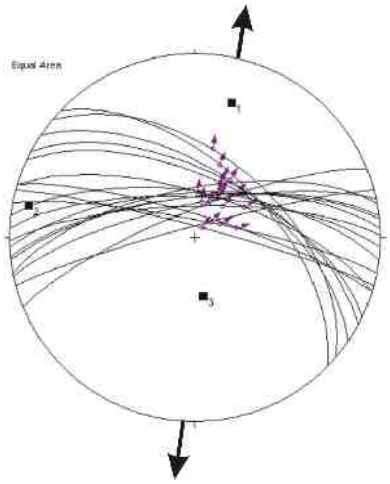

Figure 2.18: Great circles of high-angle normal faults at location 1a. Strain axes represented by heavy black squares. Equal Area, lower hemisphere projection.

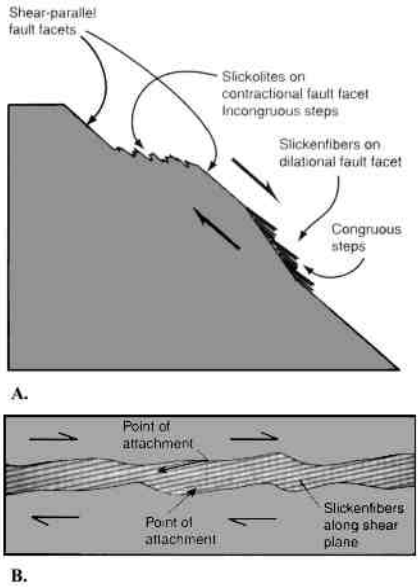

Figure 2.19: Scheme illustrating slickenfibre development. Source: Twiss & Moores: Structural Geology

Figure 2.20: Close up of one of the slickensides at location 1a. There are two generations of slickenlines and slickenfibres present.

2) Deepdell Footwall 1

The next outcrop lies structurally deeper than the Golden point road drivewall and is located c. 100m south of the mining road bridge in the Deepdell creek valley (figure 2.10, location 2). Like the rock at the drivewall, this outcrop it is psammitic TZ IV schist but compared to the drivewall it is less deformed by brittle faults and the foliation dips gently to the SW with c.02°. Shearbands are abundant in this outcrop, showing both ductile and brittle ones (figure 2.21). Samples for thin section examination have been taken at this location and will be discussed in Chapter 3 (sample HM06/10). Furthermore, this outcrop hosts s-folds which represent an additional kinematic indicator.

Figure 2.21: Photograph of a footwall schist, showing ductile and brittle shear bands and s-folds. Hammer for scale.

3) Deepdell Battery 1

North of the carpark of the historic battery and on the southern margin of the Deepdell Creek is an outcrop containing a typical Riedel arrangement for normal faults (figure 2.10, location 3). The schist is classified as TZ IV with a pelitic protolith. Two main faults can be distinguished which are accompanied by several subsidiary faults (figure 2.22). Both are high-angle normal faults and dip to the NE. The first fault, located in the western part of the outcrop, has a R'-shear accompanying it. Due to the definition of a Riedel arrangement the angular relation between R'-shear and fault plane allow an estimation of the orientation of principal strain axes (figure 2.23). This R'-shear is also subsidiary to the eastern normal fault. The calculated angle between those two faults is 85° which leads to the assumption that the eastern normal fault is a P-shear to the western fault. The typical 10° relationship between main shear and P-shear is also met. The eastern fault also has subsidiary faults which look like Riedel shears (figure 2.24).

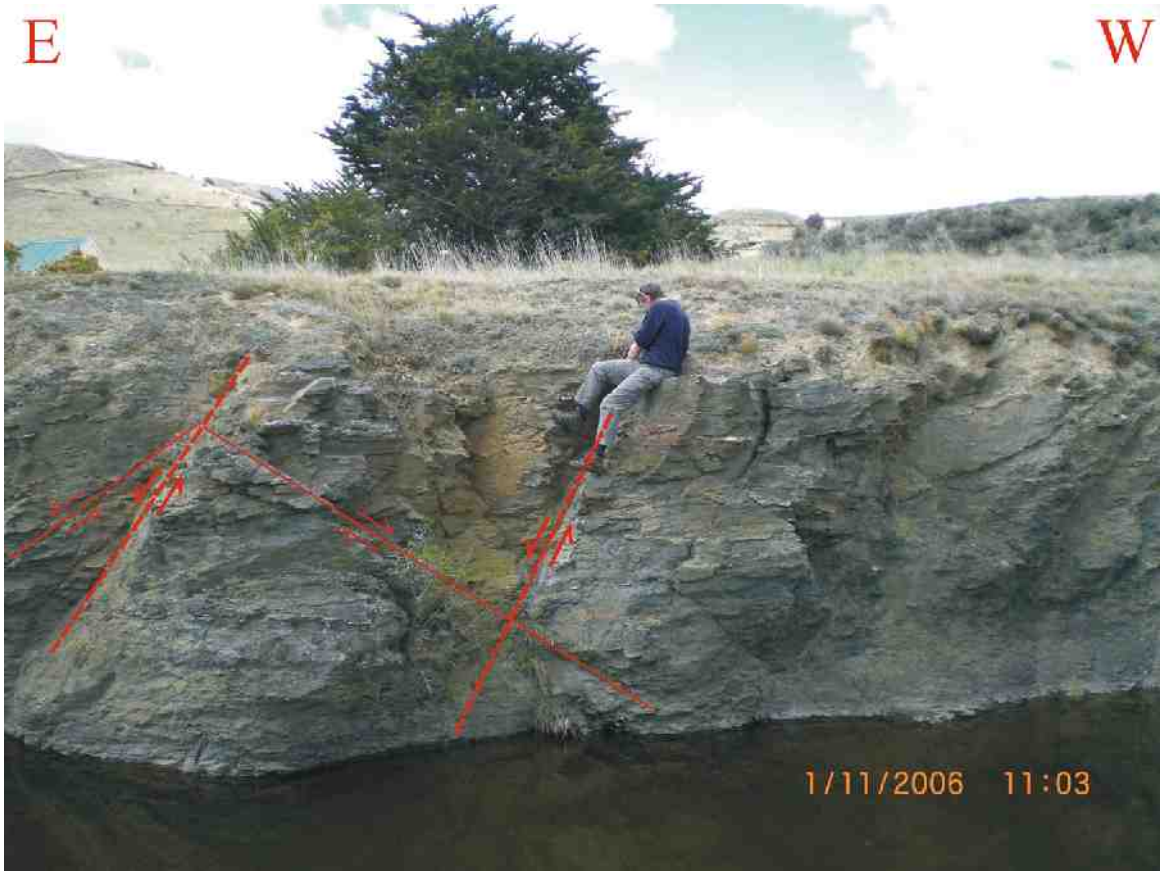

Figure 2.22: Photograph of the Riedel arrangement at location 3. View is towards south.

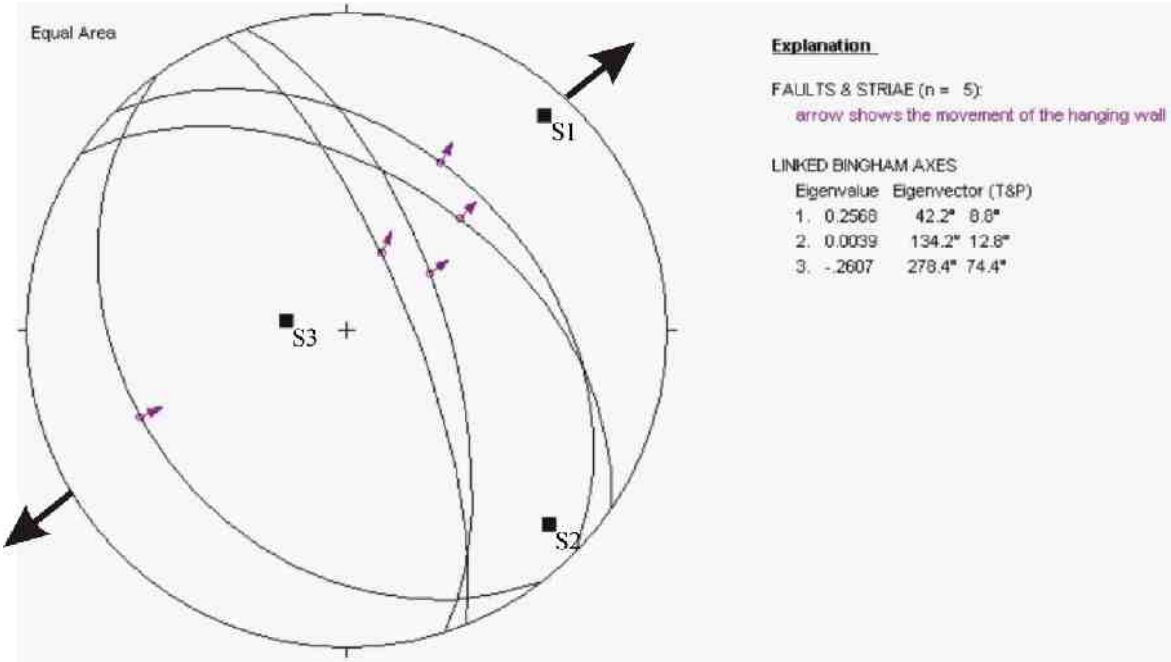

Figure 2.23: Great circles of main shear, P-shear, R'-shear and other subsidiary fractures. Black squares are strain axes. S 1 reflecting the direction of maximum extension. Equal area, lower hemisphere projection.

Figure 2.24: Photograph of the eastern fault at location 3, showing subsidiary fractures.

4) Deepdell Battery 2

South of the historic miners quarters is an old little pit (figure 2.10, location 4). In its walls are eleven brittle normal faults. Six of these faults are dipping towards SW, four towards N and NE and one dips approximately to the NW (figure 2.25). The stereoplot shows that some of these NE and SW trending faults are directly related and estimation of the principle strain axes also indicates maximum extension trending NE-SW.

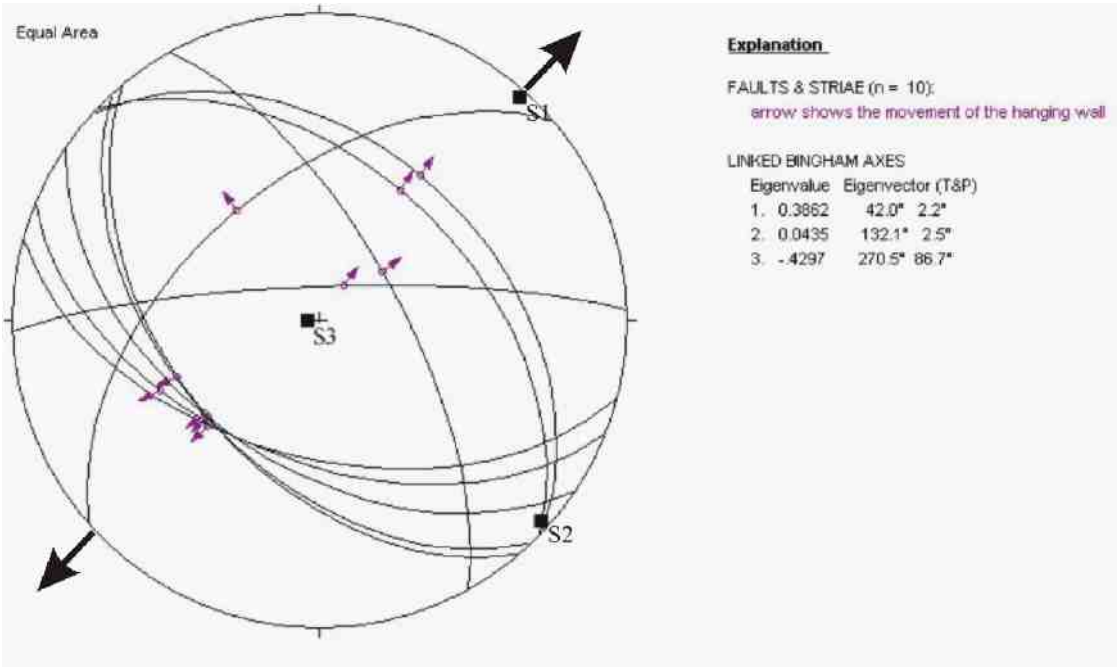

Figure 2.25: Great circles of late normal faults and Bingham strain axes (black squares)

5) Deepdell Footwall 2

Approximately 1.5 km east of the settlement Deepdell at the southern margin of the Deepdell valley are some tors, remnants of schist which were able to resist erosion, containing many shearbands (figure 2.10, location 5; figure 2.26). These shear bands are dipping gently to the NE and are well lineated (dip c. 42/32). The lineations also dip to the NE (c. 35/37).

Figure 2.26: Photograph of outcrop 5, showing many shear bands.

6) Gully Shear Zone

A brittle shear zone is located in a gully approximately 1.6 km NE of the settlement Deepdell (figure 2.10, location 6). Three main faults can be distinguished which dip gently to moderately N to NE (figure 2.27). Lineation trend is to the NE. The schist in this shear zone is highly deformed. According to foliation curvature the shear sense is normal. Strain axes have been determined by means of the Bingham method. The axis of maximum extension trends approximately NE-SW (figure 2.28).

Figure 2.27: Shear zone NE of the settlement Deepdell. Two of the main shears are seen, the third is located further to the SW.

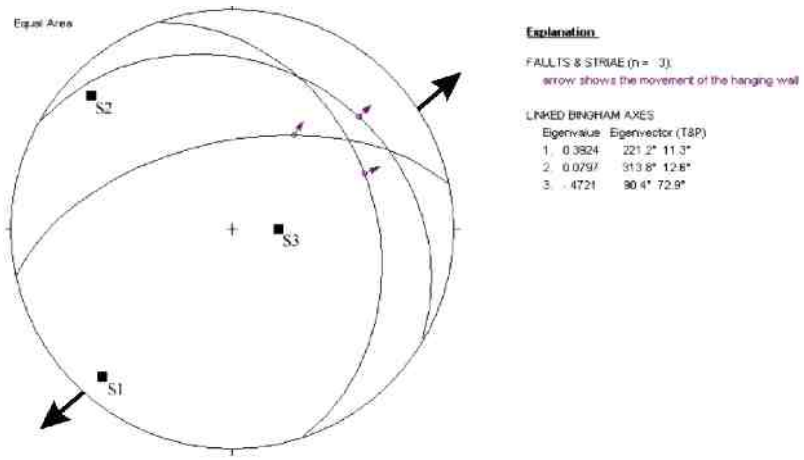

Figure 2.28: Great circles of main fault planes. Equal area, lower hemisphere projection

2.3.2 Hangingwall

2.3.2.1. Foliation Pattern in Hangingwall

The hangingwall of the Footwall Fault in the study area consists of a pelitic TZ III schist. The regional foliation dips usually gently to moderately to the NE with values between 20° to 39° (appendix A, map A). However, very close to the HMSZ the foliation orientation is not completely consistent. To the south eastern margin of the Deepdell creek valley the foliation dips basically to the SW. Towards the northwestern margin the foliation dips mainly to the SE. This pattern changes within c. 100m NW of outcrop C to C1 through the gully.

2.3.2.2. Outcrop Locations in Hangingwall

Outcrop A

Outcrop A lies c. 200m NE of the historic Battery. At this location the foliation dips very gently towards NW (dip 305/10). There are not many structures other than the penetrative cleavage except for a few kink folds (figure 2.29). The axis of the kinks plunges to the NNE (014/10), the kinks itself dip to WNW.

Figure 2.29: Kink band in pelitic TZ III schist.

Outcrop B

This outcrop shows two minor extensional fractures, dipping to the NE (008/50; 055/87) (figure 2.10, location B) and kink folds with axes dipping to the NW (340/10). Very few structures have formed after the penetrative cleavage.

Outcrop C

The first good outcrop in the hangingwall is located c.500m NE of the historic battery adjacent to a gully (figure 2.10, location C). It consists of a pelitic TZ III rock containing several brittle faults. Attention is drawn to a moderate angle brittle normal fault crosscutting this outcrop (figure 2.30a) which is accompanied by several Riedel shears. The main fault dips at c. 50° to the NE (060/51) and is therefore synthetic to the Hyde-Macraes shear zone. Lineation trends approximately NE to E and plunges at an angle of 39° (087/39). A prominent Riedel shear is located above the main fault, strikes approximately parallel to it but dips only with 33° (063/33). The foliation dips moderately to the S – SE. The relationship of both faults is illustrated in figure 2.30b also showing principal strain axes.
However, in the footwall of the main fault there is an older ductile fold indicating a thrust sense of movement (figure 2.30c). This movement was either still active after passing the ductile-brittle transition as indicated by small brittle reverse faults in its hinge or was later reactivated.

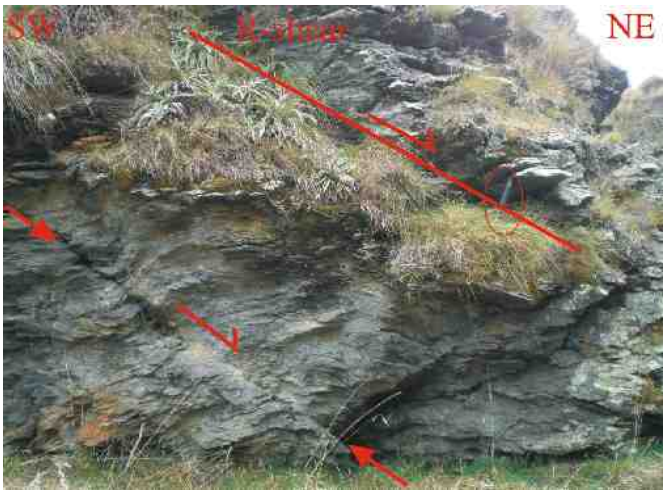

Figure 2.30 a: TZ III Schist containing two normal faults.

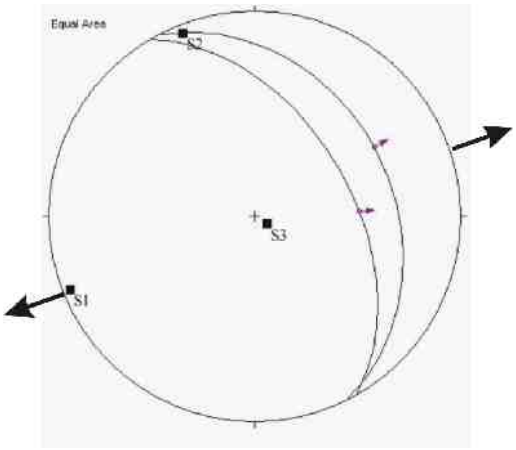

Figure 2.30 b: Stereoplot showing the relationship between the two normal faults. Principal strain axes (s1,s2,s3) illustrated by black squares

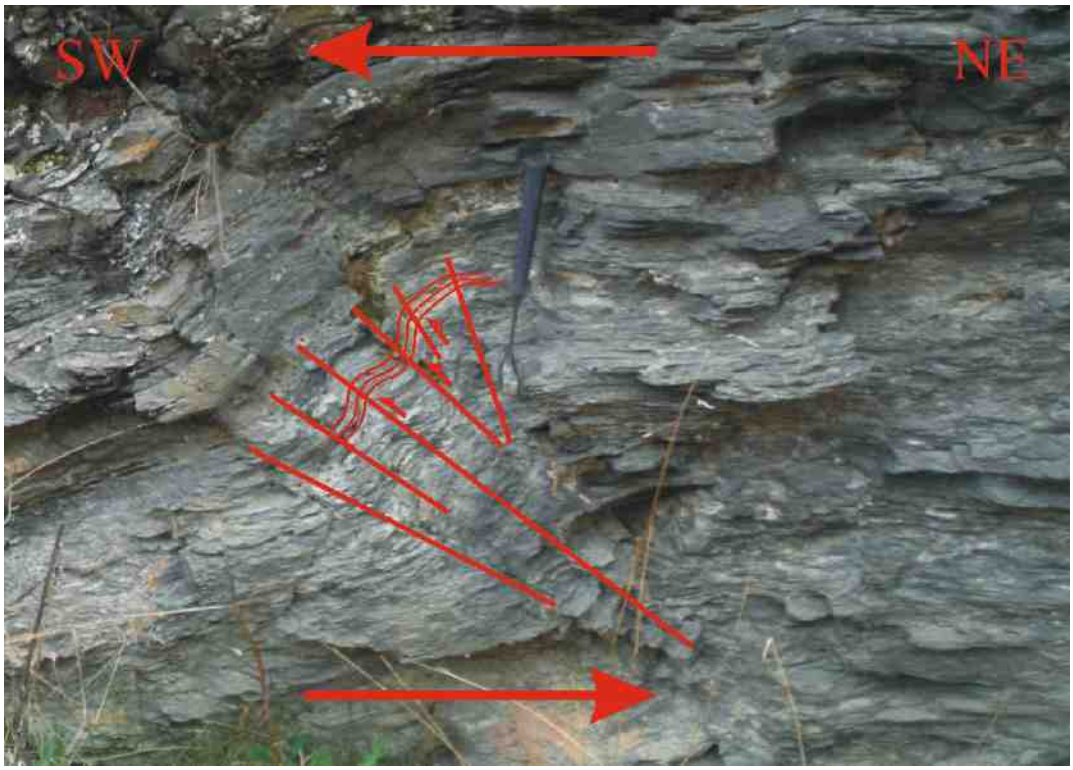

Figure 2.30 c: Photograph of a ductile fold which was reactivated by brittle faults

Outcrop C_1

On the opposite side of the gully, NW from Outcrop C another fault system can be found (figure 2.10, location C_1). The sense of movement of late structures at this location is normal and the main fault dips c. 29° to NE (074/29 upper part; 033/31 lower part). An offspring of the main normal fault cuts through an older ductile fold and offsets it by c. 30 cm (figure 2.31).

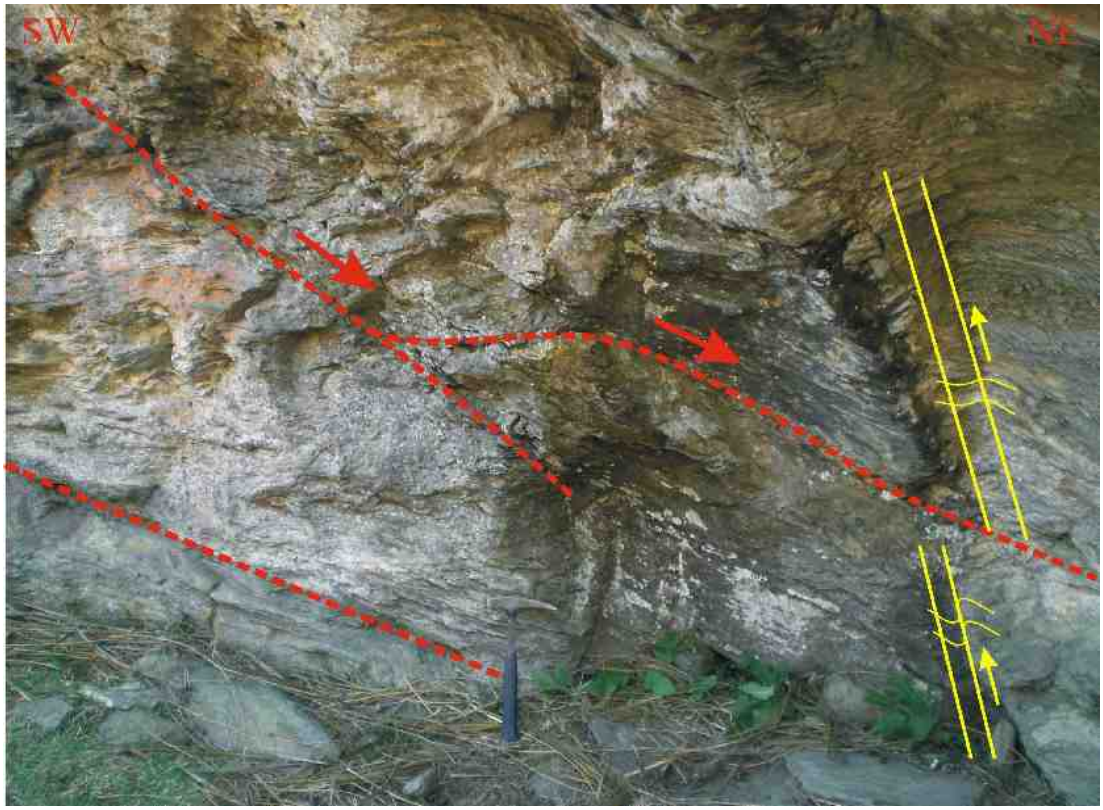

Figure 2.31: NE dipping brittle normal fault, cross cutting an older ductile fold, causing offset of c.30 cm.

Outcrop D: Highlay Creek fault

At the intersection of the Highlay Creek with the Deepdell Creek, the remnant of a brittle normal fault is found in an outcrop near an old farmtrack (figure 2.10, location D). This normal fault dips SSW (196/44) and contains slickenlines plunging at 40° to 230°.
At another location in the Highley Creek (intersection Horse Flat Road and Highlay creek, figure 2.10, location D_1) more moderate to high angle normal faults are exposed (figure 2.32). Lineations show a generally west to southwest oriented direction of transport. The majority of the faults strike approximately parallel to the Highlay Creek valley. Strain axes have been calculated using the Bingham method and indicate S 1 running NE-SW.

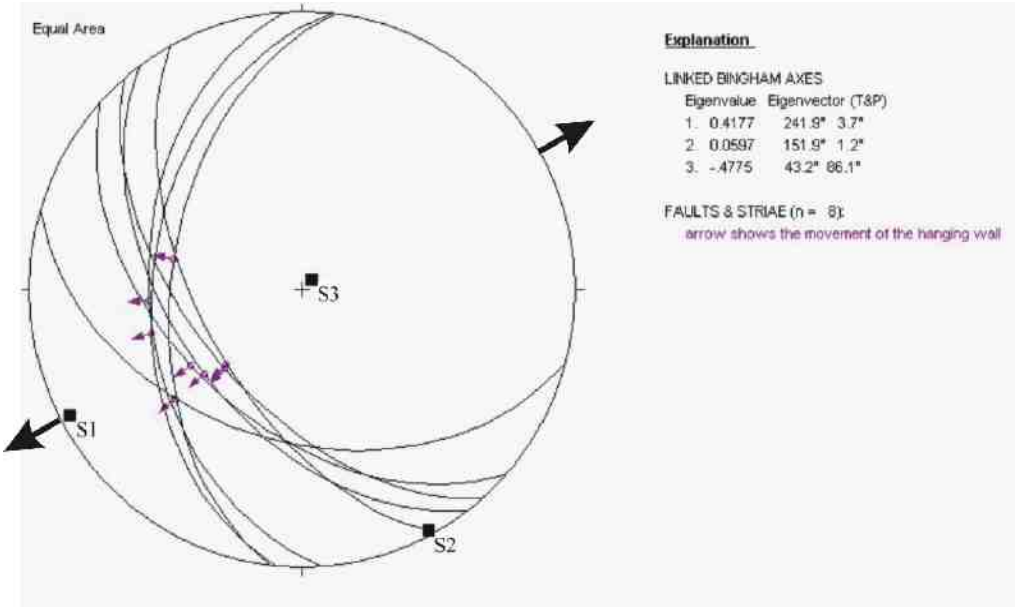

Figure 2.32: Stereoplot showing great circles of fault planes and lineations. Principal strain axes represented by black squares.

Outcrop E: Gully fault

Approximately 2 km NE of the historic battery in the Deepdell creek valley another gully occurs which is striking approximately parallel to the HMSZ or Footwall Fault. In this gully, a late normal fault can be found which is approximately strike parallel to the gully and dips to the SW (figure 2.33a/b). The foliation is dipping with c. 20° towards NE.

Figure 2.33 a: Brittle normal fault at the Deepdell creek. Hammer for scale.

Figure 2.33 b: Close up of the normal fault shown in Fig 2.33a, showing truncation of the foliation.

Outcrop F: Old survey track.

East of the historic battery on the SE side of the creek approximately half way up the slope runs an old rarely used survey track of the mining company. Some road cuts are still preserved and contain late structures. Especially one drivewall contains a brittle fault system (figure 2.34) of two NE dipping approximately parallel brittle normal faults (~060/75) which are truncated by one conjugated SW dipping normal feature (~220/34). In the footwall of the SW dipping normal fault the foliation is locally dipping moderately to the SW, indicating significant normal deflection of the foliation (dip 220/34; figure 2.28), but is not observable in direct vicinity of the fault due to erosion.

A few meter along the track to the NE another outcrop can be found which contains kink folds (figure 2.35). The axes of the kink folds plunge c. 291/13 with vergence to the SW.

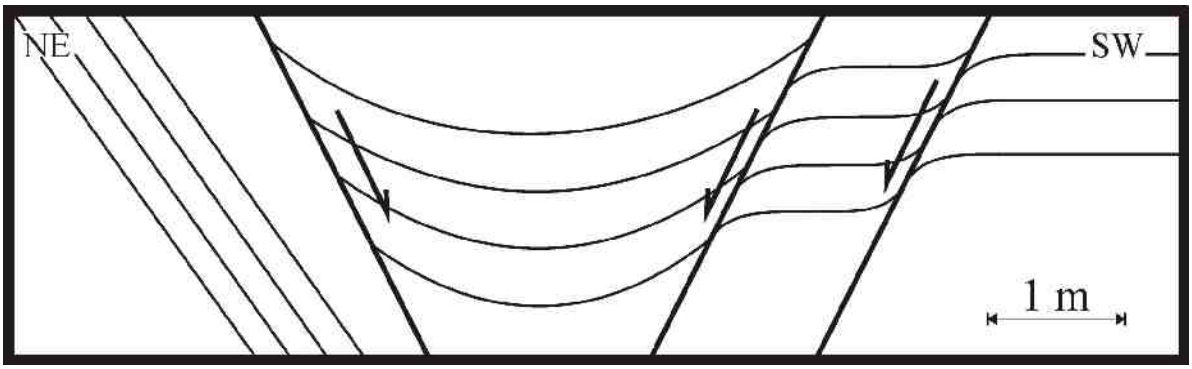

Figure 2.34: Scheme of the normal faults in the drivewall at the old survey track illustrating foliation behaviour around the faults.

Figure 2.35: Kink bands in TZ III schist in drivewall along the old mining track. Dashed red lines represent kink axes.

Outcrop G

The last outcrop in the hangingwall is located c. 4.5 km NE of the historic battery, at the northern margin of the Deepdell Valley (figure 2.10, location G). This outcrop hosts a thin normal fault which is dipping to the NE subparallel to the foliation (figure 2.36). This feature is accompanied by a Riedel shear. There are two generations of slickenlines on the fault plane. The first one is gently plunging to the north and the second one to SE. The second generation of lineations might have developed with respect to the Waihemo Fault.

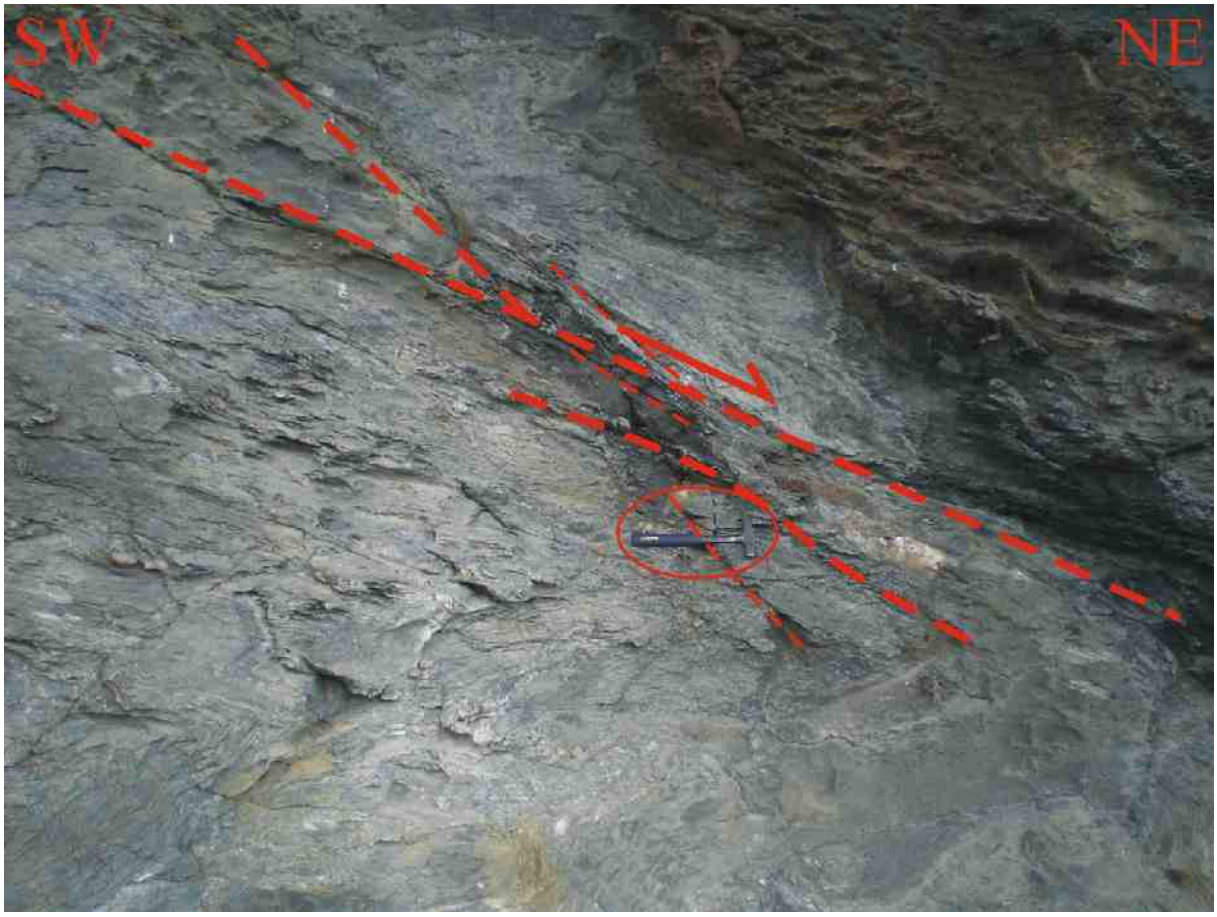

Figure 2.36: Photograph showing a NE dipping normal fault with Riedel fractures at outcrop location G. Hammer for scale

2.3.2.3 Intrashear schist of the HMSZ

Introduction

Outcrops of the mineralised schist of the Hyde-Macraes Shear Zone are very rare in the study area. Some outcrop is present in the historic pits and in the Deepdell North pit, a currently unused open pit of the recent mining operation. Foliation at the historic pit does not show a unique pattern but is almost horizontal. Parts of the intrashear schist are brecciated and do not show a preferred orientation.

I) Historic Pit

The historic mine is divided into one pit that is open to the general public and some other pits which have mostly been filled up. At the entrances to those pits, late normal faults crop out which usually dip NE (figure 2.37). The schist is highly fractured and shows black shear planes at several locations. These black shears are an indication for intrashear schist because of graphite mineralisation within the HMSZ.

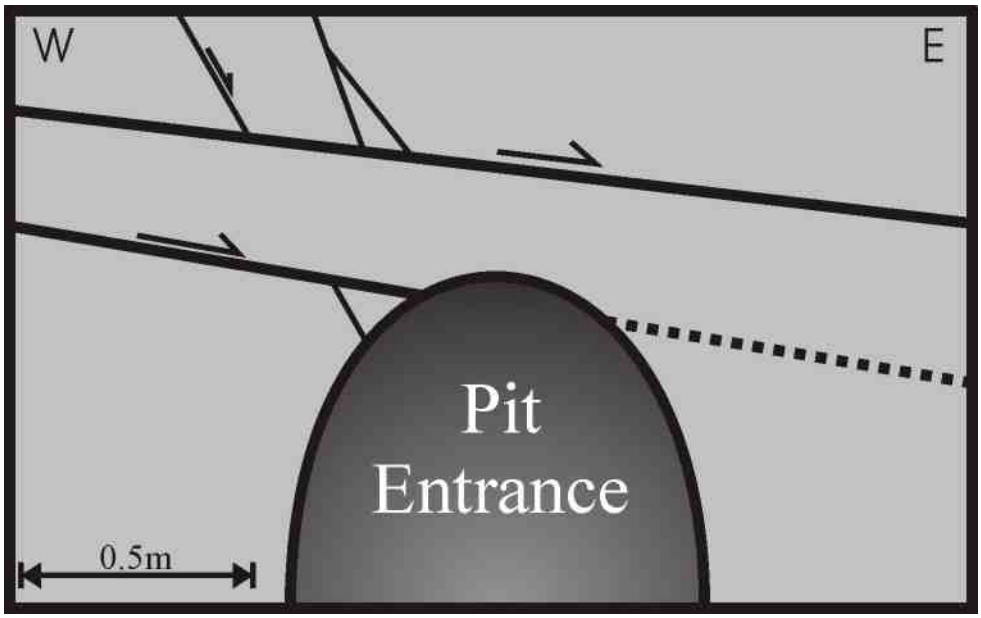

Figure 2.37: Scheme of the outcrop at the historic mine showing some normal faults above the pit entrance.

II) Shear zone

In a drivewall west of the recent mining pit, a prominent (m-scale) shear zone is situated (figure 2.38). This shear zone is a completely brittle feature and probably part of the hangingwall shear of the HMSZ. The feature is a NW dipping normal sense shear zone (dip 300/30) as indicated by Riedel shears (dip 350/84) and foliation curvature. It has well defined upper and lower shear planes filled with gouge material. The dip to the NW of the feature is anomalous relative to the other features of the hangingwall that have been analysed. This may be due to the Deepdell Fault which cuts approximately perpendicular through the Footwall Fault and HMSZ and is located a few hundred meters south of this feature (figure 2.40). However, further brittle features structurally above the shear zone and located to the NW reflect the pattern of this shear zone (figures 2.39a/b).

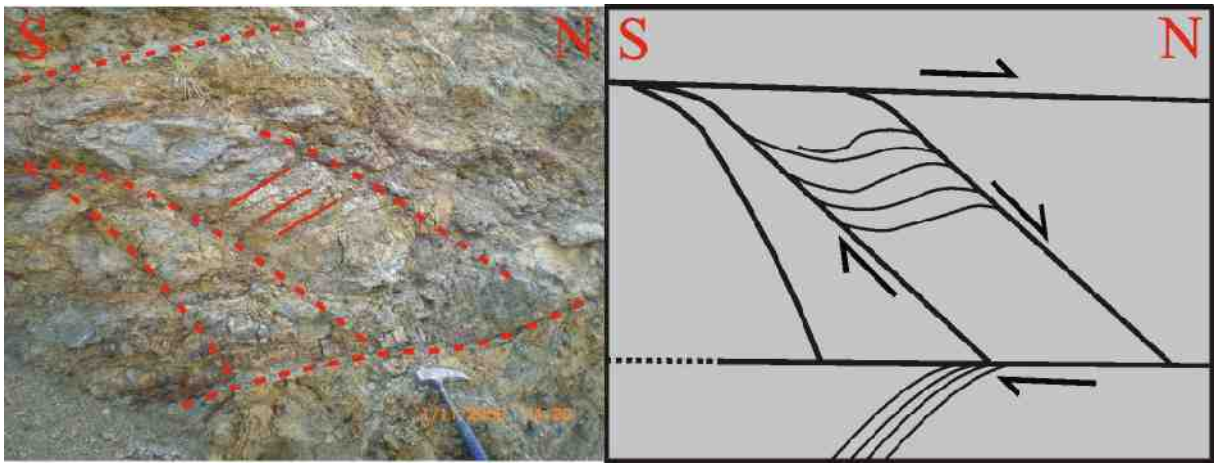

Figure 2.38: Normal sense brittle shear zone at a road cut. Hammer for scale.

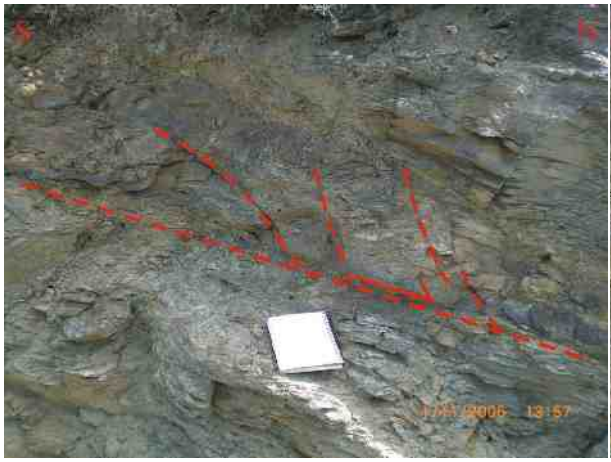
Figure 2.39a: NW dipping normal fault with Riedel fracture. A5 notebook for scale.


Figure 2.39b: NW dipping c. 40cm thick fault zone.

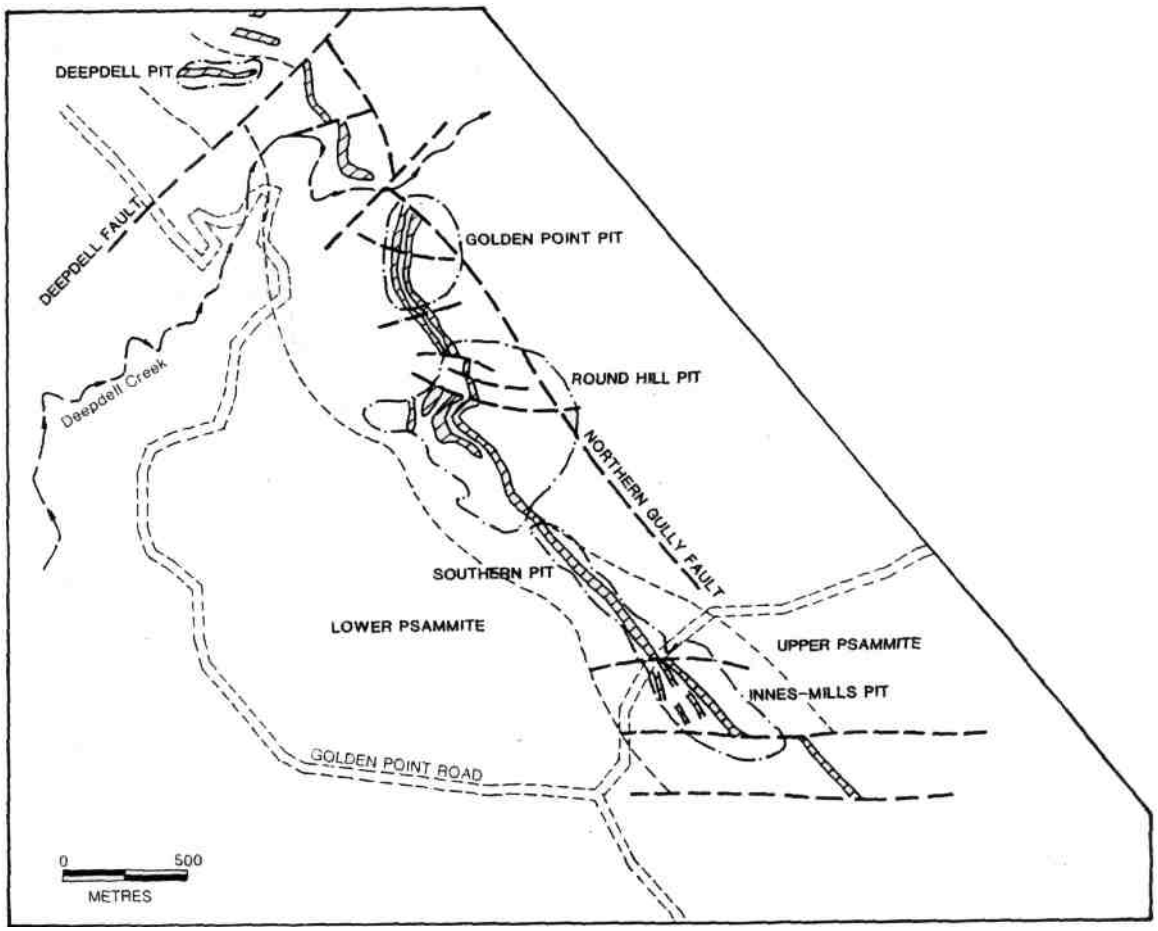

Figure 2.40: Map of the Macraes mine pits, also showing late faults at the Deepdell Creek. (Angus 1992)

2.4. Collection of Hand Specimens

Hand specimens have been collected for thin section examination of kinematic features. The specimens were selected on the basis of shear band occurrence and their location relative to the Footwall Fault. Except for two specimens, samples were taken in the footwall because shear bands did not occur in the hanging wall. The two remaining samples were collected in intrashear schist at the historic mining pit which is de facto hangingwall to the Footwall Fault. The orientation of the hand specimens have been taken prior to their removal from the host rock. This was necessary for making oriented thin sections which will be discussed in chapter 3.

Alltogether, 16 samples have been collected. They were named HM for Hyde-Macraes, 06 or 07, representing the years 2006 and 2007 and a number given by the order of collection. Samples HM06/ 04, 07 and 08 are gouge zone material. A larger version of the map is in appendix A, map C.

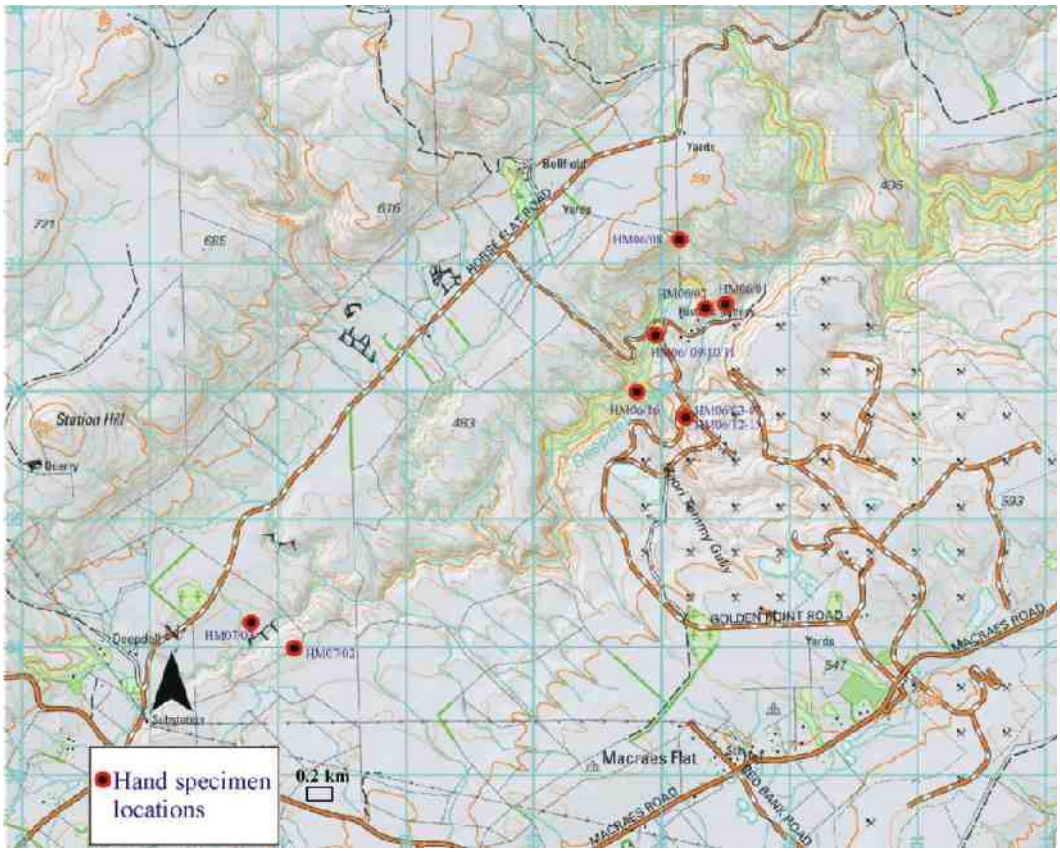

Figure 2.41: Map of hand specimen locations

2.5. Summary

The structural mapping of the study area shows two different patterns for the orientation of the foliation (appendix A, map A). In the footwall of the Footwall Fault, the foliation changes its dip direction from a gentle to moderate dip angle in the SW to the SW, to an almost horizontal orientation that dips very gently to the NE in the very vicinity of the Footwall Fault. In the hangingwall, the foliation dips to the SW for a few hundred meters in dip direction of the Footwall Fault and changes quite abruptly to a gentle to moderate dip angle to the NE.

The foliation in the footwall rotates over a distance of approximately 2 km. Close to the Footwall Fault this pattern is quite consistent, however, in the south-western part of the study area the foliation varies in its orientation (appendix A, map A). Particularly on the northern side of the Deepdell Creek valley, the foliation tends to dip to the west and NW. This inconsistency might be explained by a fault that strikes subparallel to Deepdell Creek. However, evidence for that fault has not been found the field.

Additional to the main foliation, a NE dipping shear band cleavage is well developed. The dip angles of these shear bands is between 20° and 50°.

The shear band cleavage becomes more prominent close to the Footwall Fault. However, especially in the far south-western part of the study area in the footwall of a shear zone near Deepdell settlement, shear bands are also very well developed and form a penetrative cleavage with brittle cleavage planes approximately every 4 cm. Between the shear zone near Deepdell settlement and outcrop 1 and 2 of the footwall of the Footwall Fault, the shear band cleavage has a much wider spacing.

Except for the shear zone in outcrop 6, brittle faults in the footwall seem to be entirely concentrated in the close proximity of the Footwall Fault. However, at the Golden point road in particular, their occurrence is of major importance. Kinematic analysis for all brittle normal faults in the footwall presents a strain pattern that indicates a maximum extension direction trending NE to SW (figure 2.42). Kinematic analysis of all measured shear bands supports that pattern (figure 2.43).

Brittle thrust/reverse faults are very rare in the study area and therefore play probably only a minor role or they may be R'-features which occur in conjunction with a normal sense shear zone.

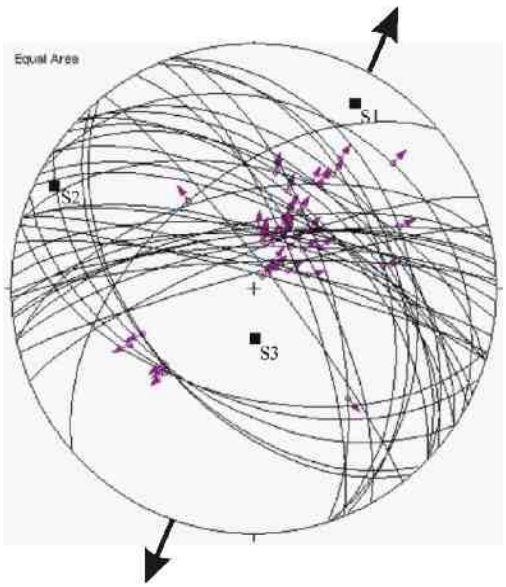

Figure 2.42: Great circles representing all brittle normal faults in the footwall of the Footwall Fault. Arrows show direction of slickenlines on the fault surfaces. Strain axes are represented by black squares and have been calculated by the Bingham method. S1 is the direction of maximum extension. Equal area, lower hemisphere projection.

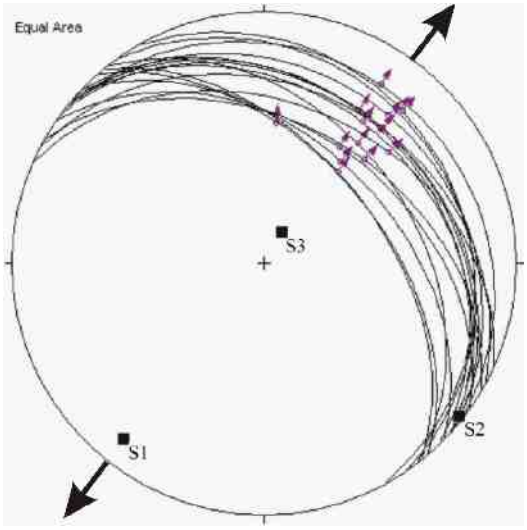

Figure 2.43: Great circles illustrating the shear band cleavage in the footwall of the Footwall Fault. Black squares are principal strain axes. S1 being the axis of maximum extension. Equal area, lower hemisphere projection.

The foliation in the hangingwall is monotonously dipping to the NE (appendix A, map A). In the first few hundred meters NE of the historic battery, the dip direction varies along the margins of the Deepdell Creek. To the southern side of the Deepdell creek valley, the foliation dips uniformly to the SW. To the northern margin of the valley, the dip direction of the foliation is quite random and dips either to the SE or NW. The dip angle is usually very gentle with 10° to 15° degrees (in both directions). Reason for this may be the Deepdell fault which is probably also the cause for the rotation of the shear zone at location II, which is dipping to the NW.

However, in between outcrop locations C and C1, the foliation changes its dip direction to the NE. This happens over distance of less than 100m through a gully. This sudden change would be explained by a fault that coincides with the gully. Outcrop locations C and C1 both show NE dipping normal faults, which leads to the assumption that the gully may also be a NE dipping fault with a normal slip sense. This would also explain the SW-dipping foliation pattern between the Footwall Fault and the gully because the common foliation pattern for a block rotation, due to a synthetic subsidiary fault, would rotate the foliation in this kind of way (figure 2.44).

Except for this, the foliation pattern along the Deepdell Valley is relatively uniform. However, at outcrop locations D and D1 as well as at location E the foliation is dipping steeper to the NE than usual. At these outcrop locations, normal faults can be found which are oriented in an antithetic manner relative to the Footwall Fault. If these faults, which also coincide with the strike of local gullies, are in fact antithetic subsidiary faults of the Footwall Fault, this foliation pattern would be readily explained: An antithetic oriented fault would cause a block rotation that rotates the foliation into the opposite direction of slip (figure 2.44).
Kink bands depict a further structure in the hangingwall. The kink band boundaries are commonly trending to the NW and the bands have a vergence to the SW. The occurance of kinks suggests minor late stage shortening, possibly due to development of the Alpine Fault. However, the kinks do not show any relationship to other structures which makes it impossible to determine the stage of their development exactly.
Nevertheless, the strain pattern that derives from the normal faults in the hangingwall is very similar to that in the footwall (figure 2.45). Like the pattern in the footwall, the mean strain axis S1 derived from the hangingwall normal faults trends approximately NE-SW. However, in contrast to the very obvious pattern in the footwall, the pattern of the hangingwall is somewhat blurred and shows probably a further reactivation which was directed NW-SE or even E-W. Evidence for a further reactivation has also been found in the footwall: At location 1a the slickensides show a second generation of slickenlines and slickenfibres which are oriented approximately E-W. Furthermore, foliation patterns along the horse flat road (NW margin of the study area) show dip orientations to the west and NW.
If all data of brittle normal faults are plot together, the strain axes show a pattern indicating that strain axis s1 trends approximately NE-SW (figure 2.46).

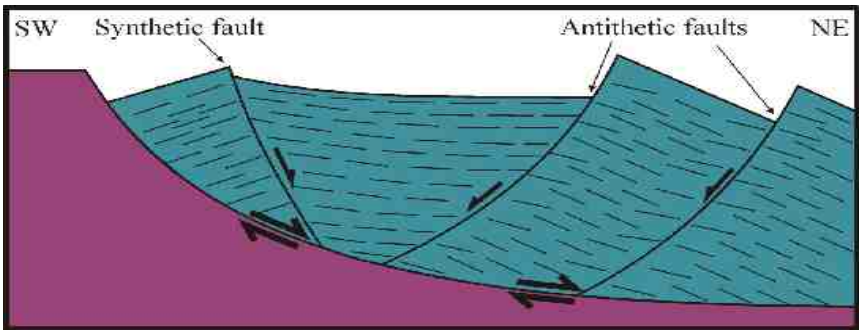

Figure 2.44: Scheme of a listric normal fault with synthetic and antithetic subsidiary faults. Also illustrating a foliation pattern that may derive from such a structure. The regional orientation of the foliation in this model is to the NE. The foliation changes at the fault zones to a shallower angle due to a deflection caused by the slip motion.

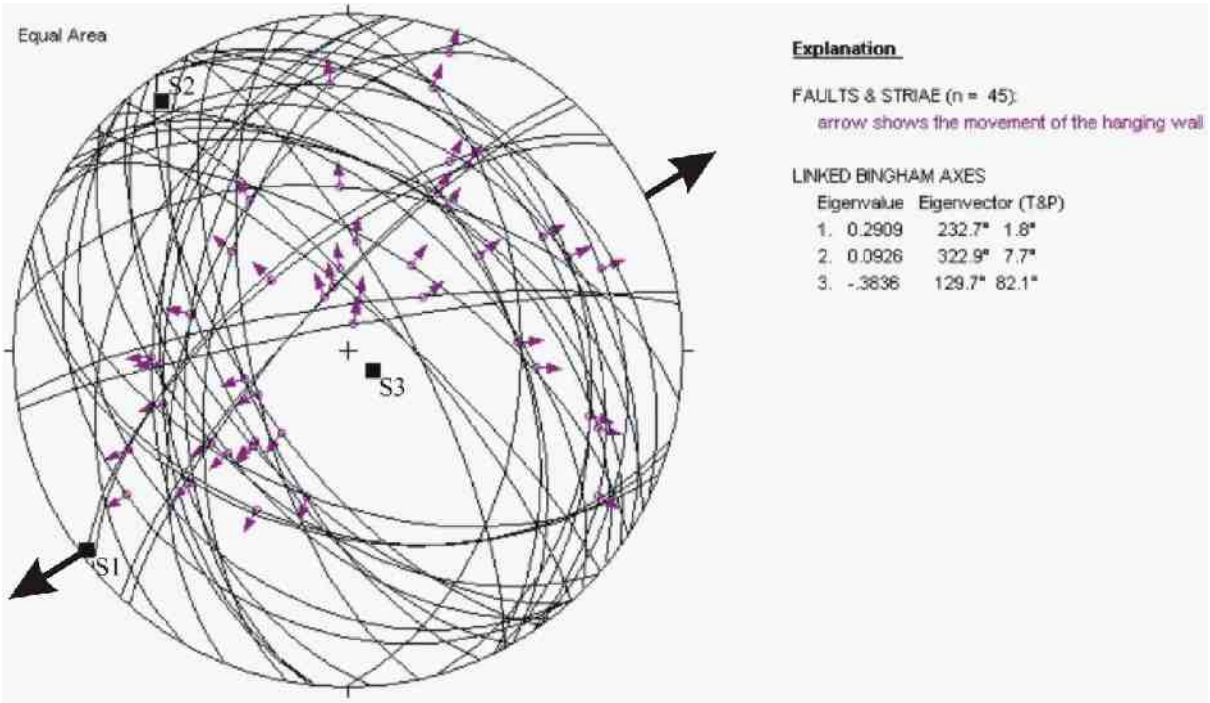

Figure 2.45: Great circles representing normal faults in the hangingwall of the Footwall Fault. Arrows show slickenline orientations. Strain axes are represented by heavy black squares. Equal area, lower hemisphere projection.

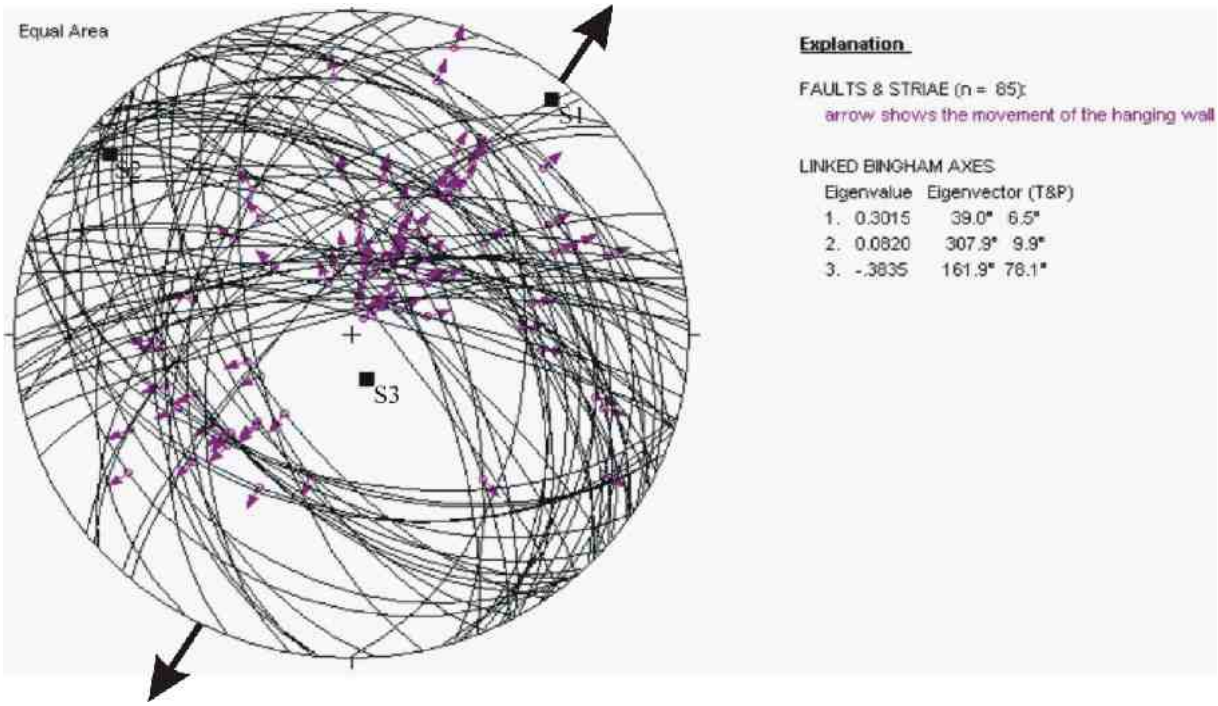

Figure 2.46: Great circles representing normal faults in hangingwall and footwall of the Footwall Fault. Arrows show slickenline orientations. Strain axes are represented by heavy black squares. Equal area, lower hemisphere projection.

CHAPTER THREE

Analysis of Hand Specimens and Thin Sections

3.1 Introduction

Thin section investigations are an important tool to explain tectonic processes because it provides a more detailed view of mineral interactions at or near to fault zones. Apart from mechanical interactions it often also provides information about pressure/temperature conditions of structures at the time they formed. If the rock was ductilely deformed it may also tell something about the conditions in which that deformation took place. One example for this may be the development of shear bands in a rock. Shear bands represent areas of high strain and usually grow in ductile shear zones where they offset a formerly developed foliation. If quartz minerals are trapped in such a shear band they may be recrystallised. This is represented by a reduced grain size. This process is also called dynamic recrystallisation and can happen in two ways: (1) Boundary migration recrystallisation and (2) subgrain rotation recrystallisation.

In the first mechanism the grain boundary of a highly strained crystal migrates into a more highly strained region. Material of the strained grain crosses the grain boundary and is added to an unstrained crystal of the same mineral. In this process individual grains will grow completely new. These new, unstrained crystals will be deformed again and become eventually replaced as well.

The second mechanism involves rotation of subgrains in a highly strained crystal. The rotation of the subgrains occurs due to lattice dislocation. Dislocations grow around a certain area that defines the subgrain. At a certain angle (c.10° of relative rotation) the subgrain boundary becomes saturated by dislocations which means that any further rotation can not be compensated and a high angle boundary between individual grains is established.

Due to the unique characteristics of individual minerals regarding their abillity to withstand heat, pressure and strain, dynamic deformation of those minerals sets minimum P/T conditions. For quartz minerals which have a grain size of c. 100µm these conditions are c. 300°C and approximately 1 kbar.
In the following section the thin sections made from hand specimens are presented. In particular, this section focusses on microtectonic structures but will also include petrographic aspects. Sample locations can be found in appendix A, map C. The orientation of the thin sections is always parallel to the lineation on the shear band cleavage.

3.2 Hand Specimen and Thin Sections

HM 06/13

This specimen is taken from the Golden point road drivewall. It is a finely laminated schist in which laminae of quartz and feldspar alternate with white micas and chlorites. These laminae vary in thickness. Quartz/feldspar laminae are usually 0.5 – 1.5 mm thick, mica rich laminae commonly <0.5mm. Some quartz veins in the hand specimen reach a thickness of >1cm. Epidote occurs as an accessoric mineral.
The mean grain size in HM06/13 is ~300µm. However, individual quartz grains may reach a size of c. 1mm. Quartz grains form subgrains and are elongated parallel to the preferred orientation. White micas reach thicknesses of c. 20 µm and length of >125 µm. These specifications identify the specimen as a TZ IV rock that derived from a fine grained psammite.
The thin section contains a major shear band (figure 3.1). Quartz recrystallisation within the shear band indicates development in a ductile environment. However, the shear band was either still active or reactivated in a brittle regime because a brittle fault plane is clearly developed.
Specimen HM06/13 contains more shear bands apart from the major one. These further shear bands are on a much smaller scale (figure 3.2) but not as much developed as the major one.

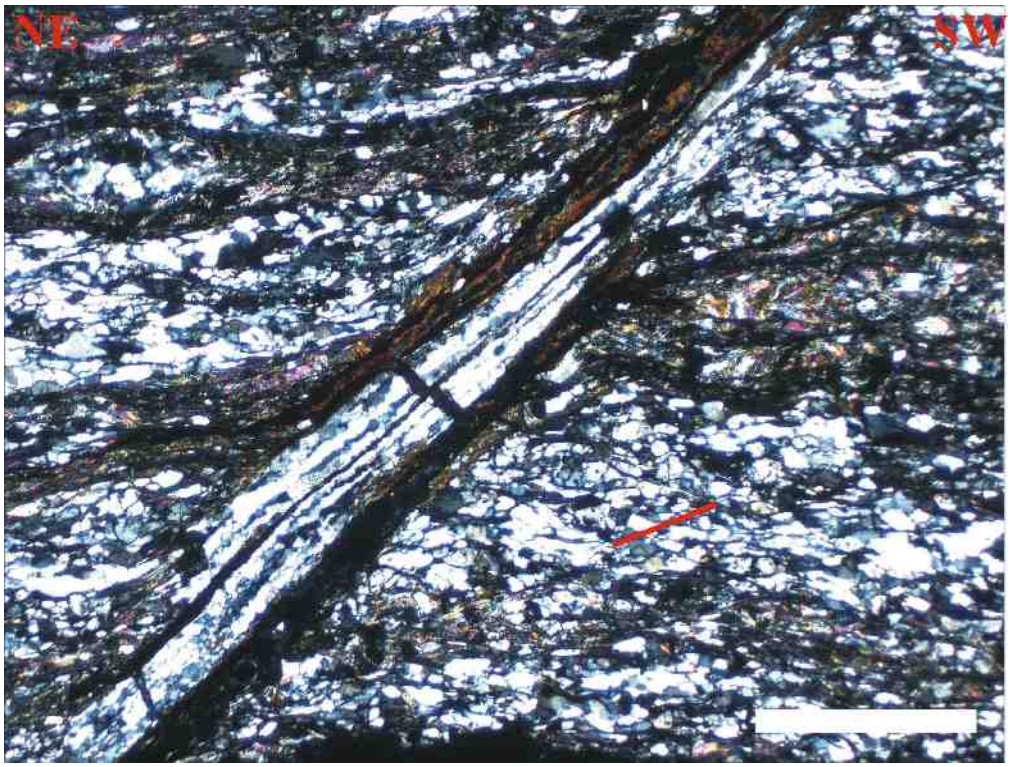

Figure 3.1: Thin section photograph of specimen HM06/13, showing a prominent shear band cutting through an older foliation. Quartz was dynamically recrystallised during shear band development. Further smaller scale shear bands are situated in the footwall of the major one, forming a second penetrative cleavage. White bar is 1mm.

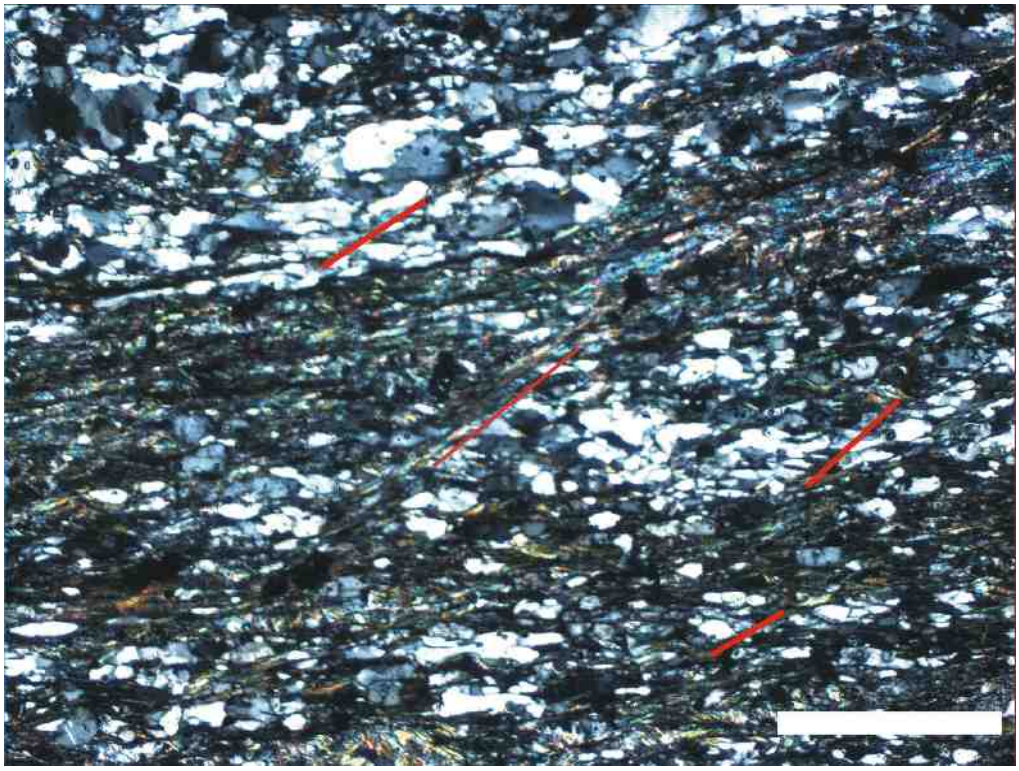

Figure 3.2: Thin section photograph of specimen HM06/13 showing a shear band parallel to the red line with minor recrystallisation of quartz. Parallel to the red line are also other smaller scale shear bands, forming a second penetrative cleavage. White bar is 1mm.

HM06/14

This hand specimen consists of three loose parts and was taken from the Golden point drivewall. Each of the three thin sections (labelled HM06/14-1, /14-2, /14-3) represent one part of the hand specimen. The rock is classified TZ IV like the previous sample. However, quartz veins play a more important role in this specimen due to their big size.

HM06/14-1: The thin section shows a 1 cm thick quartz vein with a shear band going through cutting it in half (figure 3.3). Quartz crystals show subgrain development and grain size reduction took place, too. The mineralogy of this sample consists basically of quartz, plagioclase, muscovite, chlorite and epidote, of which the latter being accessoric. Feldspar and micas are the main minerals outside of the quartz vein. Quartz is more or less restricted to the vein. However, the grain size within the vein, except for the sheared part, is relatively large (~ mm-scale).

HM06/14-2: This sample shows a shear band adjacent to a thick (5cm) quartz vein. The shear band cuts through the strain shadow of the quartz vein and deforms it slightly. It is mainly concentrated in a mica rich part of the thin section so there are only a few places where quartz is involved. However, at least at one location quartz is recrystallised (figure 3.4). The mineralogy is the same as in HM06/14-1.

HM06/14-3: This is the best thin section of sample 14. Several ductile shear bands can be seen (figures 3.5 and 3.6). The mineral composition stays the same as in the previous two thin sections but the occurrence of muscovite and chlorite has increased. The shear bands are located mostly in parts of the thin section where micas dominate but also cut through a few mm-scale quartz veins causing displacement and dynamic recrystallisation.

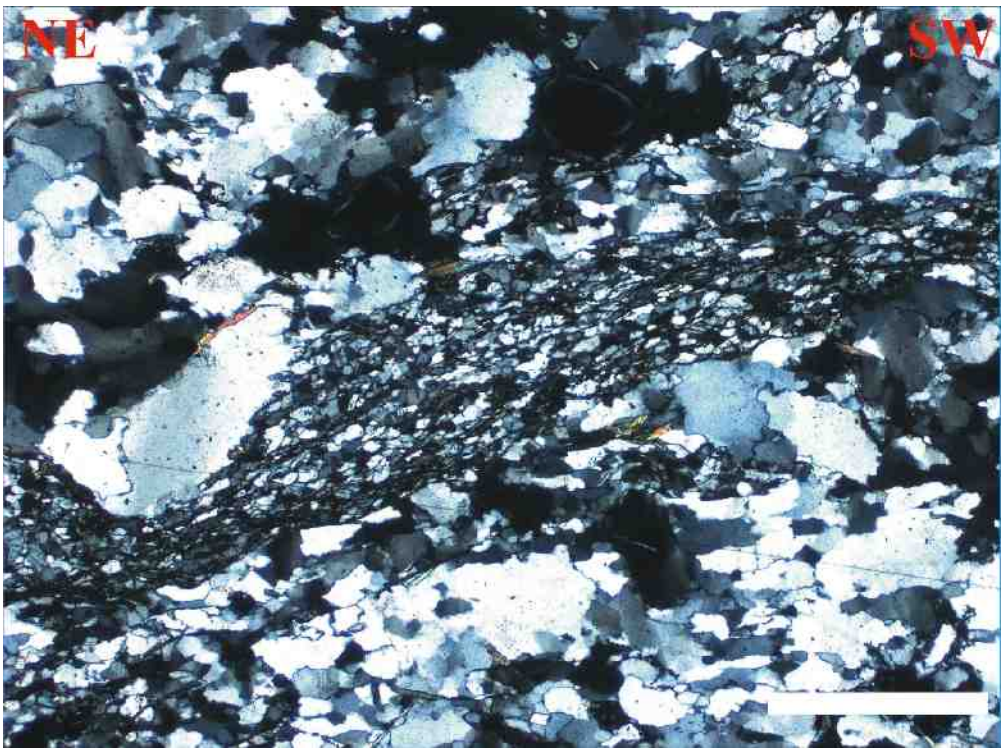

Figure 3.3: Photograph shows a mica rich shear band cutting through a quartz vein in specimen HM06/14-1. The photo shows a portion of a larger shear band structure in the hand specimen. White bar is 1 mm.

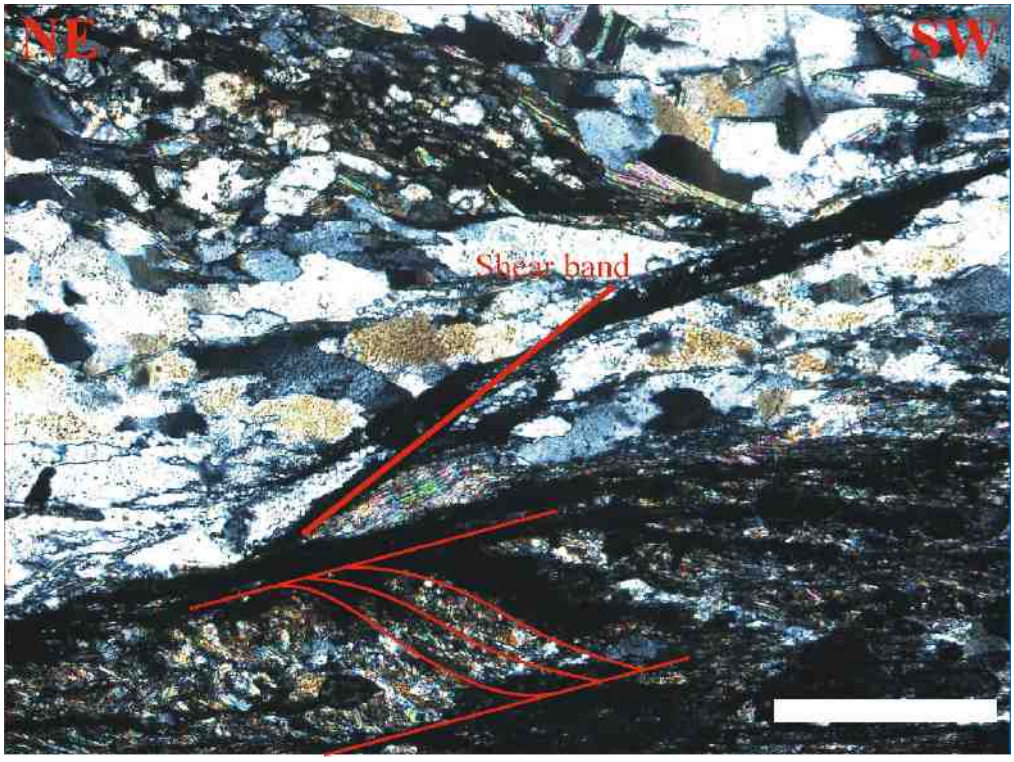

Figure 3.4: Picture of a shear band beneath a thick quartz vein in specimen HM06/14-2. Quartz has been recrystallised dynamically during shear band development. The larger quartz crystals show significant subgrain development and stretching and are deformed by the shear band. Remnants of an old C-S structure are observable in the lower half of the picture. White bar is 500 μm.

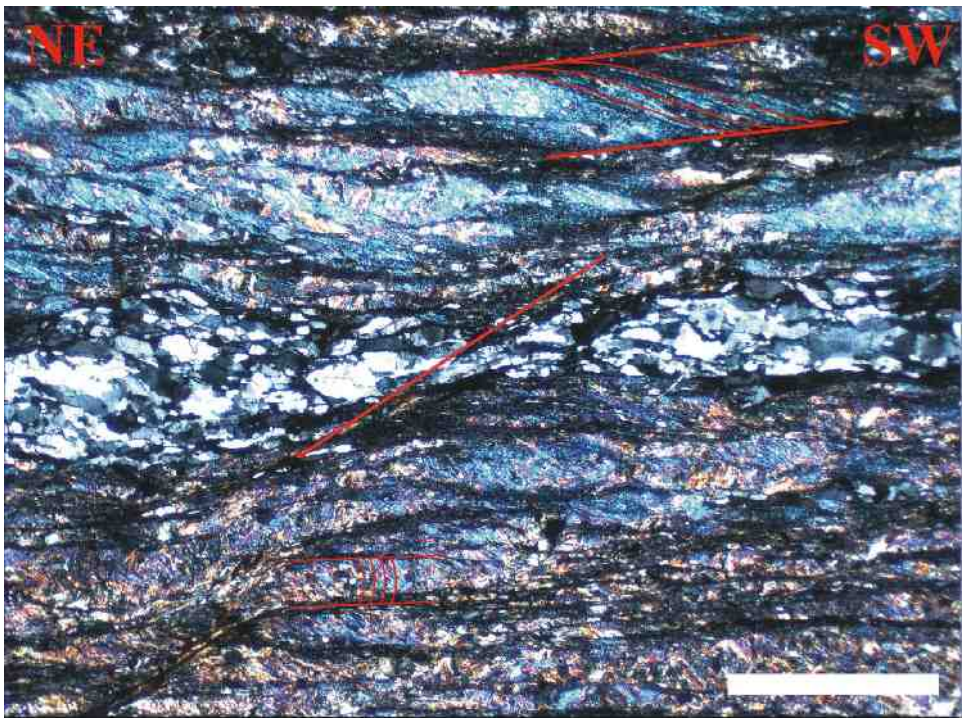

Figure 3.5: Small shear band parallel to the red line cutting through a mm-scale quartz vein in specimen HM06/14-3. Quartz has been reduced in grain size along the shear band. The mica rich sections of the thin section show an older crenulation cleavage which has been deformed by the shear band cleavage. White bar is 1mm.

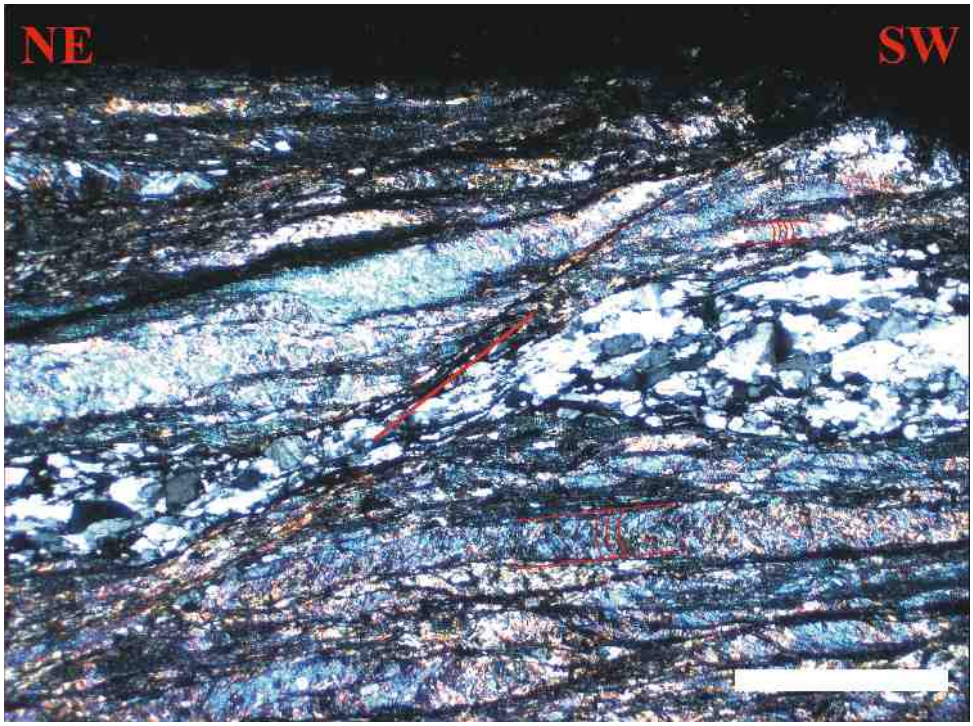

Figure 3.6: Shear band with quartz grain size reduction parallel to the red line in specimen HM06/14-3. The shear band also cuts through an older crenulation cleavage. White bar is 1mm.

HM06/16

This specimen is a massive quartzofeldspathic schist. It contains a 3 cm thick quartz vein that is deformed by shear bands. Structurally the specimen is located approximately 100 m below the Footwall Fault. Its mineralogy consists of quartz, feldspar and muscovite in particular. Accessoric minerals in this sample are calcite and garnet. This thin section does not show distinct quartz recrystallisation in the shear bands because the shear only occurred within mica layers (figure 3.7). However, a few quartz grains in the mica layers suggest reduction in grain size.

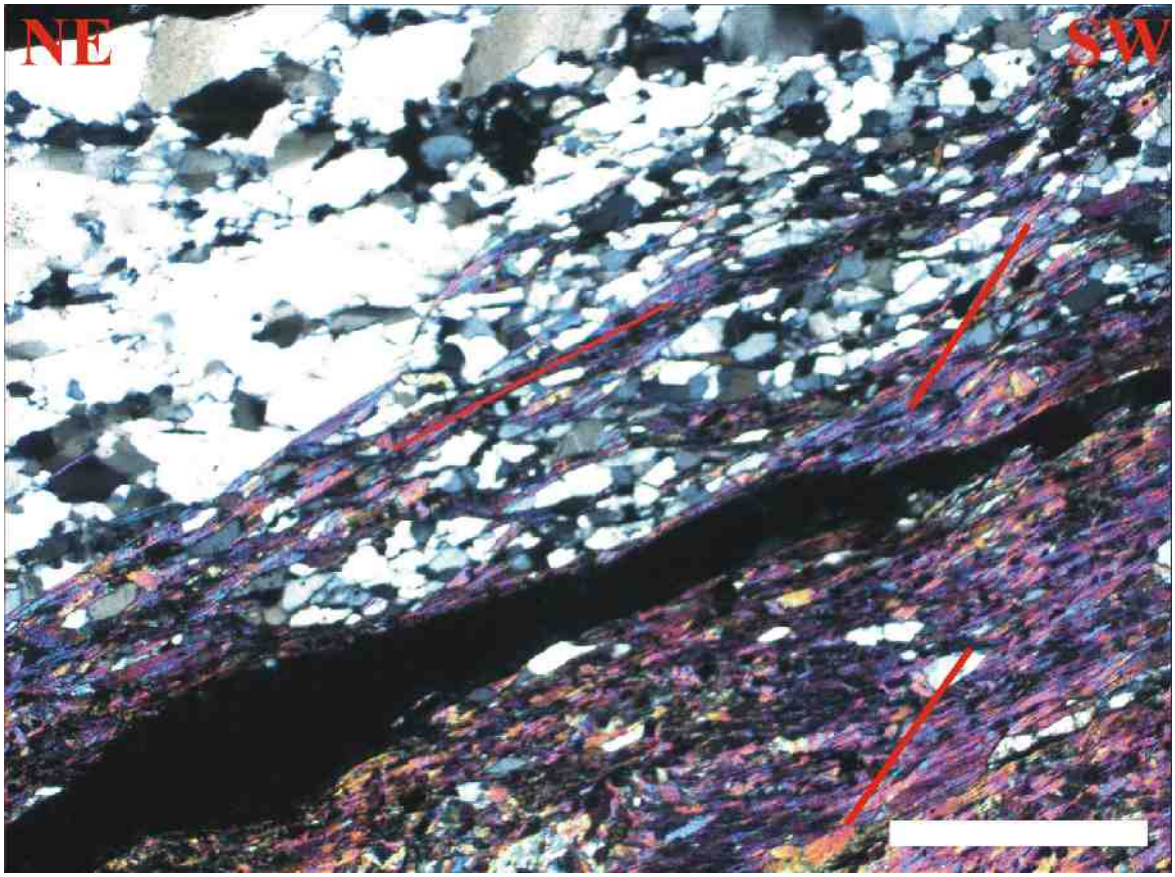

Figure 3.7: Shear bands in mica rich layers of a TZ IV psammite in specimen HM06/16. Vein quartz shows significant subgrains but no dynamical recrystallisation is observable in this specimen. White bar is 1mm.

HM06/06

The thin section of this sample is located between two 5 cm-scale quartz veins. It is about a massive quartzofeldspathic schist of TZ IV (figure 3.8). Main minerals are quartz, feldspar and mica. No accessoric minerals have been found. Shear bands are not very well developed in this section. Quartz grains show distinct subgrain development and minor grain size reduction.

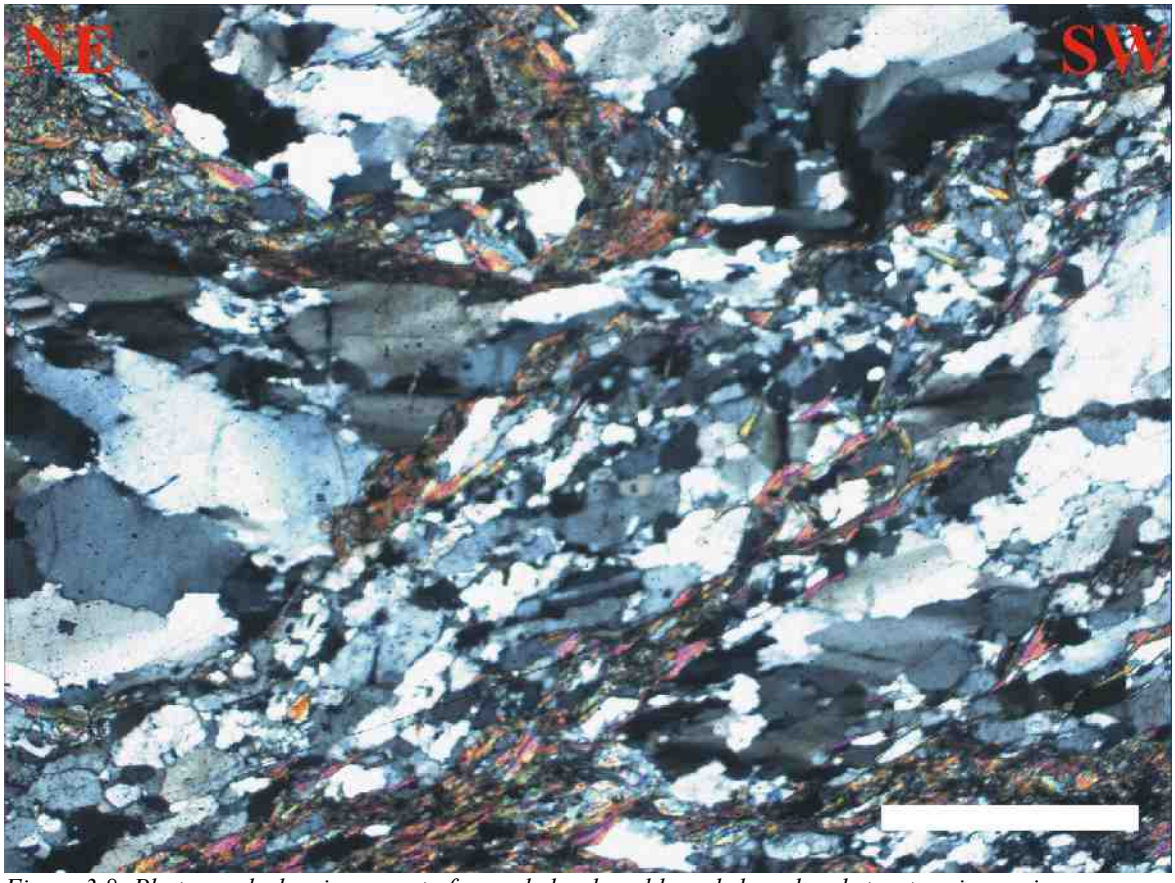

Figure 3.8: Photograph showing a part of a weak developed broad shear band structure in specimen HM06/06. Quartz has only been weakly reduced in grain size. However, a significant subgrain development within the shear band is observable.

HM06/10

The hand specimen to this thin section is part of the “Deepdell footwall 1” outcrop. The thin section was cut parallel to the stretching lineation directly adjacent to a brittle shear band plane. The mineralogy of the specimen consists of quartz, feldspar, muscovite, chlorite and accessoric epidote. The brittle shear band shows well developed quartz recrystallisation (figure 3.9). However, the grain size of the quartz crystals is generally reduced except for some mm-scale quartz veins. Ductile folds prior to the shear bands are also present.

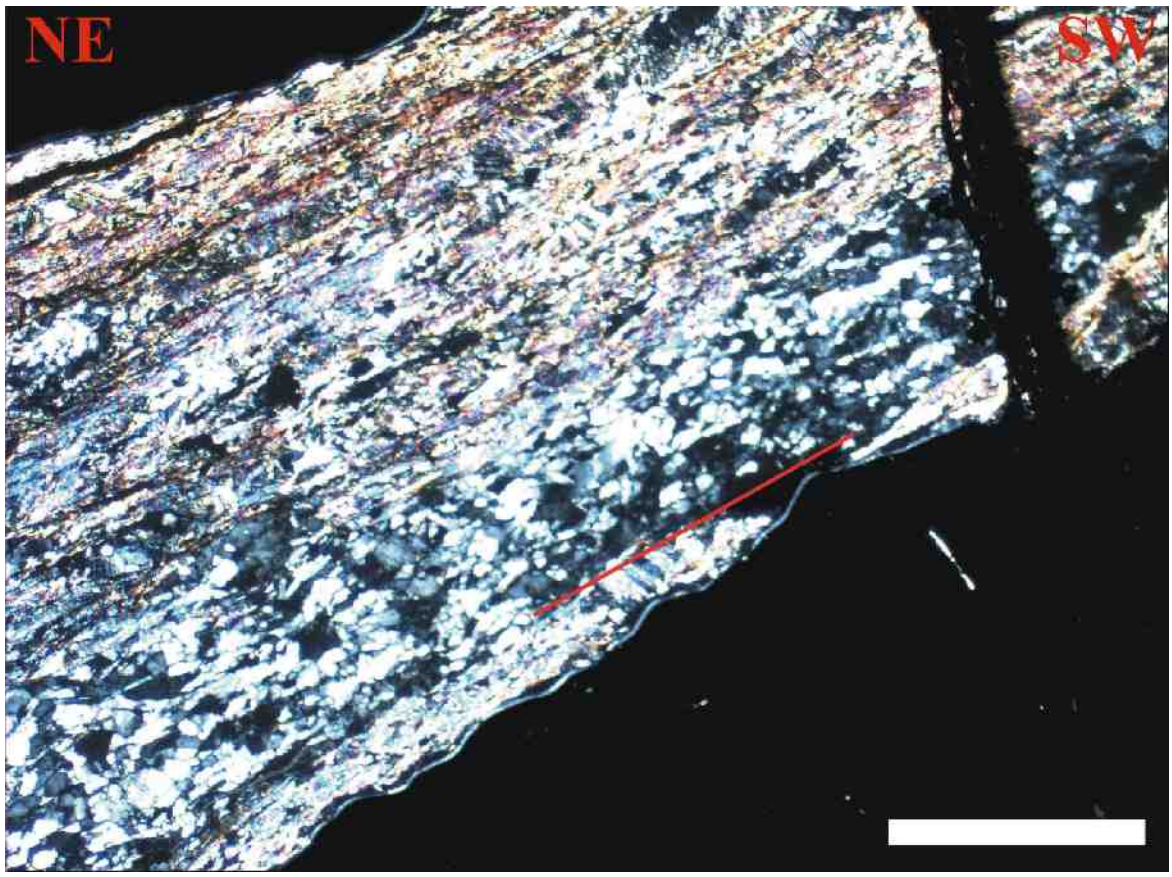

Figure 3.9: Photograph of a part of a major shear band in specimen HM06/10. Quartz crystals have been reduced in grain size (parallel to red line). White bar is 1mm long.

HM07/02

Macroscopically, this sample consists of strongly deformed cm-scale quartz veins with layers of mica and chlorite anastomosing around them, which also contain feldspar. The white mica grains are visible by naked eye which classifies the schist as TZ IV. The shear band cleavage is well developed and brittle cleavage planes, spaced at the 3-4cm scale, cut through the schist (see also figure 2.26). The cleavage planes show well expressed mineral lineation and slickenlines.

On the microscopic scale, the quartz grains show extensive subgrain development which often resulted in a reduction of grain size. This reduction climaxes in the shear bands where quartz grains only reach grain sizes of a few micrometers (figures 3.10 and 3.11). Quartz grains outside of the main veins are usually heavily elongated.

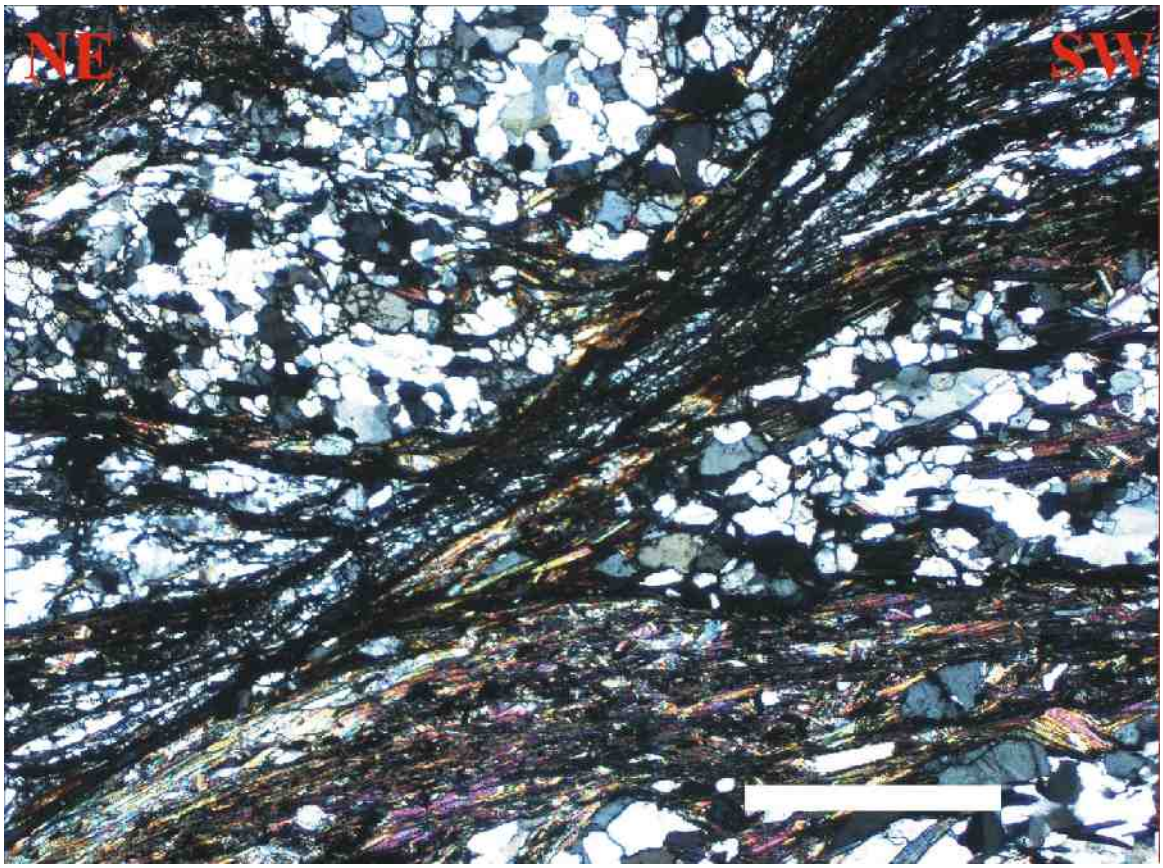

Figure 3.10: The picture shows a strong shear band in specimen HM07/02, cutting through an older foliation. The shear band shows extensive grain size reduction of quartz crystals and deforms larger grains in its vicinity. Larger quartz grains in this thin section commonly show distinct subgrain development. White bar for scale (1mm).

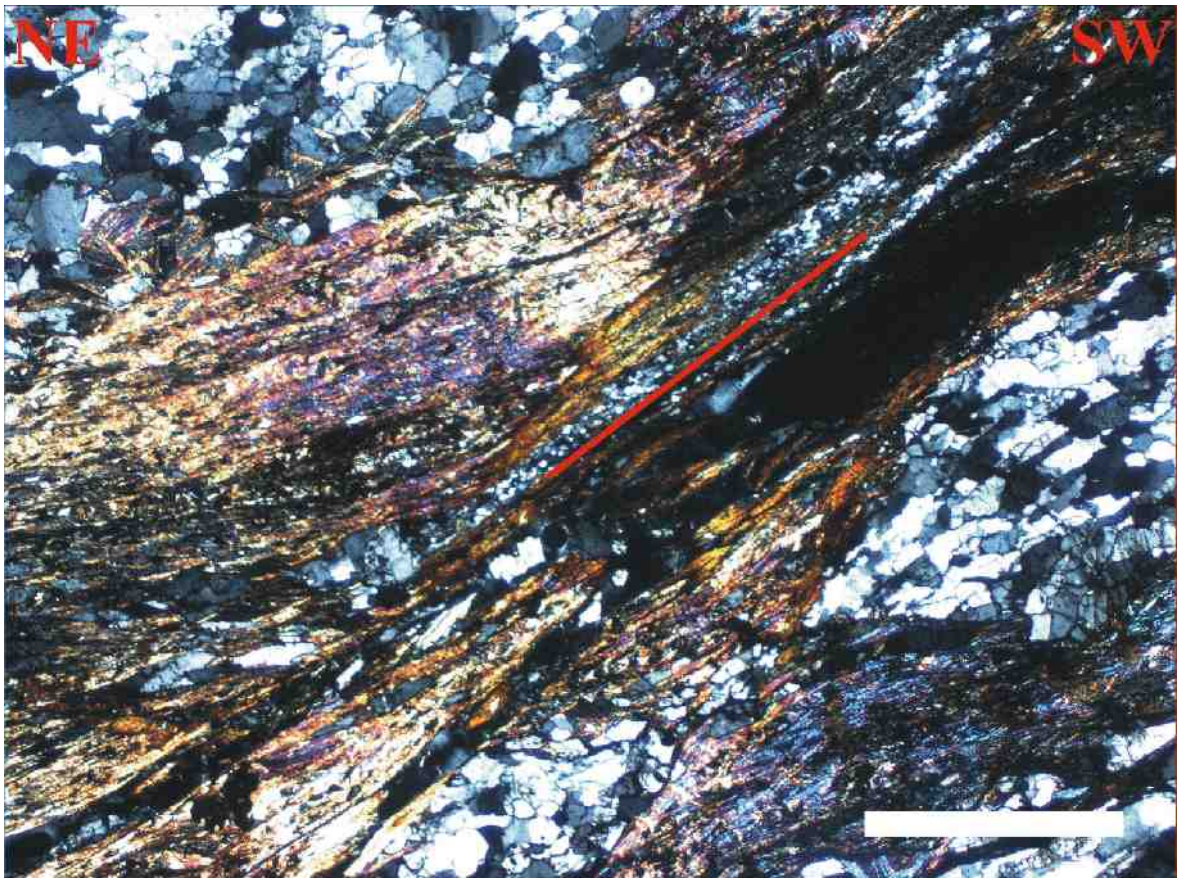

Figure 3.11: Thin section photograph of sample HM07/02. A well developed shear band runs from the top right to the bottom left corner. The shear band shows well developed reduction of grain size of quartz crystals. The deformation pattern of mica grains suggests displacement along the shear plane. Quartz crystals in this specimen commonly show distinct subgrains. The ductile shear band has a well developed brittle shear plane which suggests reactivation under brittle conditions. White bar for scale (1mm)

HM07/03

The thin section shows a psammitic TZ IV rock that consists of deformed cm-scale quartz veins that are surrounded by anastomosing layers of muscovite and chlorite. NE dipping shear bands are well developed in this thin section and show grain size reduction of quartz grains in some locations (figure 3.12). Apart from the main foliation and the second shear band cleavage there is also a third cleavage present which is not as well developed as the first two but also seems to form shear bands. This third foliation seems to dip into the opposite direction to the NE dipping shear band cleavage (figure 3.13). However, due to its weak development in the hand specimen the true dip could not be specified.

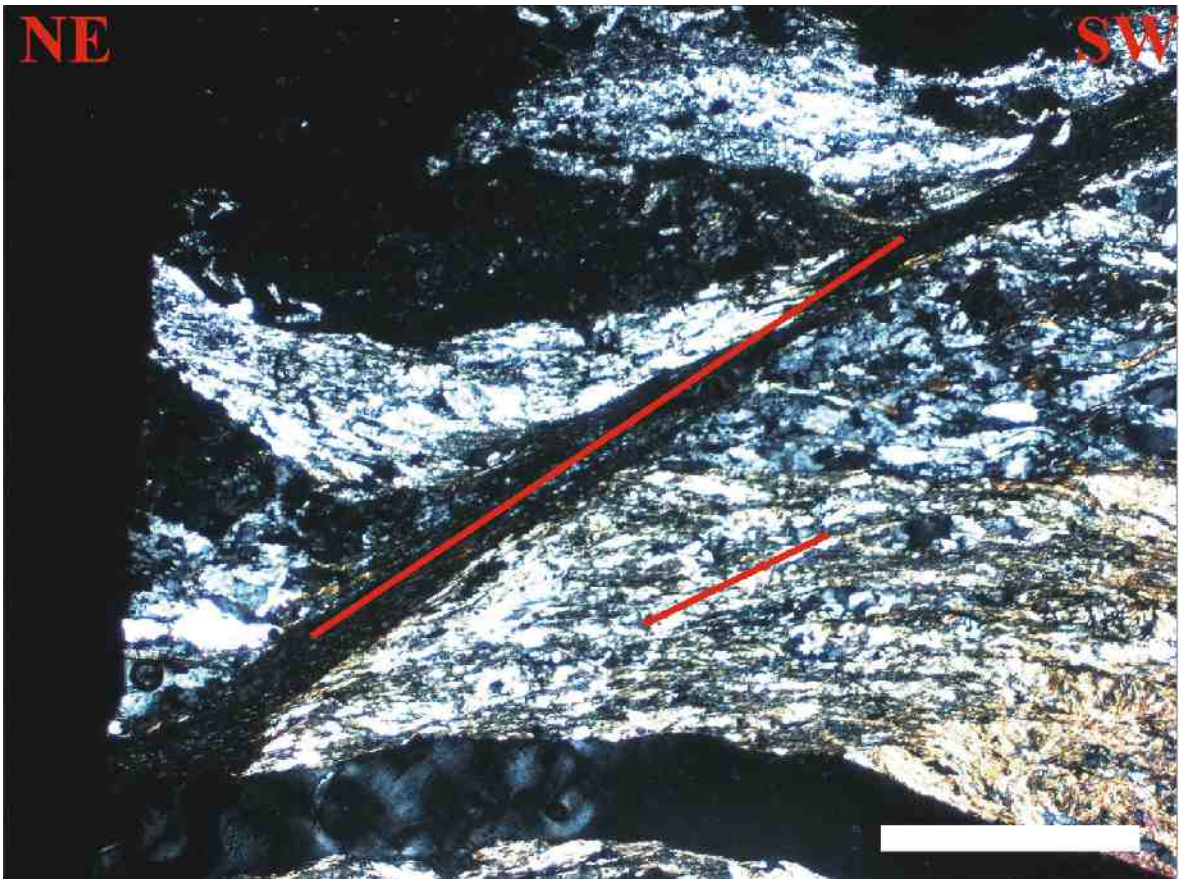

Figure 3.12: Thin section photograph from specimen HM07/03, showing a shear band with distinct reduction of the grain size of quartz crystals.The black band that forms the shear band looks like its containing very tiny micas and therefore is black. The shear band cuts through an older foliation and deflects and displaces individual layers. The photograph also shows a less developed shear band below the major one, additionally deforming the quartz and mica rich layer.

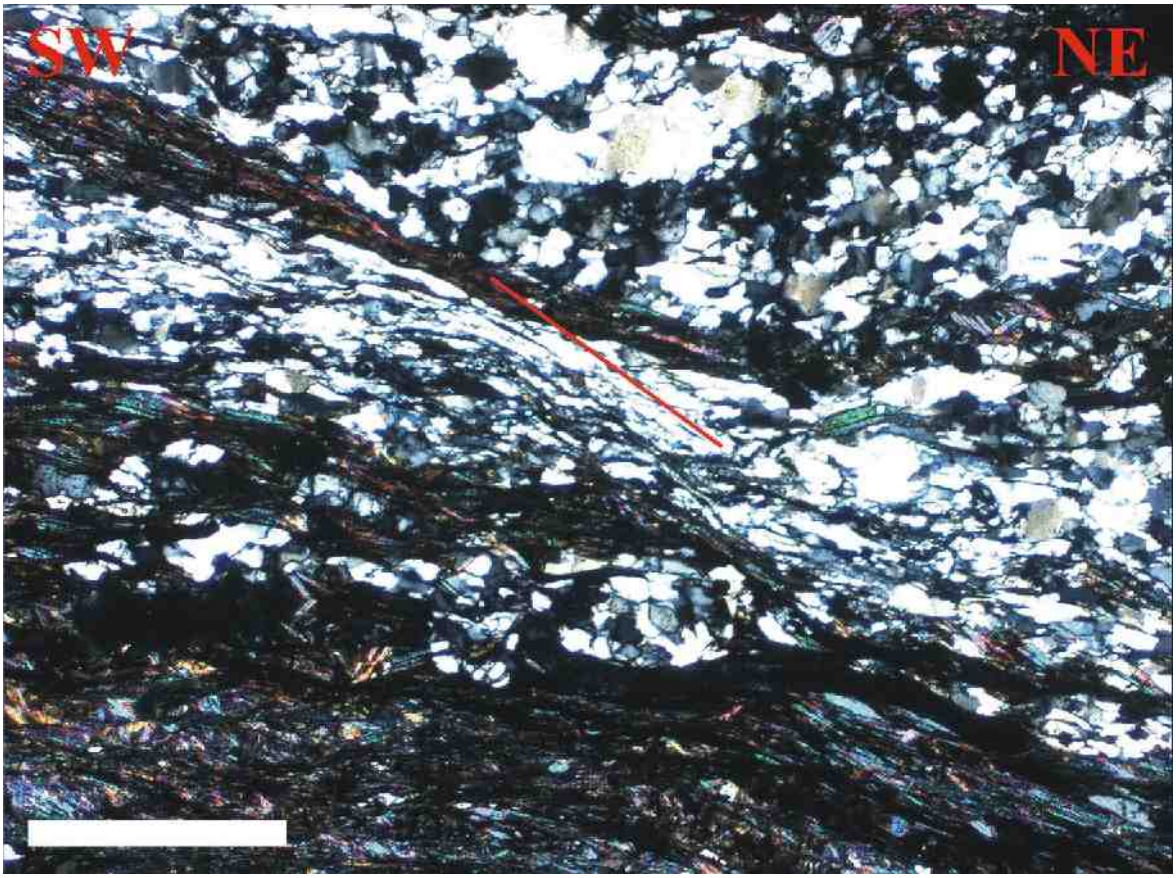

Figure 3.13: Small shear band in section HM07/03, dipping approximately to the SW, representing a part of a further cleavage which is only poorly developed. However, quartz has been dynamically reduced in grain size. This cleavage is probably a local coaxial component superimposed on general top-NE noncoaxial flow. White bar is 1mm.

HM06/01

Sample HM06/01 is taken from intrashear schist of the HMSZ at the historic mining pit. The thin section shows a change in the textural zone from TZ IV to TZ III. This is obvious due to the overall reduction of the mean white mica grain size but also other minerals are clearly reduced in size (figure 3.14). The mineral composition of this thin section is quartz, feldspar, muscovite, chlorite and accessory calcite and pyrite. The latter forms idiomorphic isotropic crystals. The texture of the schist is finely laminated and divided into small (mm-scale) layers of quartz veins and layers of mica, quartz and feldspar. However, the micas do not show a distinct preferred orientation but are rather chaotically arranged.

The grain size within the small veins is usually a little larger than in the surrounding layers. Some of the veins indicate reconditioning and some have been almost completely destroyed.

The thin section does not show any shear bands.

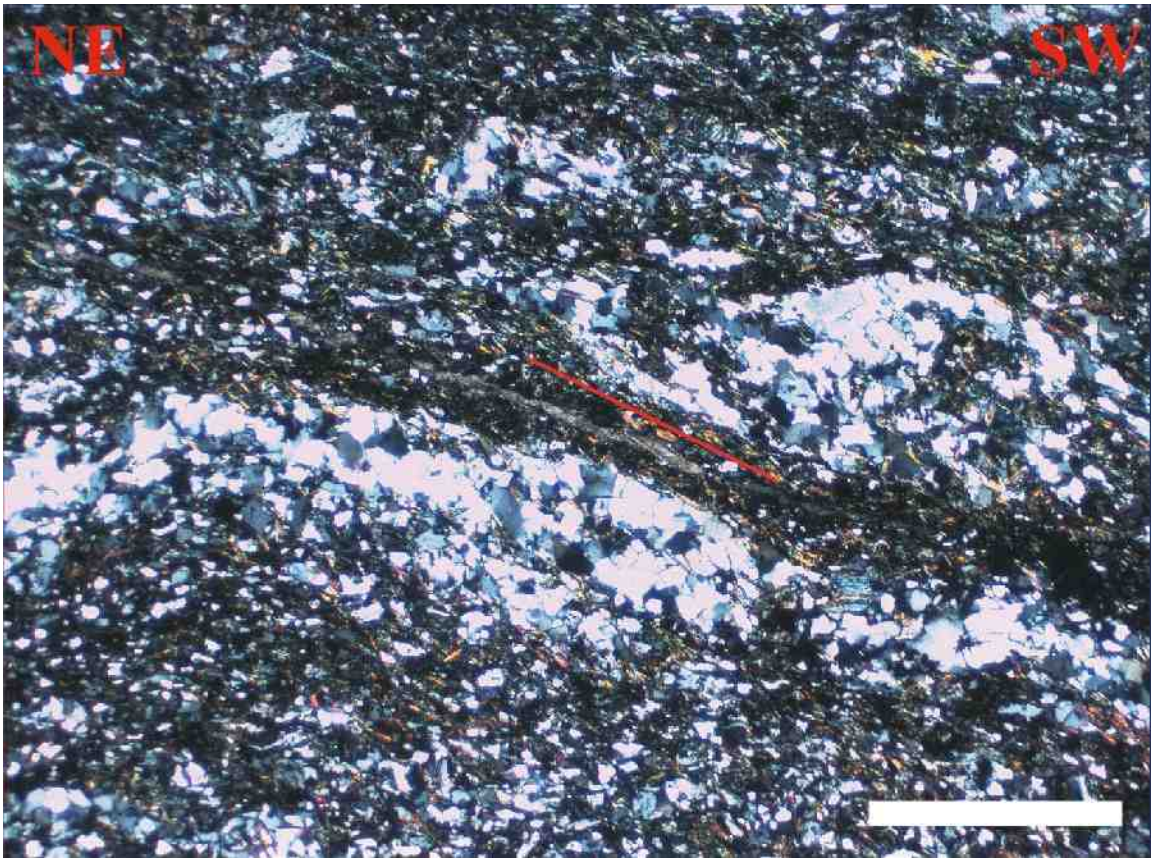

Figure 3.14: Thin section of a TZ III schist showing mm-scale deformed quartz veins and a micro-fracture parallel to the red bar that has been filled with calcite. The white bar is 1mm long.

HM06/02

In this thin section the original foliation has been destroyed completely. The rock is best described as a cataclasite. Mineral solutions run along the fractures and grainsizes of minerals vary a lot. In remnants of quartz veins the original grain size is preserved and approximately of mm-scale but show strong subgrain development (figure 3.15). However, most of the quartz grains have been strongly reduced in grain size (sub-mm-scale).
The hand specimen also belongs to the intrashear schist of the HMSZ and has been taken from an outcrop at the historic pit.

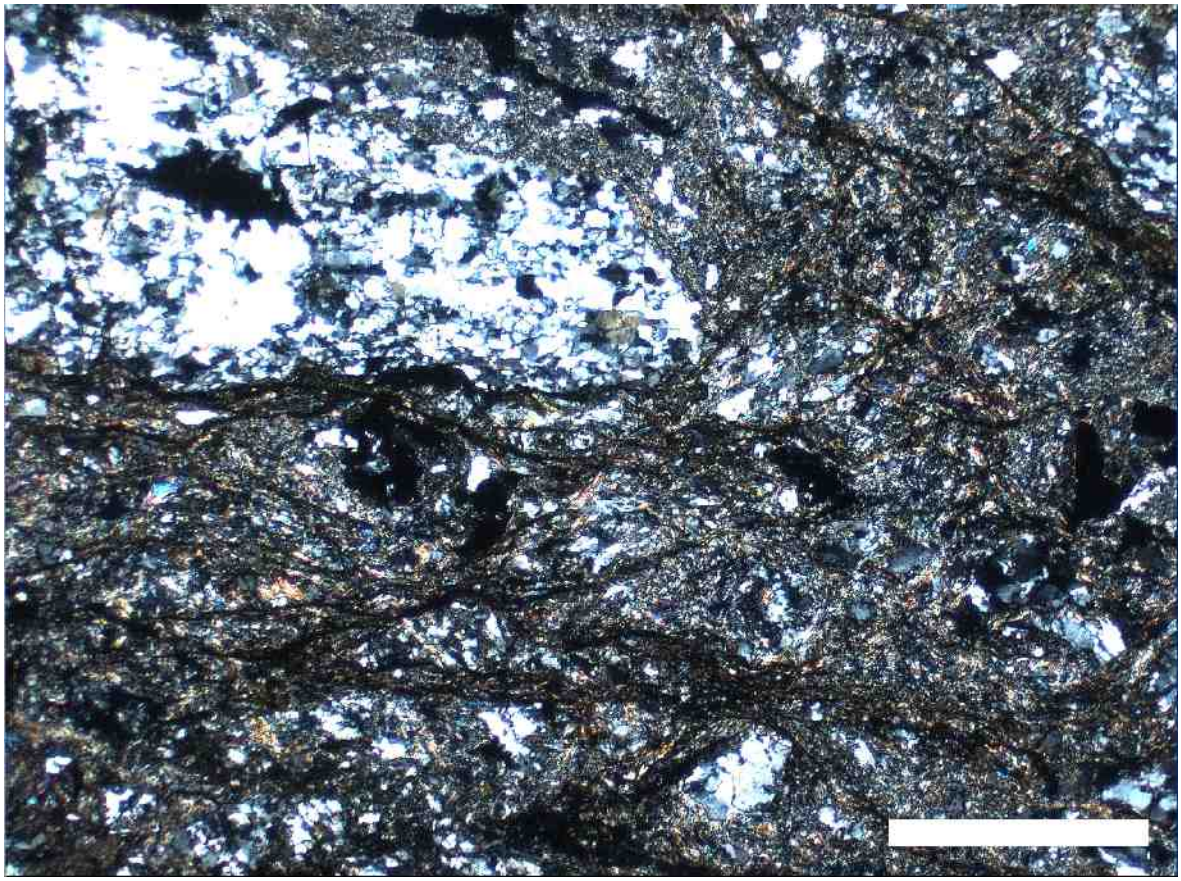

Figure 3.15: Highly deformed TZ III schist. Fractures are filled with iron-precipitals. The mean grain size has been reduced a lot.

3.3 Summary

This chapter presented the thin sections and mineral composition of the rocks in the field area. It has been shown that many shear bands have caused dynamic recrystallisation of quartz grains.

In one specimen a third shear band cleavage opposite to the first one is present but is very weakly developed and is not penetrative. This may be due to the same source that causes the foliation on the NW margin of the Deepdell creek valley to dip more to the west and NW. The 1:250.000 scale geologic map of Omaru shows a fault that runs parallel to the Deepdell creek in that area, which might be responsible for these phenomena.

The intrashear schist of the HMSZ is clearly distinct to the schist in the footwall of the Footwall Fault and is highly sheared. The shearing is very different to the shear bands in the footwall which is expressed by strong mineral-solutions in the hangingwall which dissolved minerals. Furthermore quartz seems not to be reduced in grain size by local high strain areas, but was reduced one a more global scale in the thin sections.

CHAPTER FOUR

Discussion and Conclusion

4.1. Extensional structures

This study has shown that extensional structures are an important structural element the shear zone. The Footwall Fault depicts a period of extension in the region but the timing of the switch from shortening to extension remains controversial. However, the occurrence of high grade schist fragments in the Kyeburn formation represents a minimum age for the exhumation of the footwall. Ar/Ar dating of tuff in the Kyeburn formation indicates an age of 112 Ma which is also supported by zircon dating of shag ignimbrite with an age of 113 Ma (Tulloch, pers. comm.).

Kinematic analysis of the extensional structures revealed a pattern resulting from NE-SW directed extension. Brittle normal faults represent one kind of those structures and are ubiquitous, especially in the hangingwall.

In the footwall, brittle normal faults are found mainly close to the Footwall Fault, but are also found in greater distance as shown by the Gully fault zone in Outcrop 6 of the footwall.

One of the main findings of this study, however, is a penetrative shear band cleavage in the footwall (figure 4.1). Shear bands of this kind are commonly found in conjunction with ductile shear zones because they represent areas of concentrated strain in which quartz crystals can be recrystallised. The conditions at which quartz recrystallises dynamically are >280°C, at pressures of >1 kbar (Rutter 1976). The presence of shear bands, resulting from NE extension in the footwall therefore indicates ductile conditions during the onset of extension in the footwall.

Thin section examination of the shear bands showed that quartz has been ductily deformed at several locations in the footwall.

The hangingwall does not show any signs of shear bands or shear band cleavages and deformed entirely in a brittle fashion. The intrashear schist of the HMSZ shows micro-fractures, cataclastic deformation and also recrystallisation of quartz.
Structural Mapping SW of the historic Battery, along the Deepdell creek valley, shows a rotation of the main regional foliation from a gentle NE dip to a moderate SW dip. The rotation occurs over a distance of approximately 2.5 km in the footwall of the Footwall Fault.
An explanation for the foliation pattern will be discussed in section 4.4.

4.3. Brittle-Ductile Transition

It is commonly assumed that brittle deformation is the main mechanism for the normal sense movement on the Footwall Fault (Craw 2002). However, this study presented evidence for ductile deformation in the footwall of the Footwall Fault. Furthermore, many of the shear bands evolved into brittle fault planes or have been truncated by brittle high angle normal faults. This places the start of the extensional reactivation of the HMSZ, represented by the Footwall Fault, in a ductile environment and indicates that normal sense of movement continued as the Footwall Fault passed through the ductile-brittle transition.
Because earlier studies (e.g. Teagle et al. 1990) showed that also the HMSZ and its hangingwall moved through the ductile-brittle transition during earlier thrusting, I conclude that footwall and hangingwall of the HMSZ must have distinctly different pressure-temperature-time (P-T-t) histories.

4.4. The Rolling Hinge Model

The regional tectonic setting of the HMSZ and the Footwall Fault involves a further feature that has not been discussed yet: The Waihemo Fault. The Waihemo fault is located approximately 10 km in slip direction of HMSZ. The Waihemo Fault is a high-angle fault that is traceable over several kilometers strike-parallel in the hangingwall of the HMSZ. According to present day knowledge the Footwall Fault is cut by the Waihemo Fault (figure 4.1). This study suggests a direct relationship between the Footwall Fault and the Waihemo Fault which could be explained by the rolling hinge model.

According to the rolling hinge model, a high-angle fault develops due to crustal extension within the brittle crust and cuts down to (and maybe through) the brittle-ductile transition. Isostatic rebound causes ductile material to rise. Exhumation of metamorphic rocks occurring in the footwall of the normal fault causes a rotational movement of the footwall block (figure 1.3c). The main effect of this process is that the steep fault becomes rotated to a shallower angle towards the surface giving the entire structure a convex shape.

After Andersons theory of faulting, this rotation of the fault causes the fault to become inactive at low dip angles. This means that if the angle becomes too shallow (that is < 30°), the shallow part of the fault will be abandoned, eventually. In this point, a new structure has to develop in slip direction in order to create a stress equilibrium. This new structure usually has a steep angle.

Applying this model to the tectonic setting of HMSZ, FWF and Waihemo Fault, some similarities become obvious:

(1) Tectonic setting: The Waihemo Fault is a high-angle fault that developed in slip direction of the Footwall Fault. The latter might be interpreted as a structure that rotated into its present low-angle orientation and therefore became inactive. At this time, the high-angle Waihemo Fault formed and took up regional extension.

(2) Timing of activation of the Waihemo fault: The development of the Waihemo Fault is linked to the occurrence of Albian volcanism in Otago, and the tuffs that have been dated in this region coincide with the first high grade schist fragments in the Kyeburn formation. This suggests that the Waihemo Fault developed at a late stage or shortly after the high grade core of the Otago region was exhumed.

(3) The foliation pattern in the footwall of the Footwall Fault: As outlined above, the foliation in the footwall rotates from a gentle NE orientation to a moderate SW orientation within a distance of approximately 2.5 km in the footwall of the Footwall Fault (figure 4.1). This pattern can derive from a simple normal movement along the Footwall Fault, but would require an originally SW-oriented foliation to be explained properly. However, there is no evidence for an originally SW-oriented foliation in this part of the Otago schist. The general orientation of the foliation NE of the Otago antiform is to the NE (Mortimer 2003), and therefore a SW-dipping foliation would be an anomaly relative to the common orientation. The rolling hinge model, however, can explain the foliation pattern without assuming an anomalously SW-dipping regional foliation. The exhumation of the high grade schist in the footwall of the crustal-scale fault causes the fault plane to rotate, and with this rotation, also the foliation becomes rotated. Due to the resistance of the overlying hangingwall block, the rotation of the foliation close to the footwall is restricted to a minimum and increases with distance.

(4) The Gully shear zone: The shear band cleavage in the footwall of the Footwall Fault has a close spacing in the cm-scale in two areas in particular: In the Outcrops 1 and 2 of the footwall, and in the footwall of a further shear zone near Deepdell settlement (Outcrop 6). This shear zone also is approximately strike-parallel to the Footwall Fault and could be explained as a part of the crustal-scale fault that has been abandoned prior to the Footwall Fault.

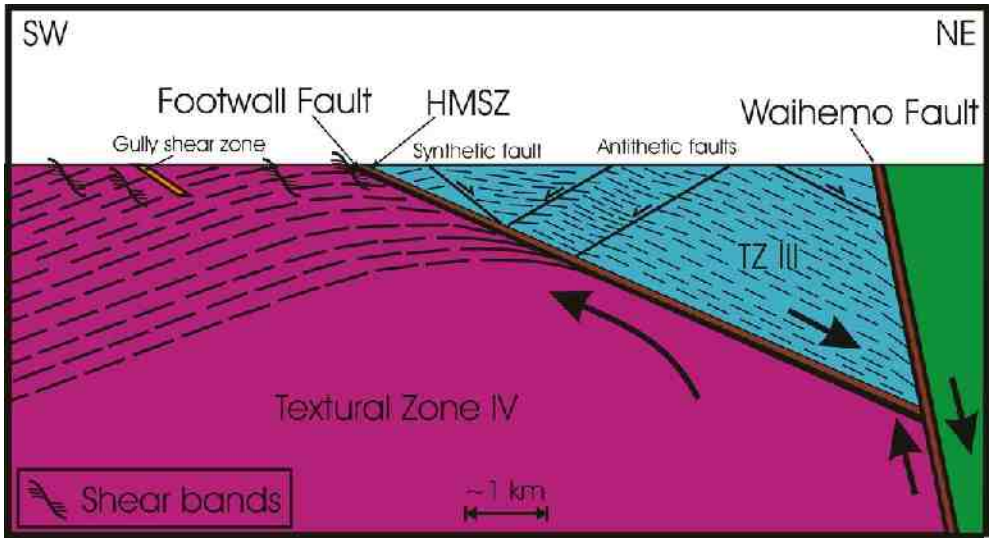

Figure 4.1: Cross section through the Deepdell creek, illustrating foliation patterns in hangingwall and footwall of the Footwall Fault. Also showing shear band locations in the footwall and suggested major brittle normal faults in the hangingwall. The section starts in the SW from the electricity substation c. 400m S of Deepdell settlement.

4.5. Implications for the Regional Geology

If my rolling hinge explanation for the Footwall Fault was correct, there should be further manifestations observeable in the region. The most obvious manifestation would possibly be the textural and metamorphic change to the NE from a high grade garnet-biotite-albite zone to a lower grade greenschist chlorite zone. The boundary of these zones is often accompanied by low-angle normal faults like the Capburn Fault and the Thompsons Gorge Fault which occur approximately strike-parallel to the Footwall Fault (figure 1.2b). The region between the TGF, CBF and FWF is often disturbed by Miocene NE-striking reverse faults like the Dunstan Fault or the Blackstone Fault, which created basins filled with a sedimentary cover. This makes it difficult to find proof for a relationship between these faults. On the other hand, the regularity at which regional-scale normal faults occur along the boundary of these two textural zones, already suggests some kind of relationship. A possible relationship could be the development of an array of individual faults which formed during the same regional extensional deformation event. However, the individual faults are probably not physically connected with each other, because a single structure of a size of c. 100 km would produce a maximum displacement of several tens of kilometers in its centre, which would be between the Capburn Fault and the Thompsons Gorge Fault. However, that is apparently not the case.

This model is not new: Deckert et al. (2002) already suggested a relationship between the extensional faults at the northern periphery of the Otago antiform but did not distinguish between the mineralised shear zones and the fault zones that caused the juxtaposition of the schist of different metamorphic grade. This resulted in some confusion in following publications and may have superseded the fundamental idea. Deckert et al. (2002) suggested that the normal faults are part of an array of faults that developed during New Zealand wide rifting in the Albian, which were replaced eventually by structurally higher faults at the margin of the Otago schist. These structurally higher faults are represented to the NE by the Waihemo Fault and Hawkdun Fault, which together form a long strike-parallel array to the boundary of the garnet-biotite-albite zone and the lower greenschist facies chlorite zone.

4.6. Further Work

Whether or not the rolling hinge model is applicable can be tested by zircon fission-track dating. For a NE-dipping normal fault, the fission track ages in the footwall of this normal fault should become progressively older in a SW direction (figure 4.2). Furthermore, the fission-track cooling ages should be around 110-115 Ma if the proposed causal relationship between the Waihemo Fault and the Footwall Fault was correct.
Using the geochronological criterion from Wheeler & Buttler (1994), a fission-track might provide additional proof for crustal extension along the Footwall Fault as well. For this purpose, eleven handspecimens for fission track dating have been collected which will be subject to further studies.
The locations of the hand specimens for fission-track dating are presented in appendix A, Map E.

A further subject of study may also be the detailed mapping of the boundary of the garnet-biotite-albite zone and the lower greenschist facies chlorite zone between the Capburn Fault and the Thompsons Gorge Fault. If the theory of an array of individual faults is true there should be evidence of further individual faults along that boundary. This is not an easy task because of many basins in which these faults (if they actually exist) are covered by sediments. However, along some of the mountain ranges, the faults may be observable.

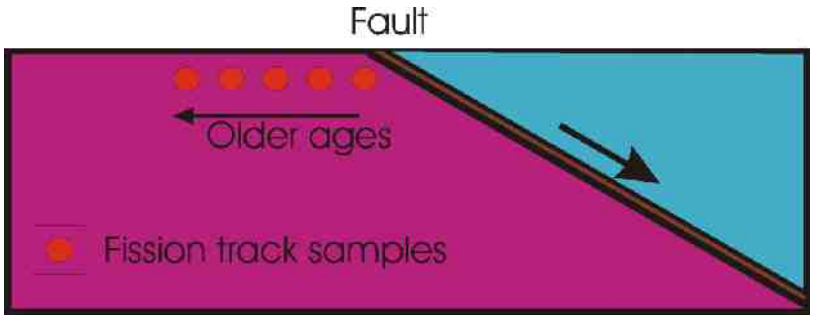

Figure 4.2: Scheme illustrating fission track dating. Fission track ages should become older in the direction of the arrow below the sample locations.

4.7. Summary

This study focussed on the kinematic evolution, responsible for the development of the Footwall Fault. For this purpose, structural mapping was carried out at the historic battery near Macraes flat. The results of this mapping were data about the foliation pattern in hangingwall and footwall, which showed a rotation of the foliation towards the Footwall Fault in the footwall and a relatively uniform NE-dipping foliation pattern for the hangingwall.

Strike-parallel faults in adjacent gullies may be subsidiary faults of the Footwall Fault, which slightly rotate the foliation either to the SW or NE. SW-orientation was observed for the foliation before the first gully NE of the Footwall Fault and indicates synthetic block rotation. NE-rotation was observed in the following gullies, indicating antithetic block rotation.

One of the main findings in this study is a shear band cleavage in the footwall of the Footwall Fault indicating that the Footwall fault started its activity under ductile conditions. Kinematic analysis of abundant brittle normal faults in hangingwall and footwall indicate that this activity continued as the schist passed through the ductile-brittle transition.

References

Adams CJ, Graham IJ 1997. Age of metamorphism of Otago Schist in eastern Otago and determination of protoliths from initial strontium isotope characteristics. New Zealand Journal of Geology and Geophysics 40(3): 275-286.

Angus PV 1992. The structural evolution of the Hyde-Macraes Shear Zone at Round Hill, Otago, New Zealand. Proceedings of the 26th Annual Conference, New Zealand Branch, Australasian Institute of Mining & Metallurgy. : 11p.

Axen GJ 2004. Mechanics of Low-Angle Normal Faults. In: Garry D. Karner BT, Neal W. Driscoll, and David L. Kohlsted ed. Rheology and Deformation of the Lithosphere at Continental Margins. New York, Columbia University Press. Pp. 46 - 91.

Begbie MJaS, R.H. 2005. Structural controls on the development of fault-hosted scheelite-gold Mineralisation at Glenorchy, northwest Otago. In: Geology and exploration of New Zealand mineral deposits. Christie, A.B. and Braithwaite, R. eds. Australasian Institute of Mining and Metallurgy Monograph
25.

Chappell DA, Craw D 2002. Geological analogue for circumneutral pH mine tailings: Implications for long-term storage, Macraes Mine, Otago, New Zealand. Applied Geochemistry 17(8): 1105-1114.

Cowan DS, Brandon MT 1994. A symmetry-based method for kinematic analysis of large-slip brittle fault zones. American Journal of Science 294(3): 257-306.

Cowie PA, Scholz CH 1992. Physical explanation for the displacement-length relationship of faults using a post-yield fracture mechanics model. Journal of Structural Geology 14(10): 1133-1148.

Cowie PA, Scholz CH 1992. Displacement-length scaling relationship for faults: data synthesis and discussion. Journal of Structural Geology 14(10): 1149-1156.

Cowie PA, Roberts GP 2001. Constraining slip rates and spacings for active normal faults. Journal of Structural Geology 23(12): 1901-1915.

Cox L, MacKenzie DJ, Craw D, Norris RJ, Frew R 2006. Structure and geochemistry of the Rise & Shine Shear Zone mesothermal gold system, Otago Schist, New Zealand. New Zealand Journal of Geology and Geophysics 49(4): 429-442.

Craw D, Norris RJ 1991. Metamorphogenic Au-W veins and regional tectonics: mineralisation throughout the uplift history of the Haast Schist, New Zealand. New Zealand Journal of Geology & Geophysics 34(3): 373-383.

Craw D, Angus PV 1993. Mafic/ultramafic clasts in deformed biotite zone metaconglomerate, Macraes mine, Haast Schist, New Zealand. New Zealand Journal of Geology & Geophysics 36(3): 395-398.

Craw D, Windle SJ, Angus PV 1999. Gold mineralization without quartz veins in a ductile-brittle shear zone, Macraes Mine, Otago Schist, New Zealand. Mineralium Deposita 34(4): 382-394.

Craw D, Norris, R J and MacKenzie, D J. 2000. Genetic classification and prospectivity of gold-bearing veins in the Otago Schist, New Zealand. N Z Minerals & Mining Conference Proceedings.

Craw D 2001. Tectonic controls on gold deposits and their environmental impact, New Zealand. Journal of Geochemical Exploration 73(1): 43-56.

Craw D 2002. Geochemistry of late metamorphic hydrothermal alteration and graphitisation of host rock, Macraes gold mine, Otago Schist, New Zealand. Chemical Geology 191(4): 257-275.

Craw D, MacKenzie, D J, Begbie, M & Norris R J. 2005. Late metamorphic structural zones in the Otago Schist: prospective hosts for gold mineralilsation. 2005 NZ Minerals Conference: Realising New Zealand's mineral potential: pp 89-97.

Craw D, Begbie M, MacKenzie D 2006. Structural controls on tertiary orogenic gold mineralization during initiation of a mountain belt, New Zealand. Mineralium Deposita 41(7): 645-659.

De Ronde CEJ, Faure K, Bray CJ, Whitford DJ 2000. Round Hill shear zone-hosted gold deposit, Macraes Flat, Otago, New Zealand: Evidence of a magmatic ore fluid. Economic Geology 95(5): 1025-1048.

Deckert H, Ring U, Mortimer N 2002. Tectonic significance of Cretaceous bivergent extensional shear zones in the Torlesse accretionary wedge, central Otago Schist, New Zealand. New Zealand Journal of Geology and Geophysics 45(4): 537-547.

Forster MA, Lister GS 2003. Cretaceous metamorphic core complexes in the Otago Schist, New Zealand. Australian Journal of Earth Sciences 50(2): 181 - 198.

Jackson J, Norris R, Youngson J 1996. The structural evolution of active fault and fold systems in central Otago, New Zealand: evidence revealed by drainage patterns. Journal of Structural Geology 18(2-3): 217-234.

Kimbrough DL, Tulloch AJ, Coombs DS, Landis CA, Johnston MR, Mattinson JM 1994. Uranium-lead zircon ages from the Median Tectonic Zone, New Zealand. New Zealand Journal of Geology & Geophysics 37(4): 393-419.

Korsch RJ, Wellman, H.W. 1988. The geological evolution of New Zealand and the New Zealand region. In: Nairn AES, F.G.; Uyeda, S. ed. The ocean basins and their margins. New York, Plenum Press. Pp. 411 - 482.

Laird MG, Bradshaw JD 2004. The break-up of a long-term relationship: The Cretaceous separation of New Zealand from Gondwana. Gondwana Research 7(1): 273-286.

Little TA, Mortimer N, McWilliams M 1999. An episodic Cretaceous cooling model for the Otago-Marlborough Schist, New Zealand, based on 40Ar/39Ar white mica ages. New Zealand Journal of Geology and Geophysics 42(3): 305-325.

MacKenzie DJ, Craw D 1993. Structural control of gold-scheelite mineralisation in a major normal fault system, Barewood, eastern Otago, New Zealand. New Zealand Journal of Geology & Geophysics 36(4): 437-445.

MacKenzie DJ, Craw D 2005. The mercury and silver contents of gold in quartz vein deposits, Otago Schist, New Zealand. New Zealand Journal of Geology and Geophysics 48(2): 265-278.

MacKenzie DJ, Craw D 2005. Structural and lithological continuity and discontinuity in the Otago Schist, Central Otago, New Zealand. New Zealand Journal of Geology and Geophysics 48(2): 279-293.

MacKenzie DJ, Corner, N. and Craw, D. 2005. The Rise and Shine Shear Zone, Central Otago. In: Geology and exploration of New Zealand mineral deposits. Christie, A.B. and Braithwaite, R. eds. Australasian Institute of Mining and Metallurgy Monograph 25.

MacKenzie Dj, Youngson, J.H. and Craw, D. 2005. Taieri River Mineralised Vein Swarm, East Otago. In: Geology and exploration of New Zealand mineral deposits. Christie, A.B. and Braithwaite, R. eds. Australasian Institute of Mining and Metallurgy Monograph 25.

MacKenzie DC, D.; Cox, L.; Norris, R. 2005. Mineralisation and structural setting of the Rise and Shine Shear Zone, Otago Schist: comparisons to the Macraes deposit. Proceedings of the 2005 New Zealand Minerals Conference: 374-379.

Markley M, Tikoff B 2003. Geometry of the folded Otago peneplain surface beneath Ida valley, Central Otago, New Zealand, from gravity observations. New Zealand Journal of Geology and Geophysics 46(3): 449-456.

McKeag SA, Craw D, Norris RJ 1989. Origin and deposition of a graphitic schist-hosted metamorphogenic Au-W deposit, Macraes, East Otago, New Zealand. Mineralium Deposita 24(2): 124-131.

Mitchell M, Maw, L., Angus, P.V. and Craw, D. 2005. The Macraes Gold Deposit, East Otago. In: Geology and exploration of New Zealand mineral deposits. Christie, A.B. and Braithwaite, R. eds. Australasian Institute of Mining and Metallurgy Monograph 25.

Mortimer N, Roser BP 1992. Geochemical evidence for the position of the Caples-Torlesse boundary in the Otago Schist, New Zealand. Journal - Geological Society (London) 149(6): 967-977.

Mortimer N 1993. Jurassic tectonic history of the Otago schist, New Zealand. Tectonics 12(1): 237-244.

Mortimer N 2000. Metamorphic discontinuities in orogenic belts: example of the garnet-biotite-albite zone in the Otago schist, New Zealand. International Journal of Earth Sciences 89: 295-306.

Mortimer N 2003. A provisional structural thickness map of the Otago Schist, New Zealand. American Journal of Science 303(7): 603-621.

Mortimer N 2004. New Zealand's geological foundations. Gondwana Research 7(1): 261-272.

Mortimer N, Richard C. Selley LRMCaIRP 2005. NEW ZEALAND. Encyclopedia of Geology. Oxford, Elsevier. Pp. 1-8.

Petrie BS, Craw D 2005. Lithological controls on structural evolution of mineralised schist, Macraes gold mine, Otago, New Zealand. New Zealand Journal of Geology and Geophysics 48(3): 435-446.

Petrie BS, Craw D, Ryan CG 2005. Geological controls on refractory ore in an orogenic gold deposit, Macraes mine, New Zealand. Mineralium Deposita 40(1): 45-58.

Pettinga JRY, M.D.; van Dissen, R.J.; Downes, G. 2001. Earthquake source identification and characterisation for the Canterbury region, South Island, New Zealand. Bulletin of the New Zealand Society for Earthquake Engineering 34: 282-317.

Pitcairn IK, Roberts S, Teagle DAH, Craw D 2005. Detecting hydrothermal graphite deposition during metamorphism and gold mineralization. Journal of the Geological Society 162(3): 429-432.

Roddick-Lanzilotta AJ, McQuillan AJ, Craw D 2002. Infrared spectroscopic characterisation of arsenate (V) ion adsorption from mine waters, Macraes mine, New Zealand. Applied Geochemistry 17(4): 445-454.

Rutter EH 1976. The kinetics of rock deformation by pressure solution. . Phil. Trans. Roy. Soc. Lond. A283: 203-217.

Teagle DAH, Norris RJ, Craw D 1990. Structural controls of gold-bearing quartz mineralization in a duplex thrust system, Hyde-Macraes shear zone, Otago schist, New Zealand. Economic Geology 85(8): 1711-1719.

Turnbull IM, Mortimer N, Craw D 2001. Textural zones in the Haast Schist-a reappraisal. New Zealand Journal of Geology and Geophysics 44(1): 171-183.

Twiss RJ, Moores, E.M. 2007. Structural Geology. Second Edition ed. New York, W.H. Freeman and Company. 689 p.

Wheeler J, Butler RWH 1994. Criteria for identifying structures related to true crustal extension in orogens. Journal of Structural Geology 16(7): 1023-1027.

Winsor CN 1991. The relationship between the Hyde-Macraes Shear Zone, deformation episodes, and gold mineralisation potential in eastern Otago, New Zealand. New Zealand Journal of Geology & Geographics 34(2): 237-245.

Winsor CN 1991. Low-angle shear zones in central Otago, New Zealand - their regional extent and economic significance. New Zealand Journal of Geology & Geophysics 34(4): 501-516.

Yardley BWD 1982. The early metamorphic history of the Haast schists and related rocks of New Zealand. Contributions to Mineralogy & Petrology 81(4): 317-327.

List of Figures

CHAPTER ONE:

CHAPTER TWO:

CHAPTER TWO (continued)

CHAPTER THREE:

CHAPTER FOUR:

List of Tables

CHAPTER ONE:

Appendix A

Maps

Toitu te Land whenua Information New Zealand

NZTopo*Online*

Custom Map

Grid co-ordinates are in terms of NEW ZEALAND MAP GRID PROJECTION

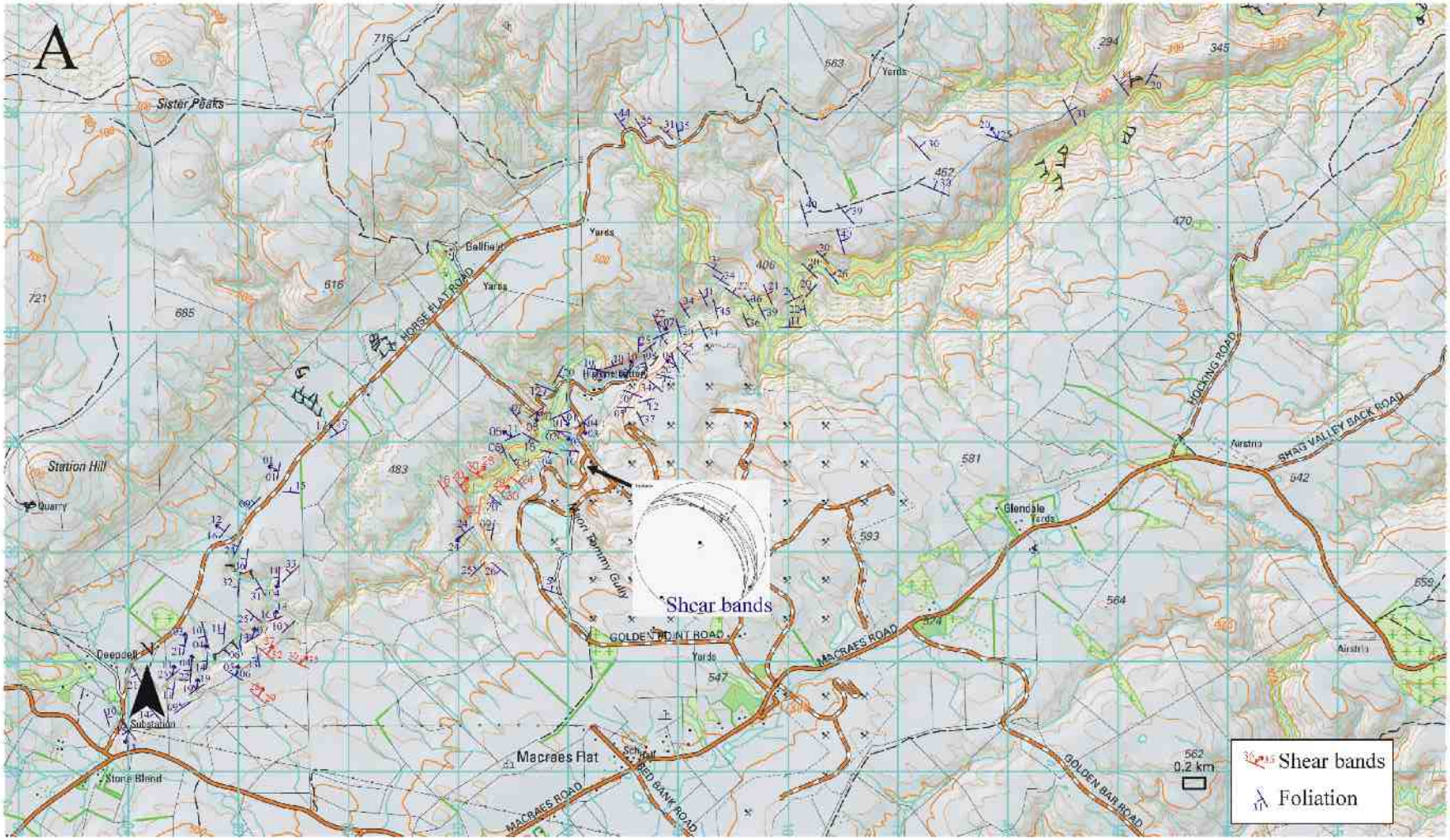

Version 4.13
Scale 1:50,000

SAFETY WARNING: Pylons and power lines are not currently plotting correctly

1. NZTopo*Online* must not be used for aircraft navigation. This map does not show all aerial wires, cableways and obstructions that could be hazardous to aircraft.
2. Closed tracks or routes on this map are no longer maintained or passable and should not be used. Contact DOC or your council for the latest information on tracks and huts.
3. The representation of a road or track on this map, or it's existence on the ground, does not guarantee a public right of way. Please respect private property.

Toitu te Land whenua Information New Zealand

NZTopo*Online*

Custom Map

Grid co-ordinates are in terms of NEW ZEALAND MAP GRID PROJECTION

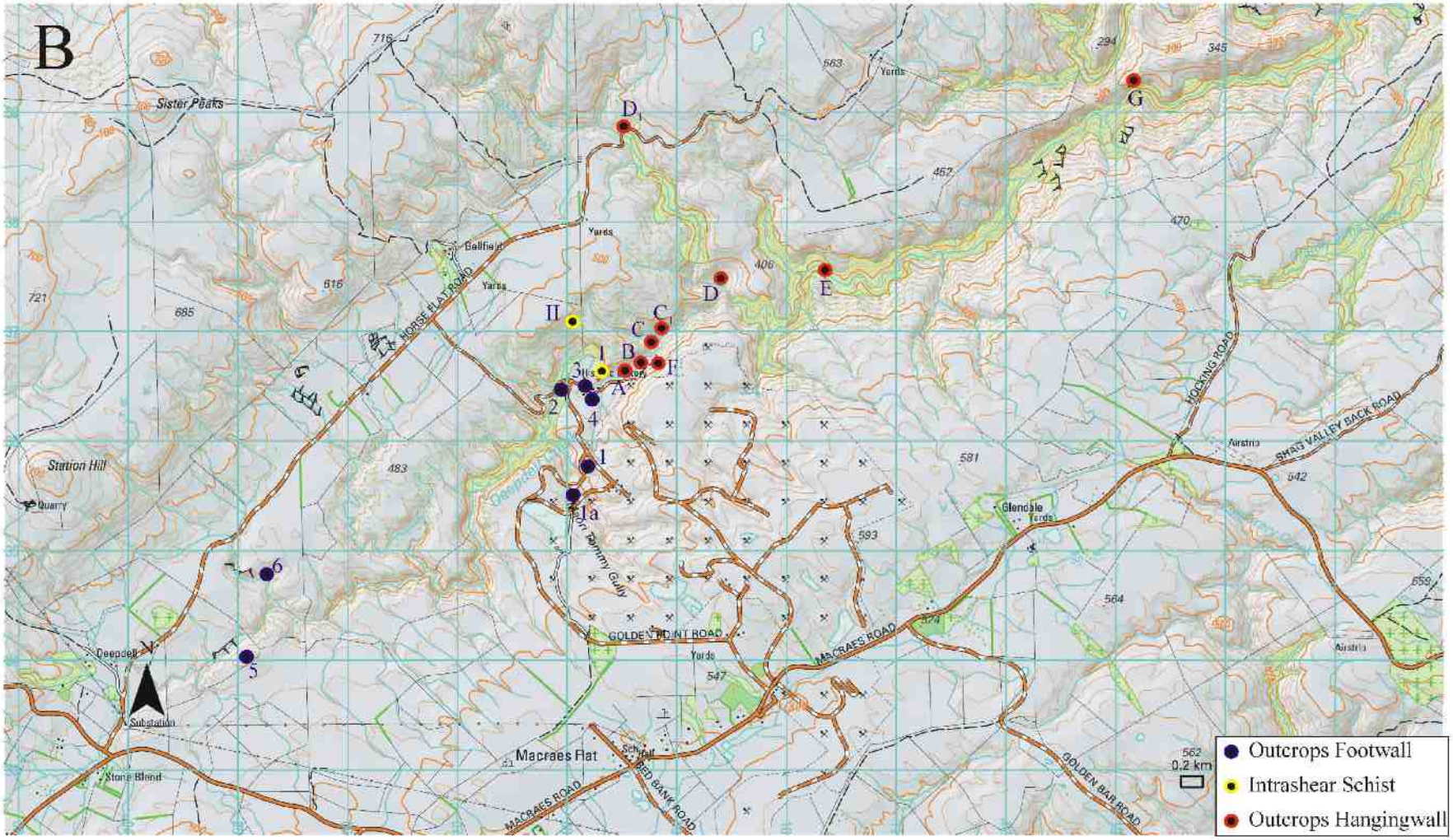

Version 4.13
Scale 1:50,000

SAFETY WARNING: Pylons and power lines are not currently plotting correctly

1. NZTopo*Online* must not be used for aircraft navigation. This map does not show all aerial wires, cableways and obstructions that could be hazardous to aircraft.
2. Closed tracks or routes on this map are no longer maintained or passable and should not be used. Contact DOC or your council for the latest information on tracks and huts.
3. The representation of a road or track on this map, or it's existence on the ground, does not guarantee a public right of way. Please respect private property.

Toitu te Land whenua Information New Zealand

NZTopo*Online*

Custom Map

Grid co-ordinates are in terms of NEW ZEALAND MAP GRID PROJECTION

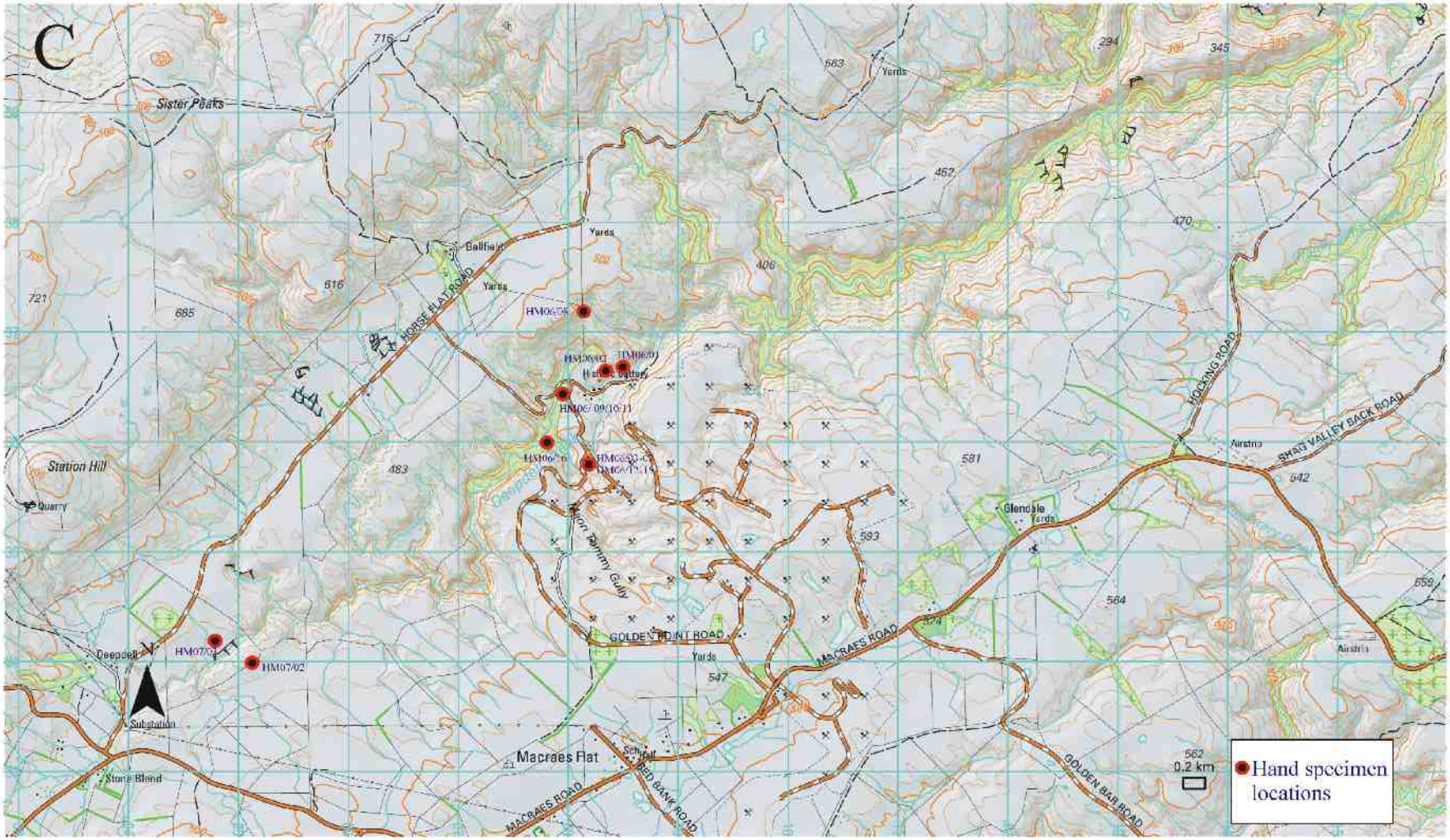

Version 4.13
Scale 1:50,000

SAFETY WARNING: Pylons and power lines are not currently plotting correctly

1. NZTopo*Online* must not be used for aircraft navigation. This map does not show all aerial wires, cableways and obstructions that could be hazardous to aircraft.
2. Closed tracks or routes on this map are no longer maintained or passable and should not be used. Contact DOC or your council for the latest information on tracks and huts.
3. The representation of a road or track on this map, or it's existence on the ground, does not guarantee a public right of way. Please respect private property.

Toitu te Land whenua Information New Zealand

NZTopo*Online*

Custom Map

Grid co-ordinates are in terms of NEW ZEALAND MAP GRID PROJECTION

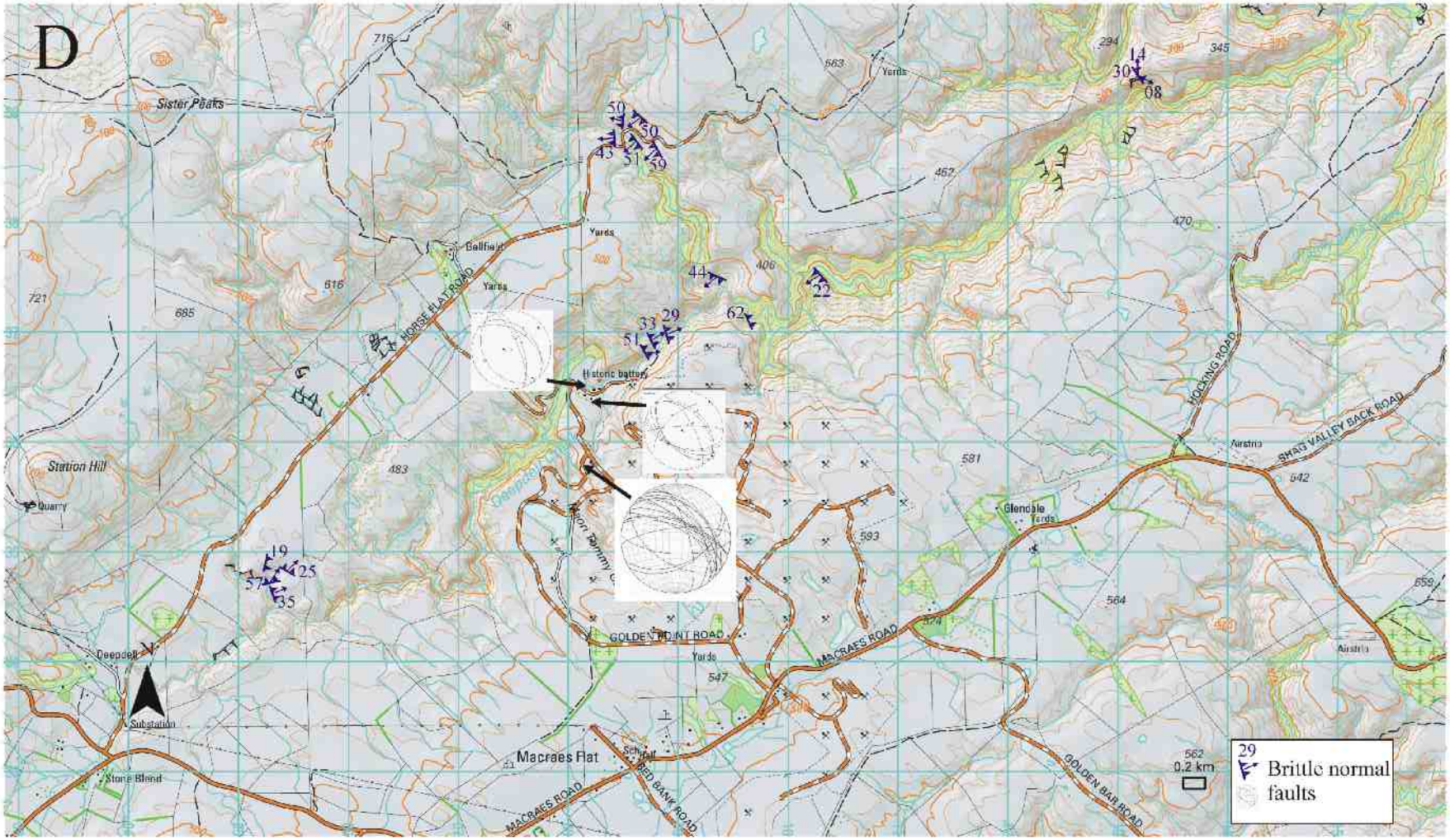

Version 4.13
Scale 1:50,000

SAFETY WARNING: Pylons and power lines are not currently plotting correctly

1. NZTopo*Online* must not be used for aircraft navigation. This map does not show all aerial wires, cableways and obstructions that could be hazardous to aircraft.
2. Closed tracks or routes on this map are no longer maintained or passable and should not be used. Contact DOC or your council for the latest information on tracks and huts.
3. The representation of a road or track on this map, or it's existence on the ground, does not guarantee a public right of way. Please respect private property.

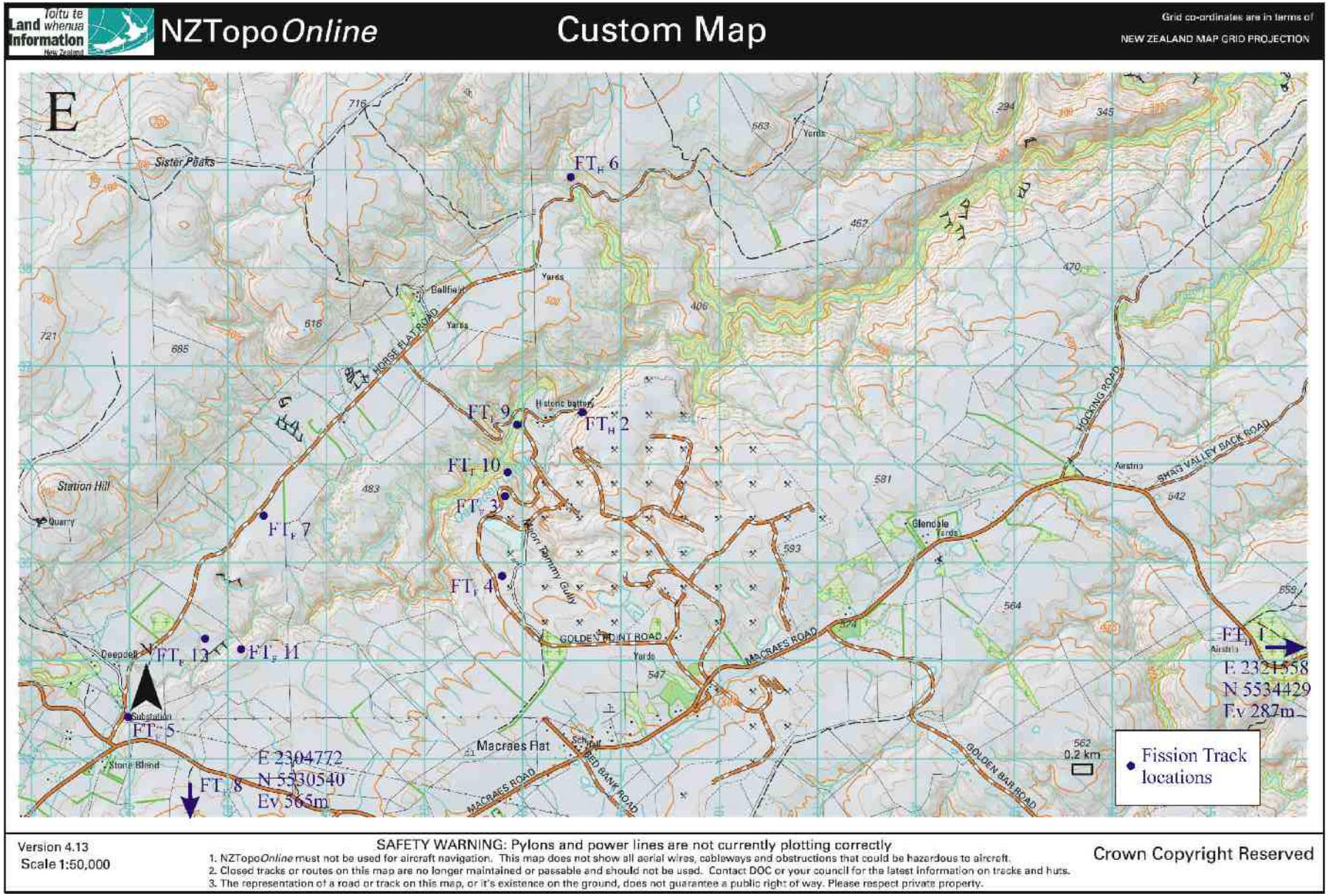

Version 4.13
Scale 1:50,000

SAFETY WARNING: Pylons and power lines are not currently plotting correctly

1. NZTopo*Online* must not be used for aircraft navigation. This map does not show all aerial wires, cableways and obstructions that could be hazardous to aircraft.
2. Closed tracks or routes on this map are no longer maintained or passable and should not be used. Contact DOC or your council for the latest information on tracks and huts.
3. The representation of a road or track on this map, or it's existence on the ground, does not guarantee a public right of way. Please respect private property.

Appendix B

Data

Outcrop	Fault planes		Lineation			Foliation		GPS			
	Dip Direction	Dip angle	Dip Direction	Dip angle	Linear	Dip Direction	Dip angle	Order	E	N	Elevation [m]
Footwall											
Golden point road											
	14	63									
	24	60									
	18	71									
	60	38									
	14	55									
	32	34									
	42	40									
	20	45									
	70	50									
	70	46									
	08	70									
	192	58									
	194	75									
	187	60									
	226	30									
	217	36									
	188	75									
	70	45	80	40	L	148	04	S1			
	85	20									
	56	50									
	66	55									
	18	25									
	18	24									
	20	74									
	24	65									
	24	64									
	54	44									
	17	72	11	70	L						
	40	43									
	54	33									
	89	55									
	26	50									
	35	66									
	24	44									
	40	60									
	70	89				140	05	S1			
	74	85				85	05	S1			
	190	55									
	172	55									
	160	50									
	211	69									
	212	55				82	07	S1			
	215	50									
	202	63									
	204	50									
	195	55									
	70	50									
	78	50									
	83	30									
	216	35									
	60	45									
	60	51									
	56	50									
	58	50									
	90	33									
	246	65									
	46	40									
	177	44									
	30	32									
	178	44									
	213	44									
	194	40									

Outcrop	Fault planes		Lineation			Foliation		GPS			
	Dip Direction	Dip angle	Dip Direction	Dip angle	Linear	Dip Direction	Dip angle	Order	E	N	Elevation [m]
Golden point road (continued)	212	58									
	111	36									
	41	29									
	58	41									
	54	52									
	78	45									
	31	40									
	20	45									
	67	40									
	67	35									
	210	74				45	15	S1			
	210	54				55	07	S1			
	215	44	213	43	L						
	184	71									
	47	32									
	174	89									
	66	58				118	05	S1			
	73	55									
	48	50									
	229	84									
	74	70									
	86	55									
	178	74									
	178	76									
	176	71									
	176	75									
	180	74				127	05	S1			
	22	80									
	34	70									
	20	50									
	51	46									
	203	84	317	81	L	160	10	S1			
	210	73	237	69	L						
	06	75				120	05	S1			
	16	69									
	20	59									
	08	59									
	09	84				96	08	S1			
	224	39									
	196	49				90	20	S1			
	262	79									
	120	05									
	26	60				75	05	S1			
	198	29									
	178	15									
	52	65									
	42	50									
	50	44									
	50	54									
	48	46									
	32	60				85	10	S1			
	31	65									
	37	67									
	42	65									
	32	57									
	48	57									
	27	50									
	38	62									
	42	71									
	14	49									
	44	51									
	55	65									
	54	80									
	08	75				95	03	S1			
	26	64									
	181	46									
	194	85									
	174	70									

Outcrop	Fault planes		Lineation			Foliation		GPS			
	Dip Direction	Dip angle	Dip Direction	Dip angle	Linear	Dip Direction	Dip angle	Order	E	N	Elevation [m]
Golden point road (continued)	52	50									
	55	45									
	60	40									
	60	45									
	147	47									
	52	78									
	14	51				126	05	S1			
	25	74				118	05	S1			
	156	55				112	10	S1			
	358	75									
	155	46									
	42	60									
	340	85									
	50	65									
	358	75									
	327	70									
	320	70									
	326	78									
	328	89									
	0	84				104	07	S1			
	30	75									
	350	71									
	36	81									
	356	75									
	06	65									
	341	75									
	355	75									
	351	75									
	152	74				56	20	S2			
	132	52				46	30	S2			
	169	50				26	27	S2			
	146	59				32	26	S2			
	167	40									
	122	45									
	26	58									
	52	83	44	81	L						
	50	85									
	65	40									
	27	84									
	38	70									
	19	81									
	48	58									
	51	56				22	06	S1	2308130	5535747	412
	48	50				17	14	S2			
	44	45				37	19	S2			
	40	48									
	60	59									
	60	70									
	58	56									
	80	61									
	39	55									
	38	55									
Shear bands			38	39	L	52	40	S2			
			05	40	L	49	52	S2			
			042	19	L	061	20	S2			
			033	15	L	037	16	S2			
			034	35	L	272	44	S2			
			11	48	L	17	50	S2			
			39	48	L	51	52	S2			
			37	44	L	44	48	S2			
			44	41	L	30	43	S2			
			41	27	L	42	29	S2			
			40	24	L	40	24	S2			
			34	38	L	67	41	S2			
			359	50	L	13	55	S2			

Outcrop	Fault planes		Lineation			Foliation		GPS			
	Dip Direction	Dip angle	Dip Direction	Dip angle	Linear	Dip Direction	Dip angle	Order	E	N	Elevation [m]
Golden point road (1a)	Everything N-normal										
	348	57	28	56	L	59	01	S1			
			129	03	L						
	03	72	30	70	L						
	349	68	25	60	L						
	359	76	41	66	L						
	357	70	05	69	L						
	338	78	21	71	L						
	44	58	19	54	L						
	40	53	11	51	L						
	348	75	10	75	L1						
			257	07	L2	-> Late, quarternairy reactivation					
	17	70	58	75	L						
	11	82	62	78	L						
	15	85	35	84	L						
	17	80	76	70	L						
	354	72	26	69	L						
	07	69	29	66	L						
	353	72	43	70	L						
	25	63	24	63	L						
	28	61	25	60	L						
	345	85	45	76	L						
	34	60	31	57	L						
	149	66	126	44	L						
	148	78	240	02	L	034	04	S1			
						170	07	S1			
			306	04	L	188	04	S1			
Deepdell Battery 1	68	74	224	67	L						
	233	31	247	30	L						
	72	65	55	37	L						
	44	40	29	38	L						
	34	49	45	47	L						
Deepdell Battery 2	195	53	227	44	L	119	20	S1			
	214	51	229	44	L						
	61	69	52	63	L						
	44	49	32	46	L						
	43	42	35	36	L						
	358	81	36	71	L						
	230	50	248	48	L						
	201	73									
	202	52	246	50	L						
	319	53	323	50	L						
	227	50	231	48	L						
6) gully shear zone	030	25	048	25	L	316	33	S1	2305368	5534826	451
	348	57	033	40	L	271	11	S1			
			195	04	Lfol						
	071	35	067	30	L						

Outcrop	Fault planes		Lineation			Foliation			GPS		
	Dip Direction	Dip angle	Dip Direction	Dip angle	Linear	Dip Direction	Dip angle	Order	E	N	Elevation [m]
Footwall Data along Deepdell Creek from Battery						201	12	S1	2307892	5536302	356
			182	08	L	145	10	S1			
	135	62	210	32	L				2307790	5536106	359
	236	75									
						053	07	S1			
						210	15	S1	2307768	5535979	361
			304	05	L	335	11	S1	2307601	5535904	361
	134	82									
						249	08	S1	2307444	5535843	346
	174	50	176	45	L	055	08	S1	2307467	5535785	347
	163	60									
	178	51	207	48	L1						
			250	20	L2						
						039	24	S2	2307268	5535633	344
						221	20	S1			
						045	30	S2			
			041	28	L	028	30	S2			
			041	20	L	055	21	S2			
						057	18	S2	2307132	5535619	387
						048	20	S2	2307140	5535580	356
			225	24	L	323	24	S1	2301707	5535293	383
						070	05	S2			
	010	30	58	28	L						
						316	25	S1			
						220	26	S1			
						296	24	S1	2304958	5535118	449
						278	32	S1	2305079	5534918	489
						276	32	S1			
Gully at gully shear zone	102	19							2305271	5534912	468
			185	01	L	275	05	S1	2305298	5534776	424
			015	04	L	303	10	S1			
						240	31	S1	2305324	5534391	443
			009	14	L	340	16	S1	2305230	5534178	473
						319	10	S1			
	039	29	032	28	L	031	06	S1	2305108	5534107	486
			016	05	Lfol						
	041	32	035	27	L						
Substation			195	13	L	234	15	S1			
						228	14	S1			
						242	21	S1	2304259	5533747	448
						324	09	S1			
						279	11	S1			
			008	19	L	324	19	S1	2304554	5533854	449
			005	04	L	274	22	S1			
			012	13	L	322	25	S1			
			002	03	L	282	21	S1			
	084	76	160	62	L						
	024	36	048	35	L				2305008	5534233	439
						260	06	S1			
			014	07	L	330	14	S1			
						221	25	S1	2305127	5534348	467
						274	11	S1	2304839	5534238	470
			182	04	L	254	10	S1			
	232	22									

Outcrop	Fault planes		Lineation			Foliation		GPS			
	Dip Direction	Dip angle	Dip Direction	Dip angle	Linear	Dip Direction	Dip angle	Order	E	N	Elevation [m]
Hangingwall											
Outcrop A	TZ III		14	10	L (Kink)	305	10	S1			
Outcrop B	335	50				260	22	S1			
		55	87 357	48	L	08	50	S1			
			340	10	L						
Outcrop C	60	51	87	39	L						
	83	40									
	70	40									
	63	33	60	30	L						
	74	29	67	28	L						
			93	33	L						
	32	29									
	33	31									
	85	15									
	65	57	93	33	L						
	67	22	122	07	L						
			132	05	L						
	55	22	72	22	L						
	198	45	210	45	L	92	25	S1			
	194	42				142	08	S1			
	346	30									
Outcrop D	196	44	230	40	L	032	34	S1			
	204	34				033	34	S1			
Outcrop E						045	20	S1			
	213	18									
	228	22	237	20	L						
	226	25				047	20	S1	2310223	5537580	291
						051	26	S1			
Outcrop F	281	56	310	49	L	165	12	S1	2308662	5536601	375
	292	61	327	30	L						
	062	75	004	66	L						
						220	34	S1			
			302	04	L	244	20	S1	2308889	5536820	368
	247	64	255	61	L						
			291	13	L	228	20				
Outcrop G	045	55	095	55	L						
			330	20	L	018	25	S1			
	056	30	120	08	L	064	31	S1			
	025	24	356	14	L	053	34	S1			

Outcrop	Fault planes		Lineation			Foliation			GPS		
	Dip Direction	Dip angle	Dip Direction	Dip angle	Linear	Dip Direction	Dip angle	Order	E	N	Elevation [m]
Hangingwall data without explicit outcrops	311	77	347	72	L	202	10	S1	2308601	5536542	358
	313	77	337	75	L						
	48	78	354	75	L	182	05	S1	2308590	5536471	381
	276	41	268	40	L	063	37	S1			
	322	65	312	60	L						
	28	45	30	44	L				2308556	5536432	392
	64	50	54	46	L						
	228	30	246	25	L						
						048	25	S1	2309129	5536933	412
	287	54	294	50	L	195	17	S1			
						198	34	S1			
	33	64	37	63	L						
	41	79	12	74	L						
	090	47	018	20	L						
	133	70							2309027	5536798	436
	92	42							2309005	5536991	333
						73	20	S1	2309242	5537166	329
						66	41	S1			
						57	34	S1			
	206	53									
	202	53	196	51	L						
	250	60				064	41	S1	2309393	5537340	314
						076	45	S1			
						034	22	S1	2309446	5537409	322
						067	36	S1	2309529	5537241	320
						065	39	S1			
						055	36	S1			
	66	62									
						068	21	S1	2309896	5537190	368
						002	11	S1	2310051	5537182	302
						334	20	S1	2310093	5537392	307
						312	20	S1			
						074	40	S1	2310268	5538053	465
						074	40	S1			
						052	39	S1			
						023	30	S1	2311698	5538666	438
						049	34	S1			
						120	20	S1	2313314	5539434	340
						043	31	S1	2308730	5538734	466
	065	55	102	45	L	079	35	S1			

Outcrop	Fault planes		Lineation			Foliation			GPS		
	Dip Direction	Dip angle	Dip Direction	Dip angle	Linear	Dip Direction	Dip angle	Order	E	N	Elevation [m]
Intrashear Schist											
Outcrop I	Upper shear										
	39	48	107	36	L	190	02	S1			
	35	47	35	38	L						
	258	64	244	64	L						
	63	33	105	13	L	344	10	S1	2308335	5536638	381
	48	45									
	353	60									
			096	40	L	082	42	S1	2308318	5536571	377
	048	60	006	53	L	145	20	S1			
	042	42	102	40	L	118	10	S1			
	263	60	272	55	L	138	06	S1			
	43	46									
	340	50	330	40	L	070	34	S1			
						150	15	S1			
	142	20									
	070	50	034	40	L						
	160	20	165	15	L						
	080	20	130	10	L				2308308	5536660	379
			114	02	L	029	25	S1			
						348	20	S1			
Outcrop II											
Big Shear zone											
Main shear	300	30	19	05	L						
Riedel shear	350	84	11	70	L						
Other faults	280	35	39	09	L						
	320	63	28	36	L	285	40	S1			
	352	79	54	63	L						
Samples											
HM 06/01						344	10	S1			
HM 06/02						007	10				
HM 06/03	Gouge										
HM 06/04	Gouge										
HM 06/05						118	05	S1			
HM 06/06						126	05	S1			
HM 06/07	Gouge										
HM 06/08	Gouge										
HM 06/09 a&b			146	01	L	155	01	S1	2307933	5536399	355
HM 06/10			174	03	L	140	04	S1			
HM 06/11			128	03	L	186	02	S1			
HM 06/12	Gouge										
HM 06/13						055	07	S1			
HM 06/14						045	15				
HM 06/15						052	20	S1			
HM 06/16						185	10	S1			
Sample HM07/01						170	07	S1			
Sample HM07/02						261	12	S1			
Sample HM07/03						275	14	S1	2304630	5533951	445
Horse Flat Road											
						59	36	S1	2308659	5538731	463
	277	50	283	46	L						
	266	43	266	42	L						
	276	44	254	40	L						
	222	50	236	48	L						
	233	51	230	50	L						
	241	59	226	54	L						
	229	57	225	55	L						
TZ III	235	65	219	62	L	55	44	S1	2308477	5538813	425
TZ IV			317	17	L	330	19	S1	2305796	5536120	458
TZ IV			299	01	L	281	01	S1	2305256	5535469	465
						315	09	S1			
TZ IV			306	12	L	308	16	S1	2304960	5535137	447
						74	10	S1	2303909	5533474	441